NAVAL POSTGRADUATE SCHOOL
Monterey, California

THESIS

EXPERIMENTAL OBSERVATIONS OF GEOMAGNETIC
MICROPULSATIONS: LAND AND SEA

by

Edward Wayne Pogue

December 1932

Thesis Advisor: P. H. Moose

83   04   25   125

DISCLAIMER NOTICE

THIS DOCUMENT IS BEST QUALITY PRACTICABLE. THE COPY FURNISHED TO DTIC CONTAINED A SIGNIFICANT NUMBER OF PAGES WHICH DO NOT REPRODUCE LEGIBLY.

REPORT DOCUMENTATION PAGE		READ INSTRUCTIONS BEFORE COMPLETING FORM
1. REPORT NUMBER	2. GOVT ACCESSION NO. $AD-A$	3. RECIPIENT'S CATALOG NUMBER
4. TITLE (and Subtitle) "Experimental Observation of Geomagnetic Micropulsations: Land and Sea"		5. TYPE OF REPORT & PERIOD COVERED Master's Thesis December 1982
		6. PERFORMING ORG. REPORT NUMBER
7. AUTHOR(s) Edward Wayne Pogue		8. CONTRACT OR GRANT NUMBER(s)
9. PERFORMING ORGANIZATION NAME AND ADDRESS Naval Postgraduate School Monterey, California 93940		10. PROGRAM ELEMENT, PROJECT, TASK AREA & WORK UNIT NUMBERS
11. CONTROLLING OFFICE NAME AND ADDRESS Naval Postgraduate School Monterey, California 93940		12. REPORT DATE December 1982
		13. NUMBER OF PAGES 37
14. MONITORING AGENCY NAME & ADDRESS(If different from Controlling Office)		15. SECURITY CLASS. (of this report) Unclassified
		15a. DECLASSIFICATION/DOWNGRADING SCHEDULE

16. DISTRIBUTION STATEMENT (of this Report)

Approved for public release; distribution unlimited

17. DISTRIBUTION STATEMENT (of the abstract entered in Block 20, if different from Report)

18. SUPPLEMENTARY NOTES

19. KEY WORDS (Continue on reverse side if necessary and identify by block number)

Micropulsations	Stokes Parameters
Geomagnetic variations	Ellipticity
Polarization	Ocean Floor

20. ABSTRACT (Continue on reverse side if necessary and identify by block number)

Data taken from the second generation of the Naval Postgraduate School's ocean floor and land geomagnetic data collection system is analyzed to determine the wave nature of Geomagnetic Pulsations in the .05 to 10 Hz range. The measurements were made in Monterey, California during June to September 1982. Three of these experiments were twenty-four hours in length. During two such

(continued)

Item 20. (Continued)

experiments land and sea data were transmitted to a central point where the signals were recorded simultaneously. Geomagnetic fluctuations were analyzed to determine various factors characterizing the waves. These factors include the power spectral densities, coherences, Stokes parameters, orientation angle, degree of polarization, and ellipicity. The software developed in this research provides an extensive capability for analysis of geomagnetic noise. Long term data collection can utilize it to establish trends in both the spatial and temporal properties of naturally occurring ELF electromagnetic fields.

Accession For

NTIS GRA&I	☑
DTIC TAB	☐
Unannounced	☐
Justification	

By

Distribution/

Availability Codes

Dist	Avail and/or Special

DTIC COPY INSPECTED 2

Experimental Observations of Geomagnetic Micropulsations:
Land and Sea

by

Edward Wayne Pogue
Captain, United States Army
B. S., United States Military Academy, 1971

Submitted in partial fulfillment of the
requirements for the degree of

MASTER OF SCIENCE IN PHYSICS
from the
NAVAL POSTGRADUATE SCHOOL
December 1982

Author _____

Approved by: _____
                                        Thesis Advisor

_____
Michael E. Thomas
                                        Second Reader
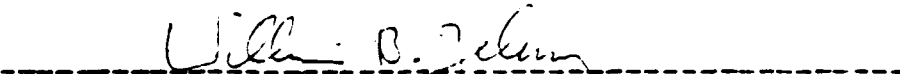
_____
                    Chairman, Department of Physics

_____
                    Dean of Science and Engineering

3

ABSTRACT

Data taken from the second generation of the Naval
Postgraduate School's ocean floor and land geomagnetic data
collection system is analysed to determine the wave nature
of Geomagnetic Micropulsations in the .05 to 10 Hz range.
The measurements were made in Monterey, California during
June to September 1982. Three of these experiments were
twenty-four hours in length. During two such experiments
land and sea data were transmitted to a central point where
the signals were recorded simultaneously. Geomagnetic fluc-
tuations were analyzed to determine various factors charac-
terizing the waves. These factors include the power spectral
densities, coherences, Stokes parameters, orientation angle,
degree of polarization and ellipicity. The software devel-
oped in this research provides an extensive capability for
analysis of geomagnetic noise. Long term data collection can
utilize it to establish trends in both the spatial and
temporal properties of naturally occuring ELF electromag-
netic fields.

TABLE OF CONTENTS

LIST OF FIGURES

7

I. INTRODUCTION

This thesis is part of the long term effort of the Naval Postgraduate School to collect and interpret ELF eletromagnetic noise on the sea floor and from a nearby land station. The project's objective is to study and interpret signals in the 0.05 to 10 Hz frequency range. It emphasizes the importance of obtaining measurements of geomagnetic noise on the sea floor and on land over a period of several years.

The specific obectives of this thesis are twofold; to calibrate, install, and operate the land data collection system; and to develope a computer program to analyze the data recorded to provide easily utilized interpretive factors.

.

A. TIME VARIATIONS OF THE GEOMAGNETIC FIELD

The earth's magnetic field has been used for centuries for navigation at sea and for survey direction on land. These common uses are dependent on the static magnetic field. The static field can be generally characterized as a magnetic dipole at a 11.5 degree inclination to the axis of rotation of the earth. It shows only minor diurnal variations in direction. Its magnitude varies greatly over the earths surface but usually is in the range of 40,000 to 70,000 nano-Teslas (nT). At Monterey, California the static field has a value of 48,600 nT.

It has only been since the discovery of magnetic induction that the underlying variations in the static field have become well known. These variations are due to many sources. The sources include, but are not limited to, solar

8

activities, lunar daily variations, magnetic storms, thunderstorms in the earth's atmosphere, earthquakes, and the detonation of nuclear devices. One of the major contributors to this is the interaction of the charged particles from the sun with the earth's magnetosphere. These events vary widely in duration, amplitude, and the frequency range they effect. Within the frequency range of this system the most common variations are characterized as micropulsations.

Geomagnetic micropulsations are defined to be fluctuations in the earth's magnetic field which have periods from 0.2 seconds to 10 minutes. They vary in amplitude from .001 nT to as high as a few tens of nT. They are attributed to the interaction of groups of charged particles propagating in the earth's magnetosphere as hydromagnetic waves. These waves inturn create the source currents, (primarily in the ionsphere), for the micropulsation field. Micropulsations are divided into two subcatagories: irregular and continuous. The abreviations for these are pc for pulsation continuous and pi for pulsation irregular. The primary difference between the two is that the pc micropulsations have a semi-sinusoidal nature while the pi micropulsations show irregularities in both amplitude and frequency. The period ranges and average amplitude for these pulsations are listed in Table I, [Ref. 1].

The overwhelming majority of the pulsations in this frequency range are due to solar activity. In addition, "Schumann" resonances will also be apparent in the vicinity of 6-8 Hz. These resonances are due to lightening transients in the concentric spherical cavity between the earth's surface and the lower region of the ionosphere, [Ref. 2].

TABLE I

Geomagnetic Micropulsation Classes

Notation	Period(Sec)	Amplitude(nT)
pc1	0.2-5	0.05-0.1
pc2	5-10	0.1-1
pc3	10-45	0.1-1
pc4	45-150	0.1-1
pc5	150-600	1-10
pi1	1-40	0.01-0.1
pi2	40-150	1-5

B. SYSTEM DESCRIPTION
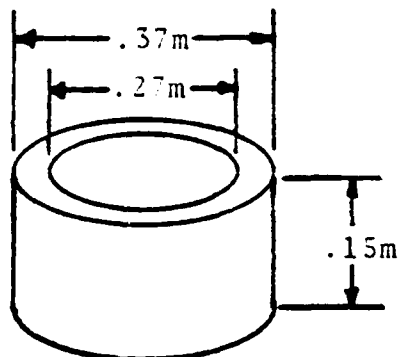
Figure 1.1   Sensing Coil Dimensions

The sensor system currently employed consists of a three coil land system deployed at La Mesa Village housing area, approximately 2 km from the Naval Postgraduate School data collection center, and a two coil sea system deployed on the bottom of Monterey Bay. Its distance to the Naval Postgraduate School (NPS) varied from 2 to 4 km. The original intention of the project was to deploy the land system approximately 22 miles from the Naval Postgraduate School at Chew's Ridge. This proved impossible due to data transmission difficulties. See Appendix B for additional information on this site.

Each sensing coil is a continiously wound coil antenna made up of approximately 5460 turns of 18 gauge copper wire. The average sensing area of each coil is 0.0825 square meters and its dimensions are as depicted in Figure 1.1. The sea system has its coils mounted orthogonally, usually in the horizontal plane. The land system coils are affixed to a wooden mount that holds them in an orthogonal configuration; see Figure 1.2. The directional orientation of the sea system cannot be determined when deployed. The land system is oriented with the X-coil in the magnetic north-south direction , Y-coil in the magnetic east-west direction and the Z-coil in the vertical.

The two systems were designed to be as similar as possible. The coils, preamplifier, signal conditioner and pulse code modulator (PCM) are identical in design and were all calibrated to insure the production of valid data. The technical description of all of these items may be found in [Ref. 3] . The land system is deployed as shown in Figure 1.3. The pre-amplifiers are battery powered and located within one foot of the coils. The coil mount and preamplifiers were positioned approximately 50 meters from the signal conditioners, and connected by three coaxial cables.
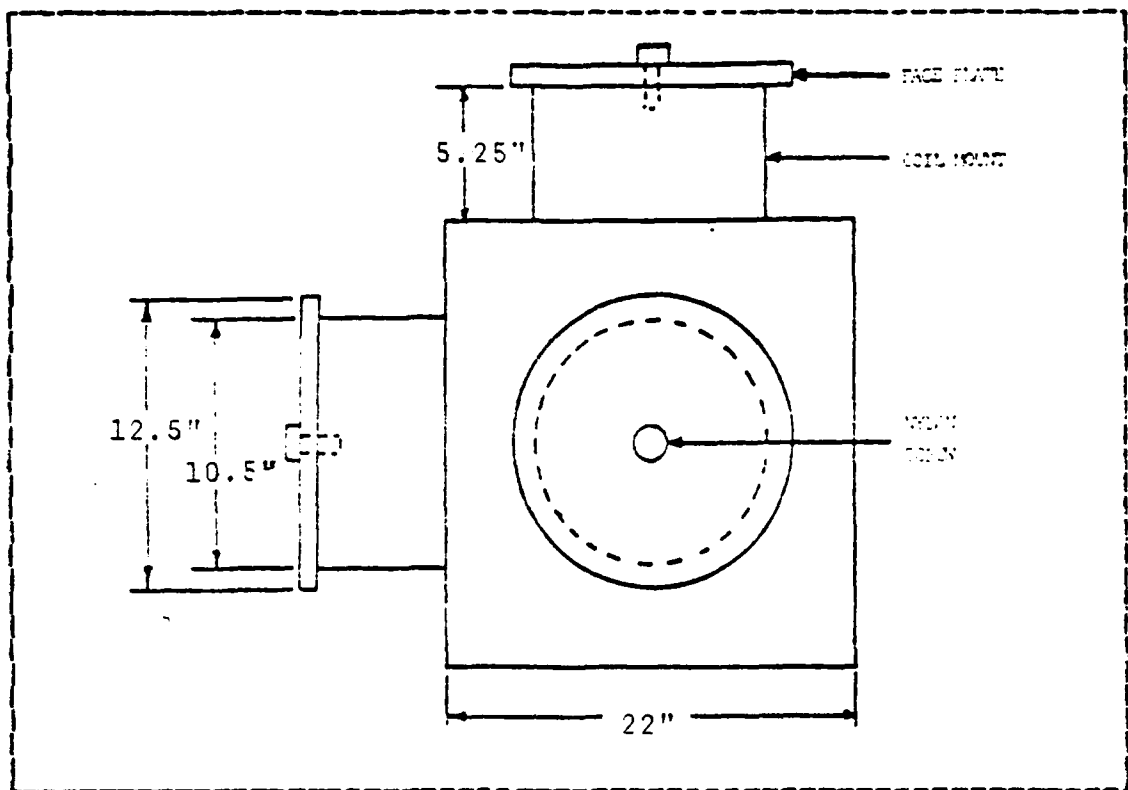
Figure 1.2   Sensor Mounting Block

The signal conditioners, PCM board and transmitter are all housed in a small wooden building and powered by D.C. power supplies. This building is the closest source of alternating current.

After the data has been encoded by the PCM, it is transmitted by VHF radio data link to the Naval Postgraduate School for recording.

C. DATA COLLECTION AND PROCESSING

Land and sea data are simultaneously received and recorded on separate channels of an analog tape recorder. Each tape holds 60 to 120 minutes of data. These tapes must
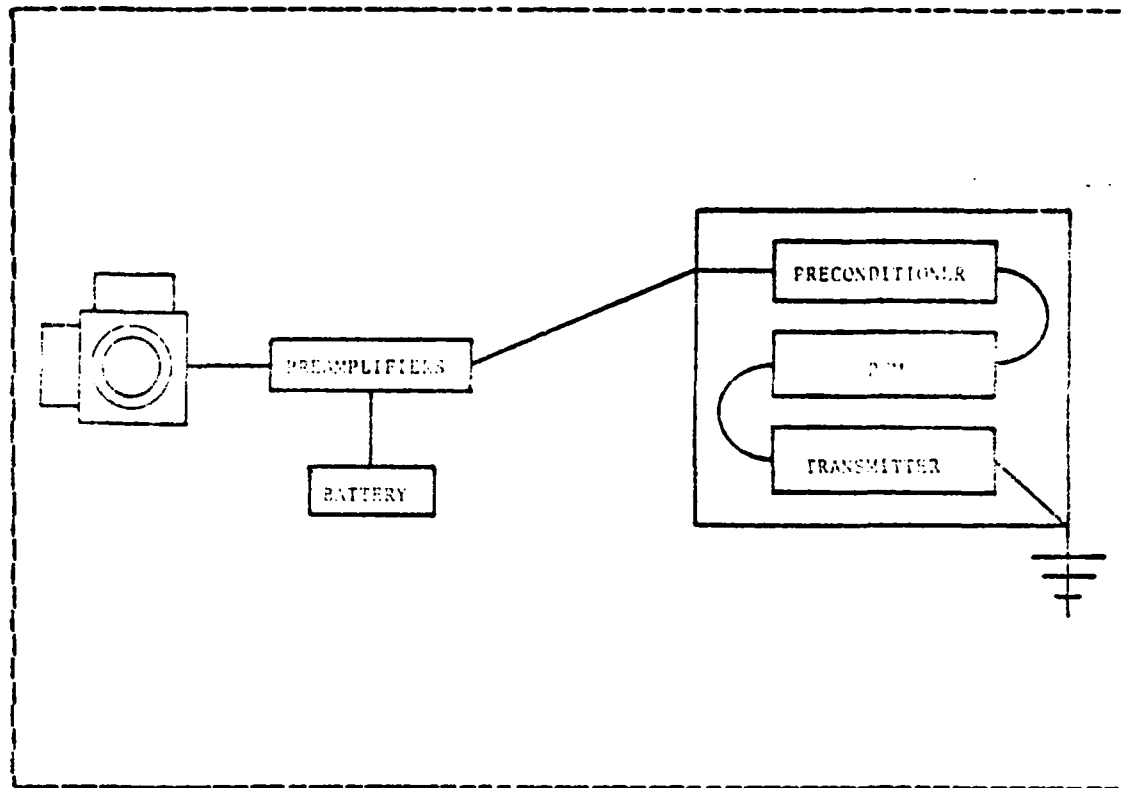
Figure 1.3   Land Data Collection System

be decoded and re-recorded onto digital tape suitable for
the main-frame computer at the Church Computer Center. Each
digital tape contains 90 minutes of land or sea data. Each
of these digital tapes is then processed through the
computer program, (See Chapter 3, Section C.), to provide
the plots of the various interpretive factors. See Reference
3 for the details of the recording, decoding and re-re-
cording on digital tape.

II. SYSTEM CALIBRATION

A. INTRODUCTION

The triaxial coil magnetometer system is diagramed in Figure 2.1. The data sensed by this magnetometer system is given by $V_x(t)$, $V_y(t)$ and $V_z(t)$; the output voltages generated by the input magnetic fields. The system transfer function must be determined so that the magnetic field components can be removed from the output voltage. In the time domain the relationship between the output voltage and the magnetic field is a convolution integral,

$$v_i(t) = \int h_i(t-t')b_i(t')dt' \tag{1}$$

where $i=x,y,z$. It is more convenient to express Eqn. (1) in the frequency domain.

$$V_i(\omega) = H_i(\omega)B_i(\omega). \tag{2}$$

The transfer function $H_i(\omega)$ can easily be determined in terms of the ratio of output to an input test signal or by analysis of the measurement system's properties.

The next section discusses the components of the system and attempts to develop a system model. The last section describes the calibration measurements and the experimental determination of the transfer function.

B. SYSTEM DESCRIPTION

The individual transfer function for the sensing coil is:

$$V_c(\omega) = j\omega KB(\omega) \tag{3}$$
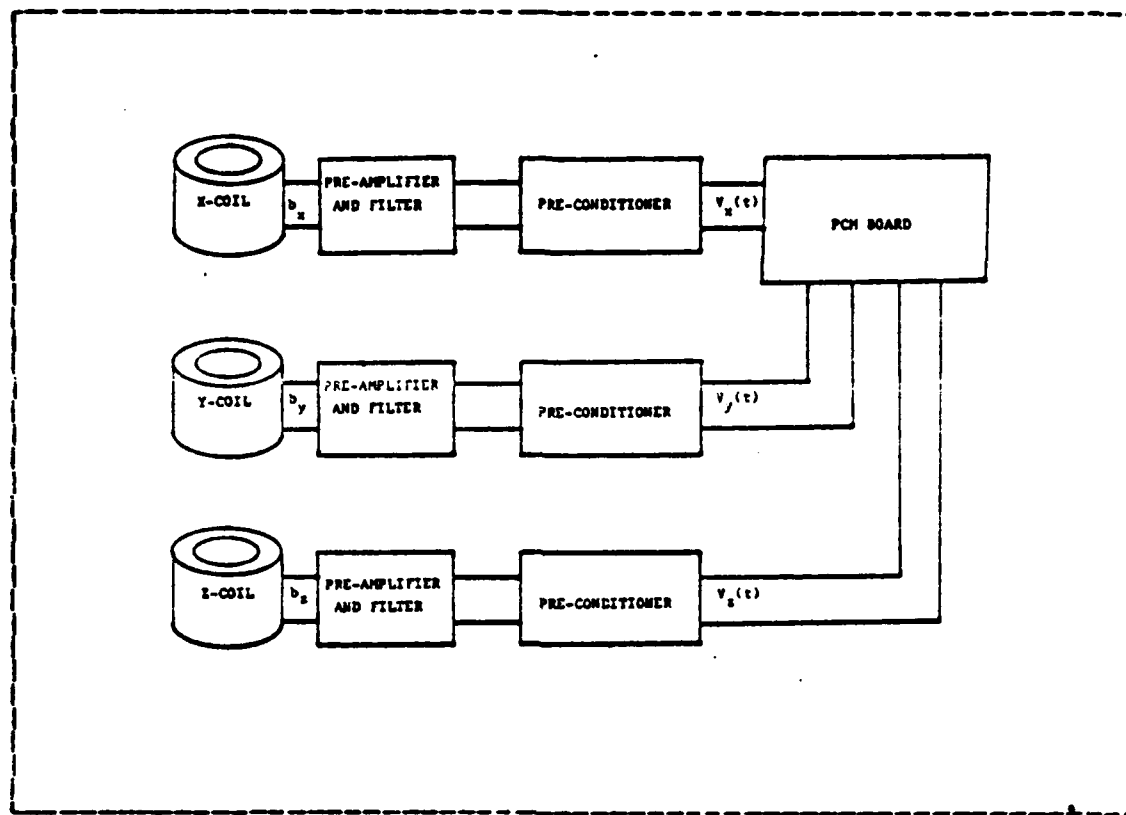
Figure 2.1   System Component Configuration

where $V_c(\omega)$ is the spectrum of the voltage directly out of the coil and K is a gain factor.

The next component in the system is the preamplifier low pass filter.   The preamplifier introduces a gain of 1000 so the voltage signal can be sent to remote instrumentation. The low pass filter is a five pole Chebyshev with a 3dB cutoff at 20 Hz.   The filter is primarily used to remove 60 Hz signals from the system and to prefilter the data before it is digitized. An additional pole is introduced because of a capacitive coupling between the second and third stages of the filter.   Figure 2.2 shows a pole-zero diagram of the preamplifier. The transfer function takes the form:

$$H(j\omega) = K/(j\omega+a)(j\omega+b)(j\omega+c-jd)(j\omega+c+jd)(j\omega+e-jf)(j\omega+e+jf) \quad (4)$$

15

where K is the gain of the preamplifier and the coeficients a - f are determined from the pole-zero diagram.

The preconditioner has additional gain of approximately 1000 and has zener diodes to limit the input voltage to the PCM board. Typically the cutoff is around 7 to 8 volts.

The magnitude and phase response of the preamplifier-filter and preconditioner are shown in Figures 2.3 through 2.8. The input test signal generating these curves had flat magnitude and phase character as shown in Figures 2.9. The figures then represent the actual transfer functions of the preamplifier-filter preconditioner system for the x-y-z channels of land and ocean sensor systems. The figures show that the channels are well matched in magnitude and phase. The phase response is linear and virtually identical in every case. This is an important point since the phase part of the transfer function is not removed from the output voltage signal. However, since the data analysis is in terms of power spectral densities and coherences, this fact has no bearing on the results.

The total transfer function of the system is the product of Eqn. (3) and (4). Based on these formulas and the figures the resulting transfer function is predicted to be fairly linear at the low frequency end.

C. DETERMINATION OF THE SYSTEM TRANSFER FUNCTION

The magnitude of the system transfer function was determined experimentally through the use of a Helmholtz coil, a source of sinusoidal current and a spectrum analyzer. The experimental set up is illustrated in Figure 2.10. A one turn Helmholtz coil with a 0.61 meter radius and a 0.61 meter seperation between coils was used to provide a calibrated magnetic field to the sensing coil. The sensing coil

15
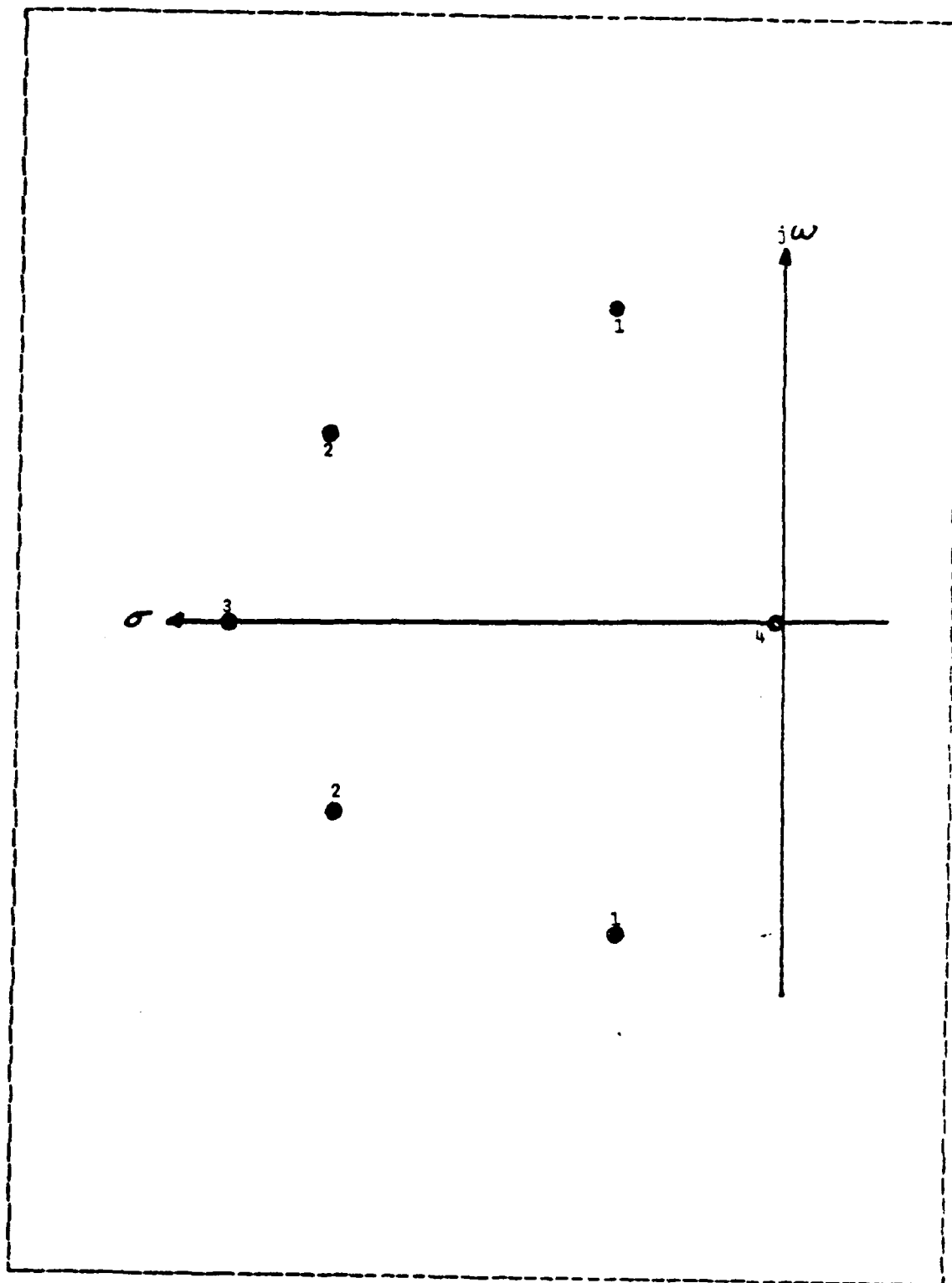
Figure 2.2   Pole-Zero Diagram for Model 13-10A Amplifier

17
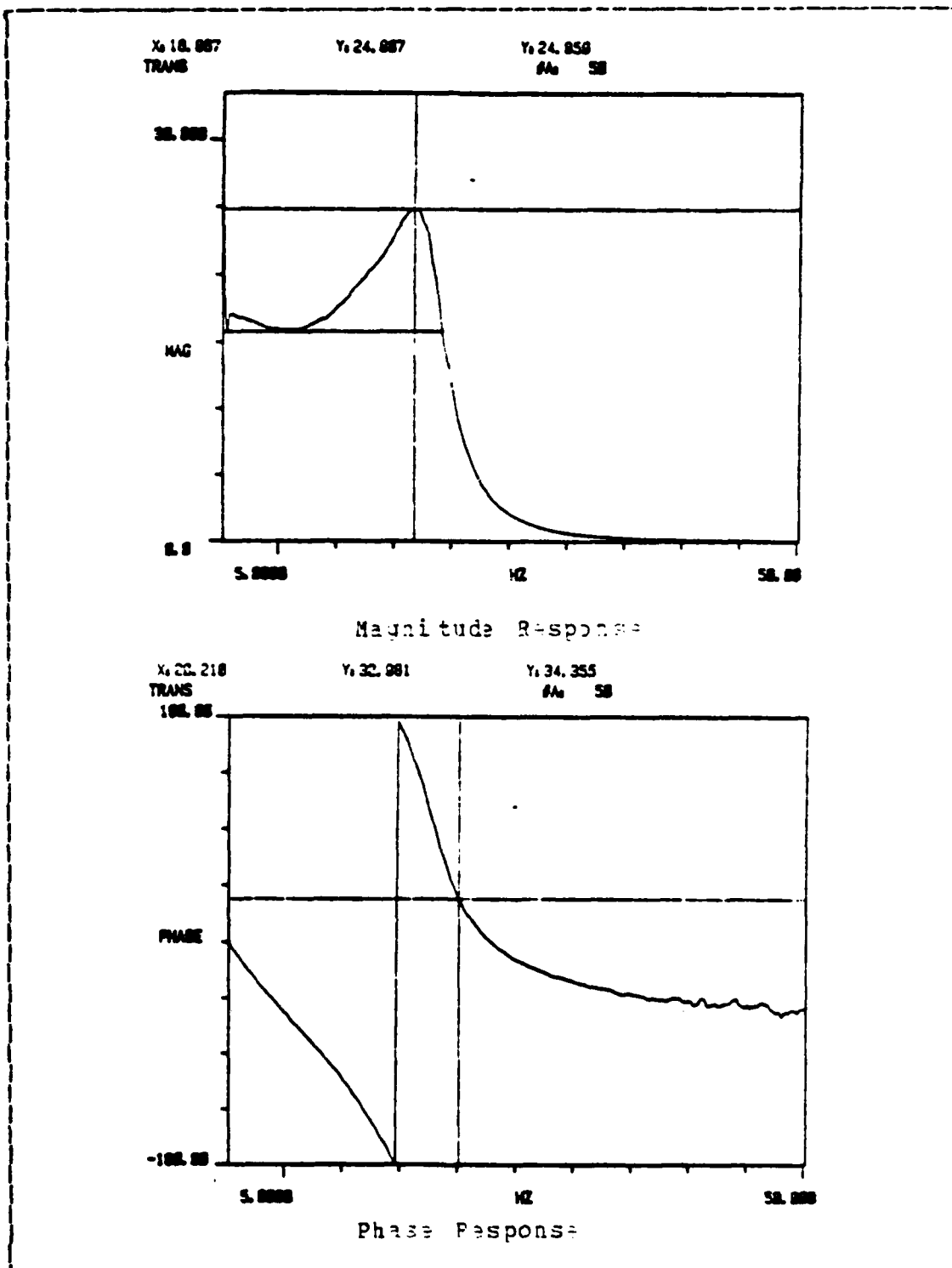
Figure 2.3   Response of the Land X System

18
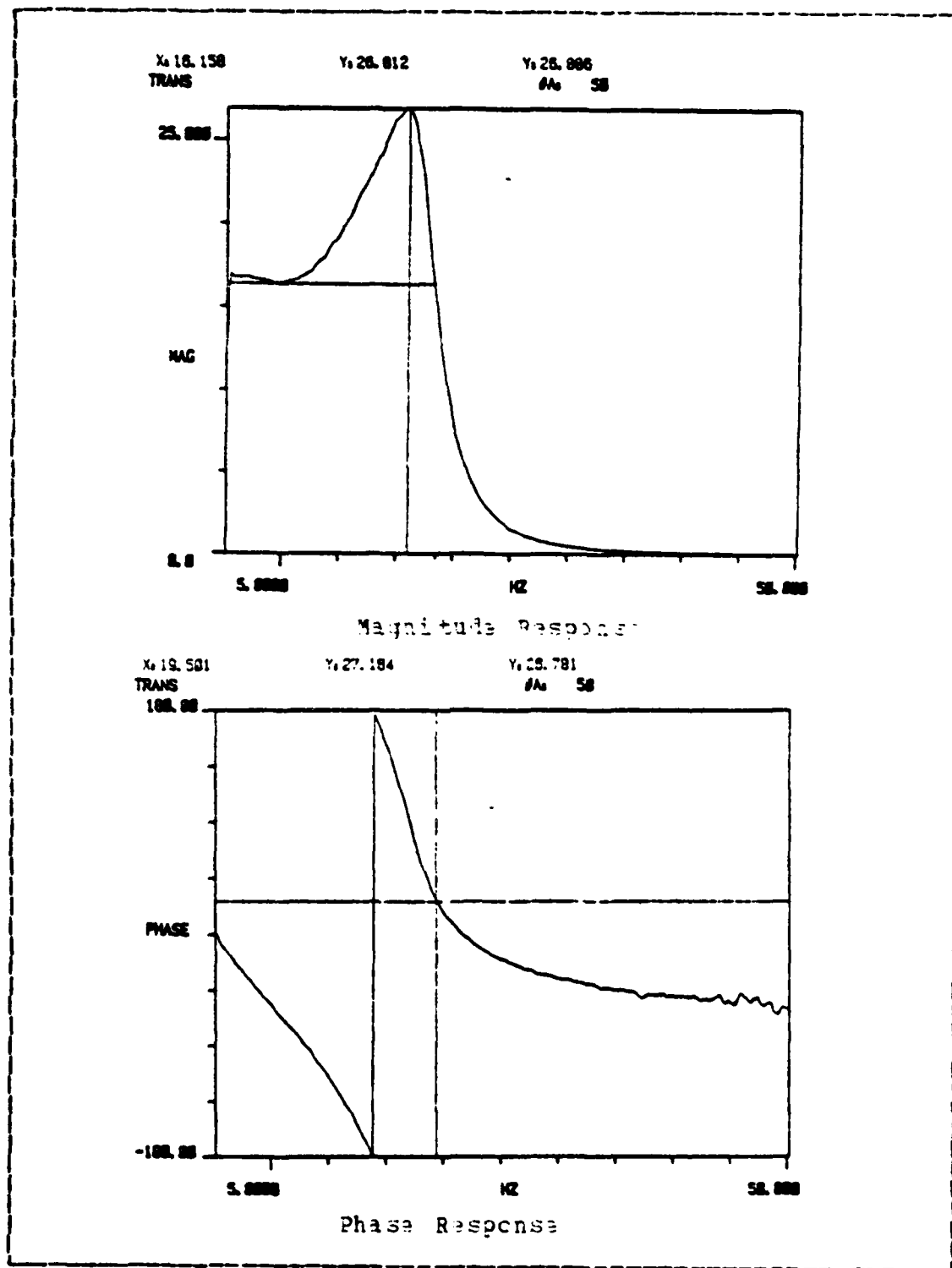
Figure 2.4   Response of the Land Y System

19
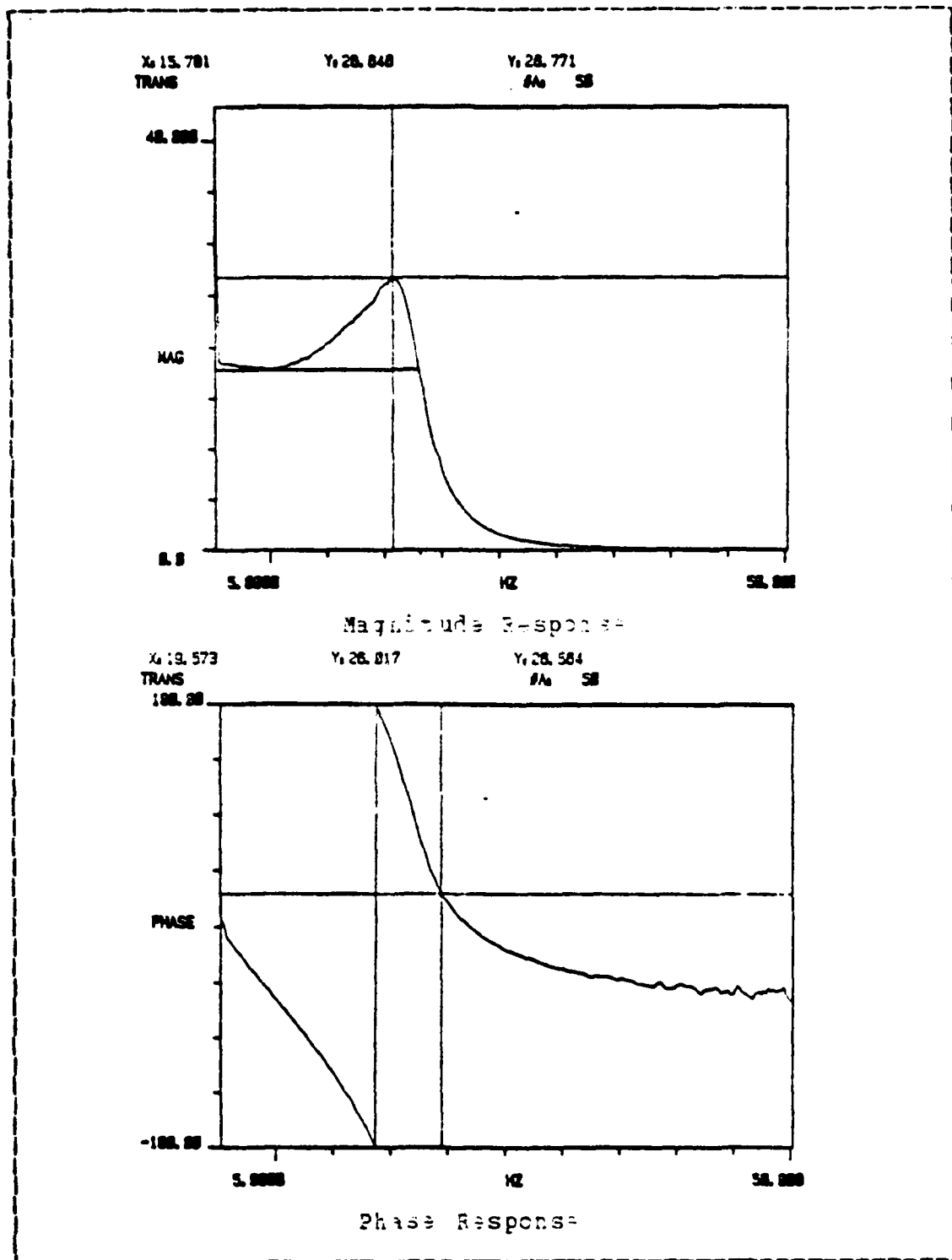
Figure 2.5   Response of the Land Z System

20
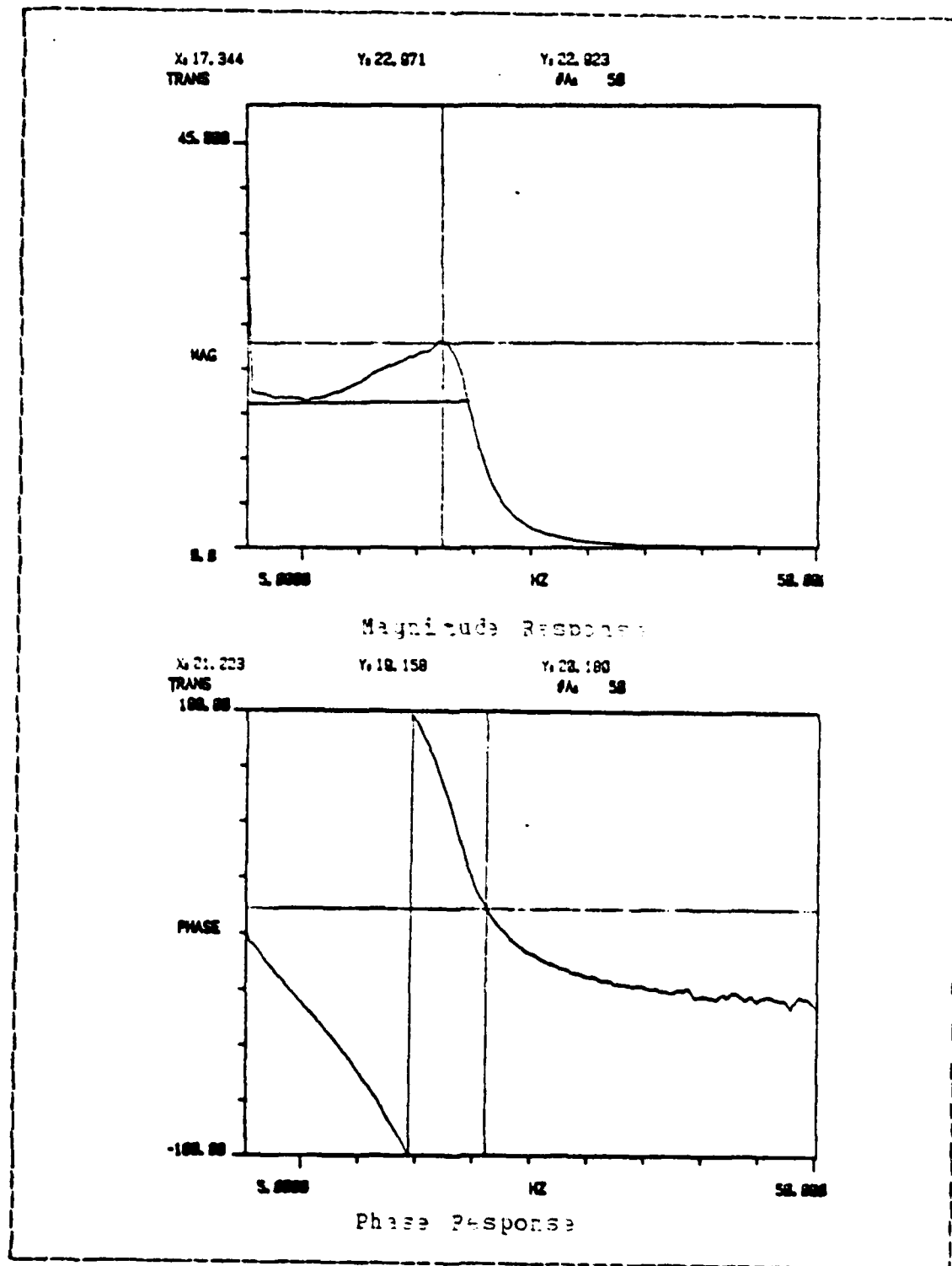
Figure 2.6   Response of the Ocean X System

21

Magnitude Response

Phase Response
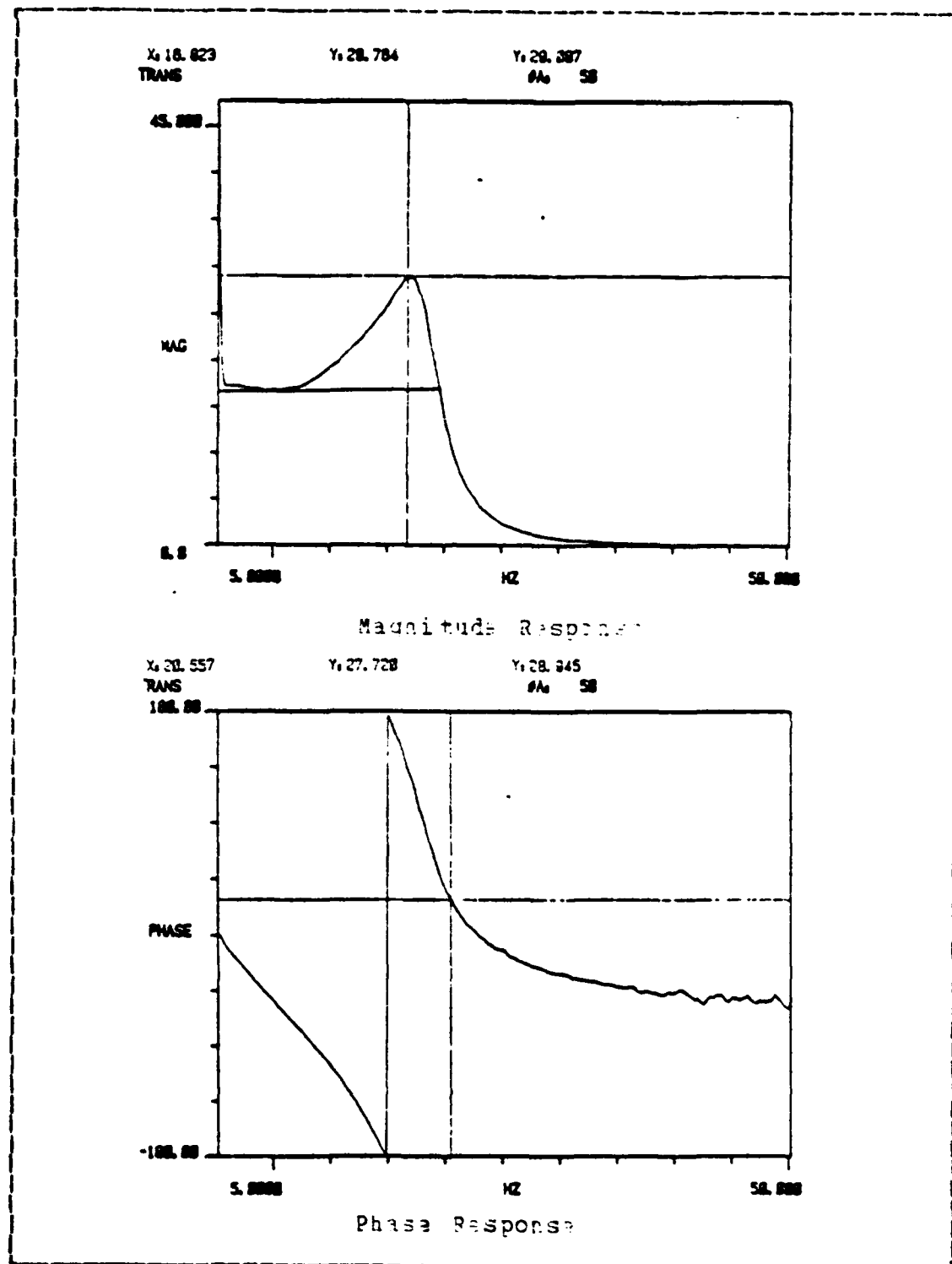
Figure 2.7   Response of the Ocean Y System

22

X: 15.362   Y: 34.113   Y: 34.876
TRANS   #A: 58
46.888

MAG

8.8

5.8888   KZ   58.888

Magnitude Response

X: 13.252   Y: 32.817   Y: 34.231
TRANS   #A: 58
180.88

PHASE

-188.88

5.8888   KZ   58.888

Phase Response
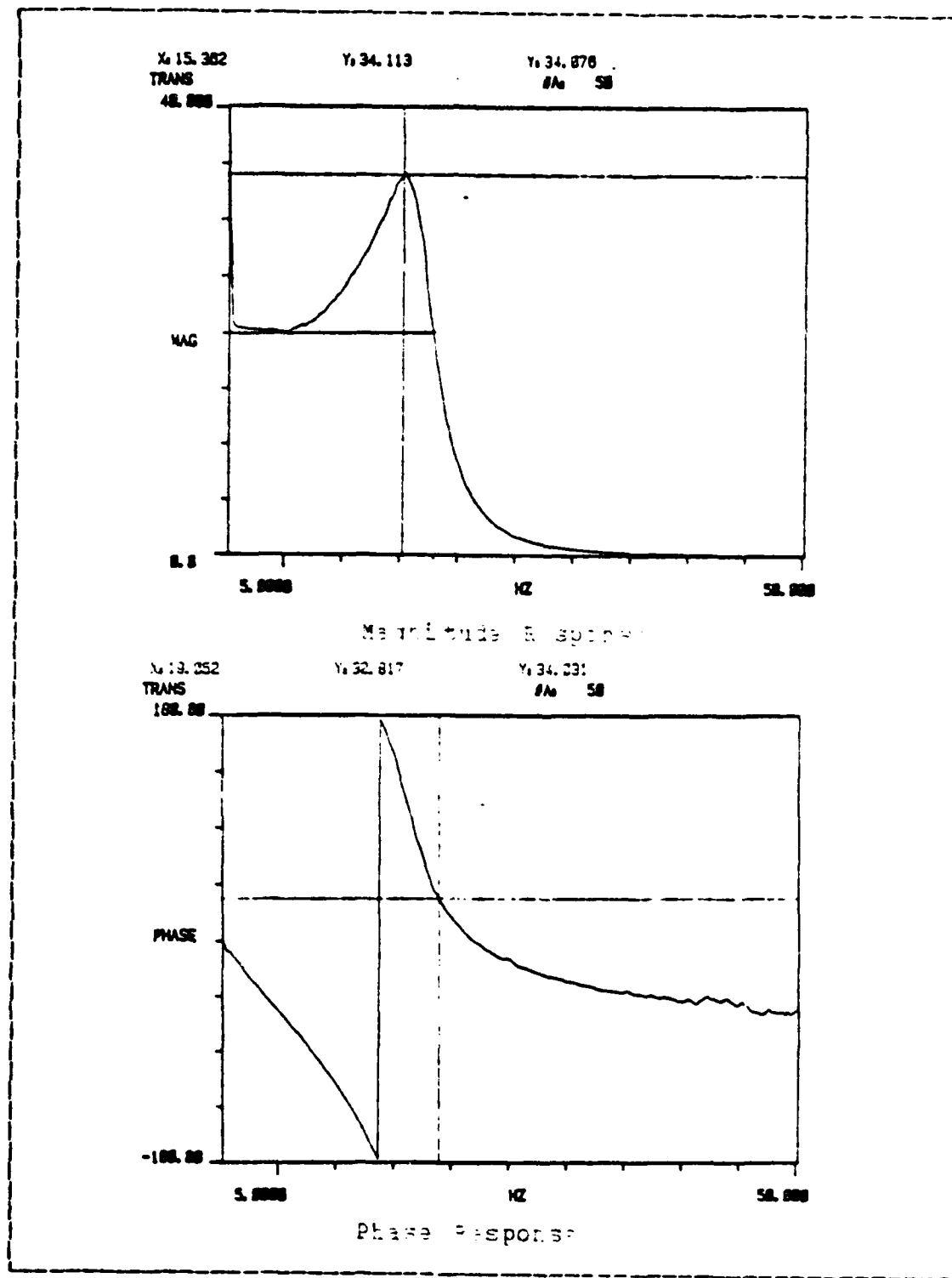
Figure 2.8   Response of the Ocean Z System

23

Magnitude Response

Phase Response
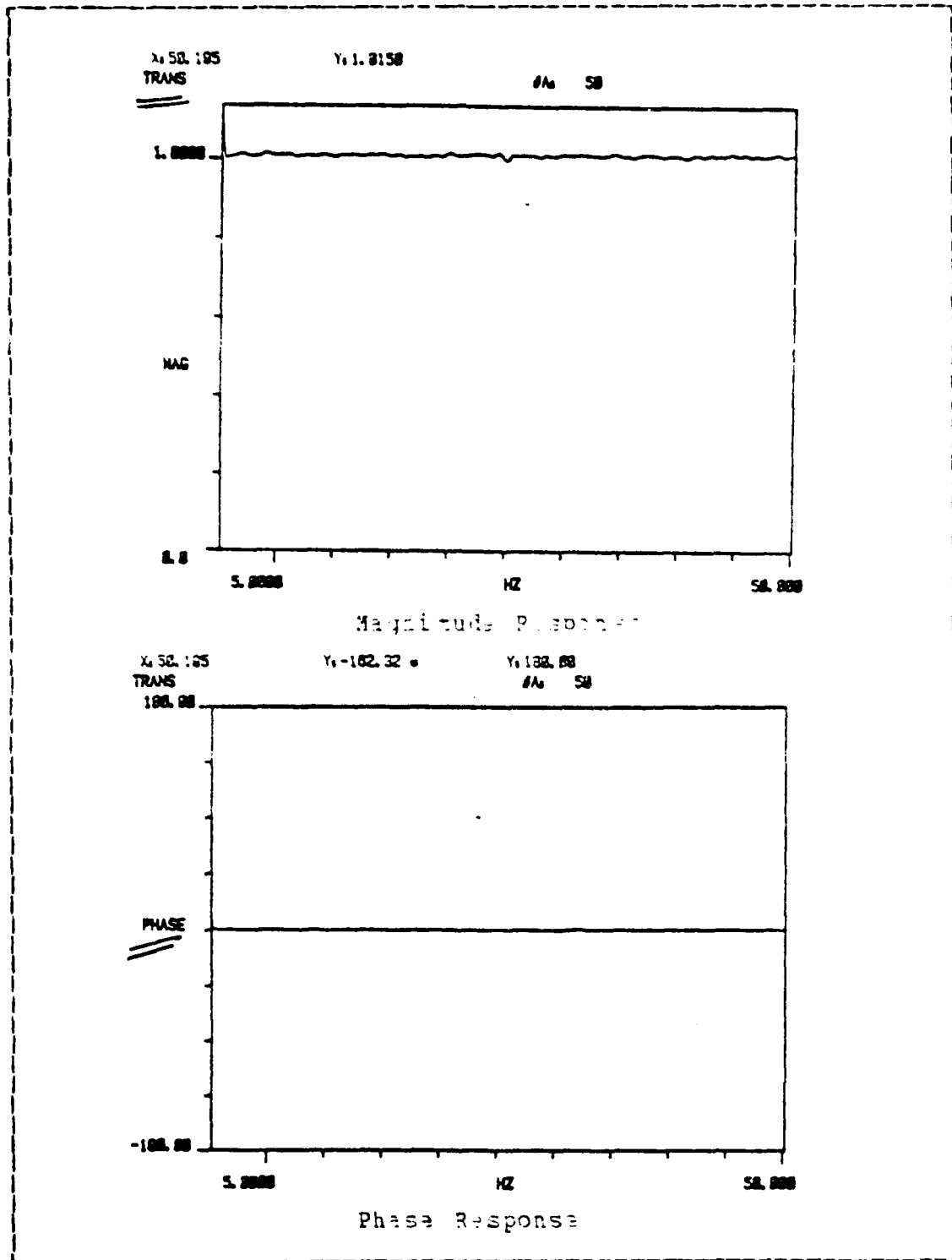
Figure 2.9   Response of the Input Test Signal

24

was placed concentric to the Helmholtz coil, and centered vertically, to ensure a uniform magnetic field about the sensing coil. The magnetic field in this region of the Helmholtz coil is directed along its axis and is given by [Ref. 4] :

$$B = \mu_0 8NI/5\sqrt{5}R \qquad\qquad (5)$$

to terms on the order of (L/R), where L is the linear dimension of the region, N is the number of turns, R is the Helmholtz coil radius and I is the driving current of the coil. The driving current was produced by a Wavetek signal generator, Model Number 142. The current was measured by reading the voltage across a 996 ohm resistor in series with the Helmholtz coil. A spectrum analyzer (HP-3582A) was used to measure the system output to avoid any spurious signals generated by harmonics. By repeating the measurements at a number of different frequencies and drive currents, the system transfer function could be measured.

The actual calibration was conducted at the La Mesa village site using the setup illustrated in Figure 2.10. The Helmholtz coil, sensing coil and preamplifier were located approximately 40 meters from the shack which housed the remainder of the experiment. With the Helmholtz coil disconnected the background magnetic noise of this location was repeatedly examined to ensure accurate readings. Figure 2.11 shows a typical background noise plot from the spectrum analyzer (the transfer function has not been removed). The distinct features are Schumann resonances, otherwise the background was low enough and stable enough to adequately calibrate the system. Only at the Schumann frequencies was the background subtracted from the measured output voltage. Calibration runs were conducted from 0.05 Hz to 20.0 Hz with applied calibrated magnetic field of 0.02, 0.2 and 1.0

25
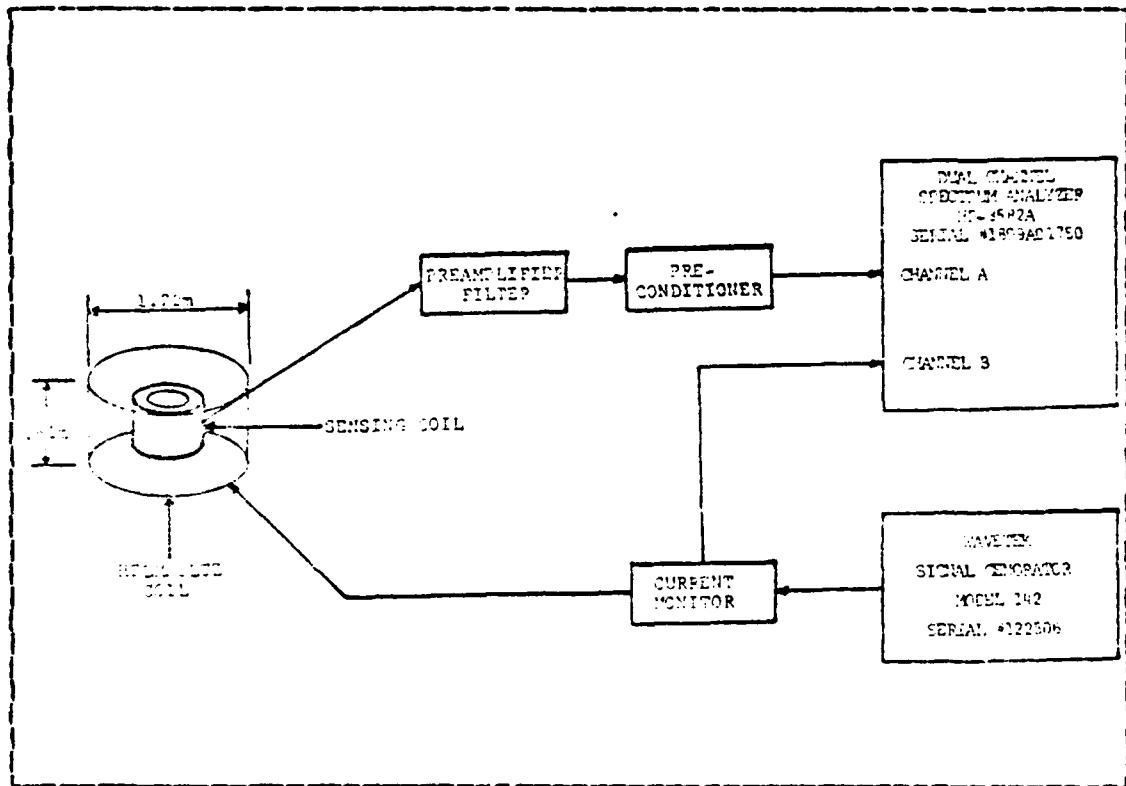
Figure 2.10   System Calibration Experiment

nanoteslas.   Figures 2.12 through 2.16 show the resulting
calibration curves of the land and ocean magnetometer
systems. The true transfer function is represented by the
0.02 nT field. The larger applied fields show saturation of
the system at the protective zener diodes in the precondi-
tioner. At the low frequency end all the systems are closely
matched.   At 1 Hz an output voltage of 1 v indicates a
measured magnetic field of 0.4 nT. A 1 nT field is saturated
above 2 Hz.

     The computation of the equations,   representing the
magnitude of the transfer functions, requires fitting the
data to the theoretical transfer function of the previous
section.   This would be desirable if the phase character of

the system transfer function need be estimated. However, since the primary area of interest is in the lower frequency region, and since the phase response is not needed if the various channels maybe assumed identical, it was decided to model the transfer functions in terms of linear segments. The equations derived in this manner have a maximum error of 1% in the range of 0 to 10 Hz and 5% in the 10 to 20 Hz range for the magnitude of the transfer funtion.

In the actual computation each curve was broken into convenient segments that could be represented by a straight line. The range of the segments were 0 to 5 Hz, 5 to 7.5 Hz, 7.5 to 10 Hz, 10 to 15 HZ and 15 to 20 Hz. The straight line parameters were computed for each segment to yield a series of five equations to model each sensing coil and amplification system. See Table II for the individual transfer functions.
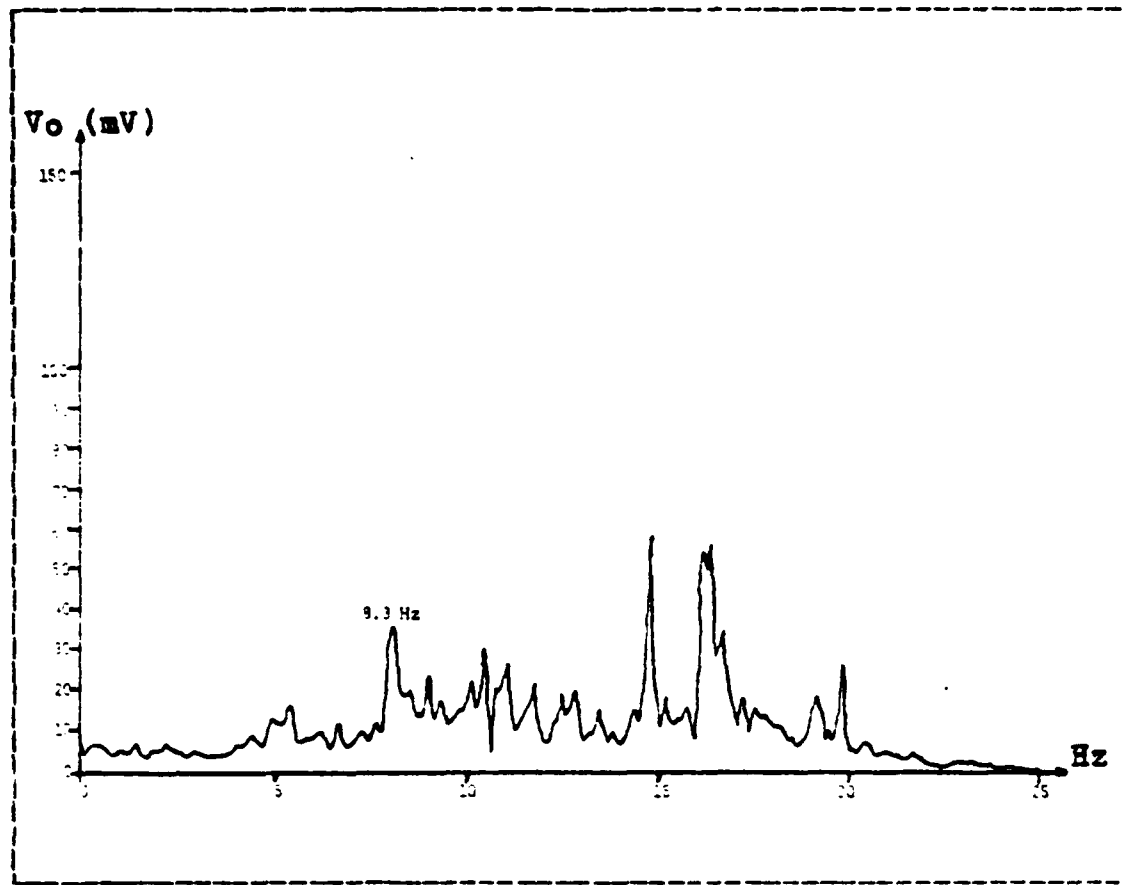
Figure 2.11   Background Geomagnetic Noise f(Hz) 05/20/82
               1513 hrs.
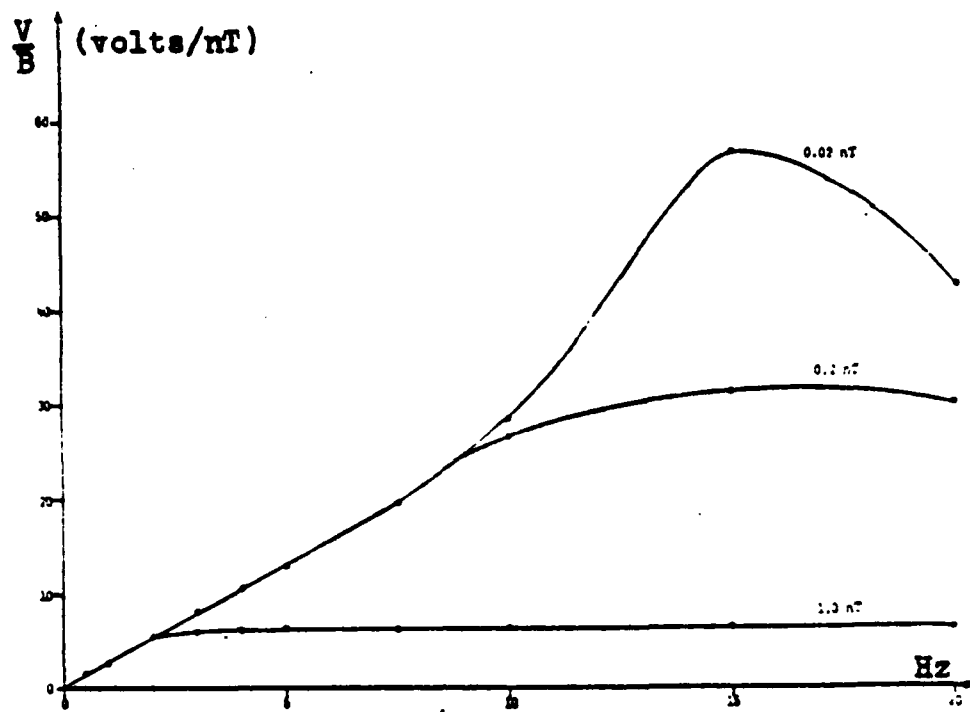
Figure 2.12   Land System X-Coil Calibration
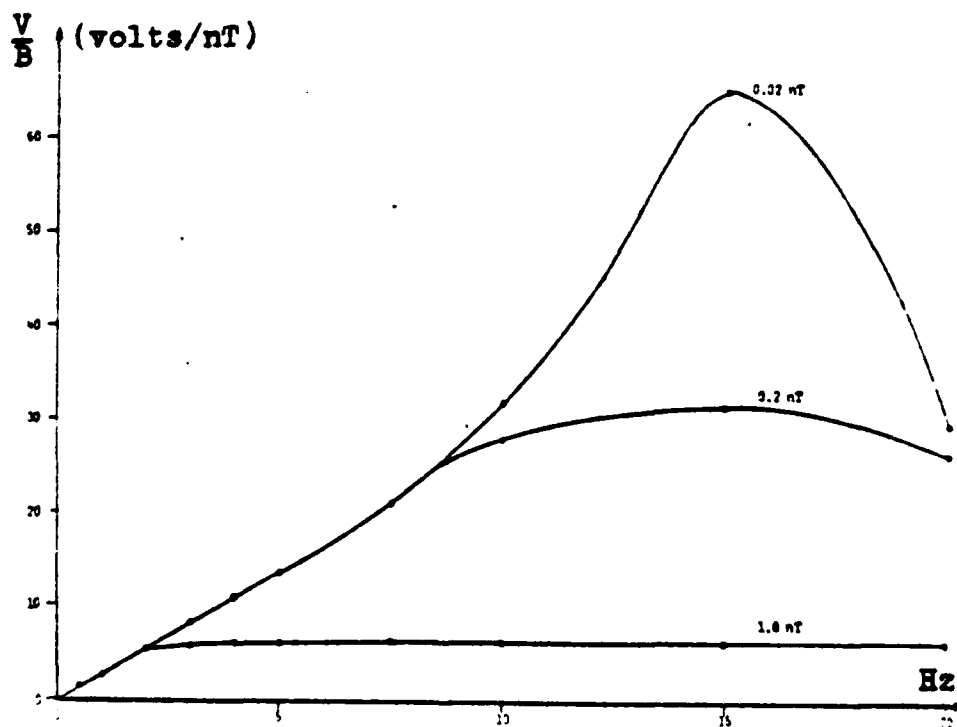
Figure 2.13   Land System Y-Coil Calibration

29
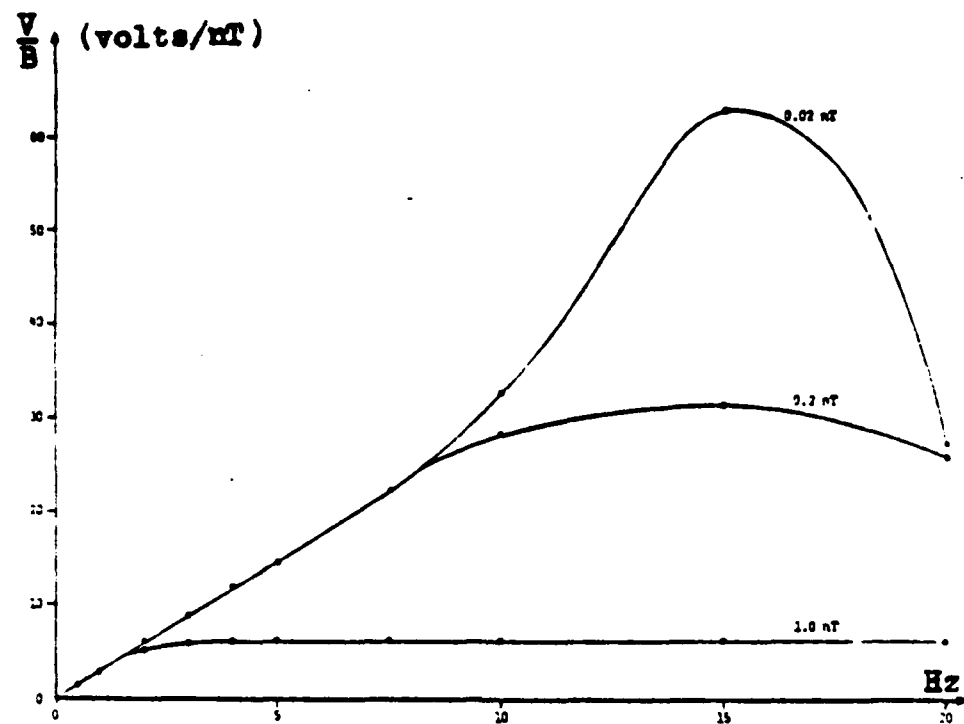
Figure 2.14   Land System Z-Coil Calibration
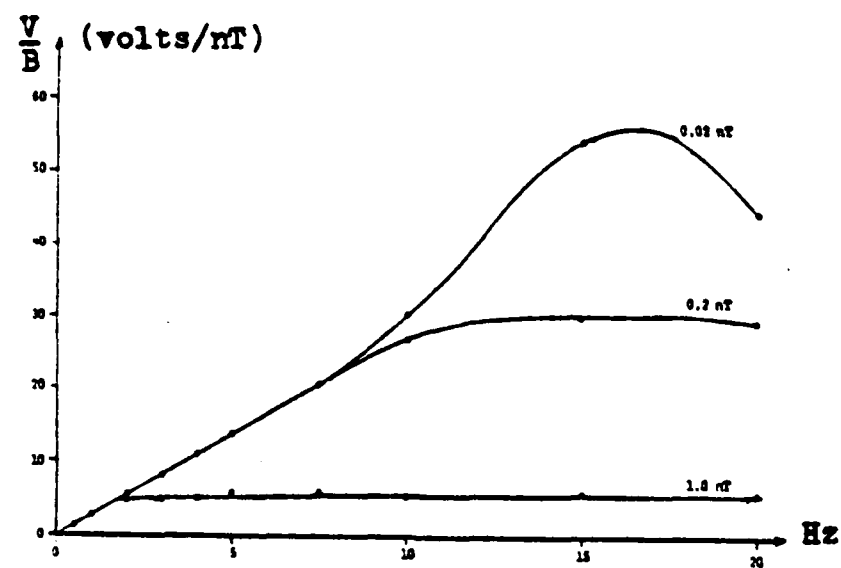
Figure 2.15   Ocean System X-Coil Calibration
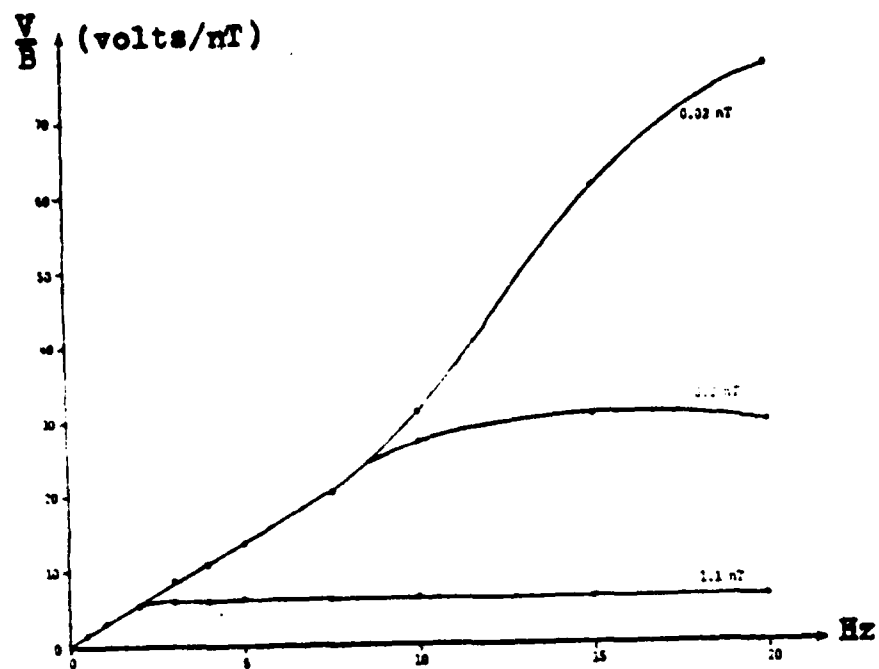
Figure 2.16   Ocean System Y-Coil Calibration

31

TABLE II

Transfer Function Computer Program

```
      CC 9 L=1,N
      FRC=FREC(L)
      IF(FRQ.LE.25.)GC TC 1
      XX(L)=XX(L)/28.
      GC TC 3
    1 IF(FRQ.LE.15.)GC TC 2
      XX(L)=XX(L)/(1C5.5-3.14*FRQ)
      YY(L)=YY(L)/(181.32-7.533*FRC)
      Z(L)=Z(L)/(177.2c-7.484*FRQ)
      GC TC 3
    2 IF(FRQ.LE.10.)GC TC 3
      XX(L)=XX(L)/(5.958*FRQ-3C.97)
      YY(L)=YY(L)/(7.166*FRQ-39.09)
      Z(L)=Z(L)/(6.49*FRC-32.35)
      GC TC 3
    3 IF(FRQ.LE.7.5)GC TC 4
      XX(L)=XX(L)/(3.492*FRQ-5.31)
      YY(L)=YY(L)/(4.252*FRQ-10.85)
      Z(L)=Z(L)/(4.044*FRC-7.39)
      GC TC 3
    4 IF(FRQ.LE.5.)GC TC 5
      XX(L)=XX(L)/(2.6311*FRQ+0.14667)
      YY(L)=YY(L)/(3.012*FRQ-1.65)
      Z(L)=Z(L)/(3.184*FRC-1.44)
      GC TC 6
    5 IF(FRQ.LE.3.)GC TC 6
      XX(L)=XX(L)/(2.6311*FRC+0.14667)
    7 YY(L)=YY(L)/(2.7C2*FRQ)
      Z(L)=Z(L)/(2.92*FRC)
      GC TC 9
    6 XX(L)=XX(L)/(2.72*FRC)
      GC TC 7
    8 CCNTINUE
    9 CCNTINUE
```

III. DATA EVALUATION

A. POWER SPECTRAL DENSITY AND ALIASING

The first step in the analysis of the data collected was the determination of the power spectral densities (PSD's) for each channel of the land and sea data. This was accomplished through the use of the computer program developed by J. M. Schweiger [Ref. 5]. After minor modification of this program, approximately twenty hours of real time data was evaluated. Samples of the PSD's are presented in Figures 3.1 to 3.5.

The overall value of the PSD's is in agreement with previous work conducted in this area. The PSD's have a decline of approximately -6 dB per octave from 0 to 5 Hz where they tend to decrease their rate of decline. Night PSD's tended to be 3 to 7 dB below the daytime level. This coincides with the findings of McDevitt and Homan (1980), M. W. Beard (1981) and A. C. Fraser-Smith and J. L. Buxton (1975), [Ref. 6].

One feature of the PSD's that differed from previous PSD's is the spike at 4 HZ in the land data. This was found to be "aliasing" of the 60 Hz power grid component by the PCM sampler. This experiment was conducted with a sample rate of 32 Hz; which, by the sampling theorem, should give a clear view of the frequency range of 0 to 10 Hz, when coupled with the 20 Hz cut-off filter in the amplifier,[Ref. 7]. The 60 Hz component of the geomagnetic field was measured by F. W. Clayton (1979) and found to be 4 (nT) /Hz, which is 10 higher than the surrounding data [Ref. 8]. The 20 Hz filter, built into the amplification system, would normally eliminate frequencies in this range but because of

33
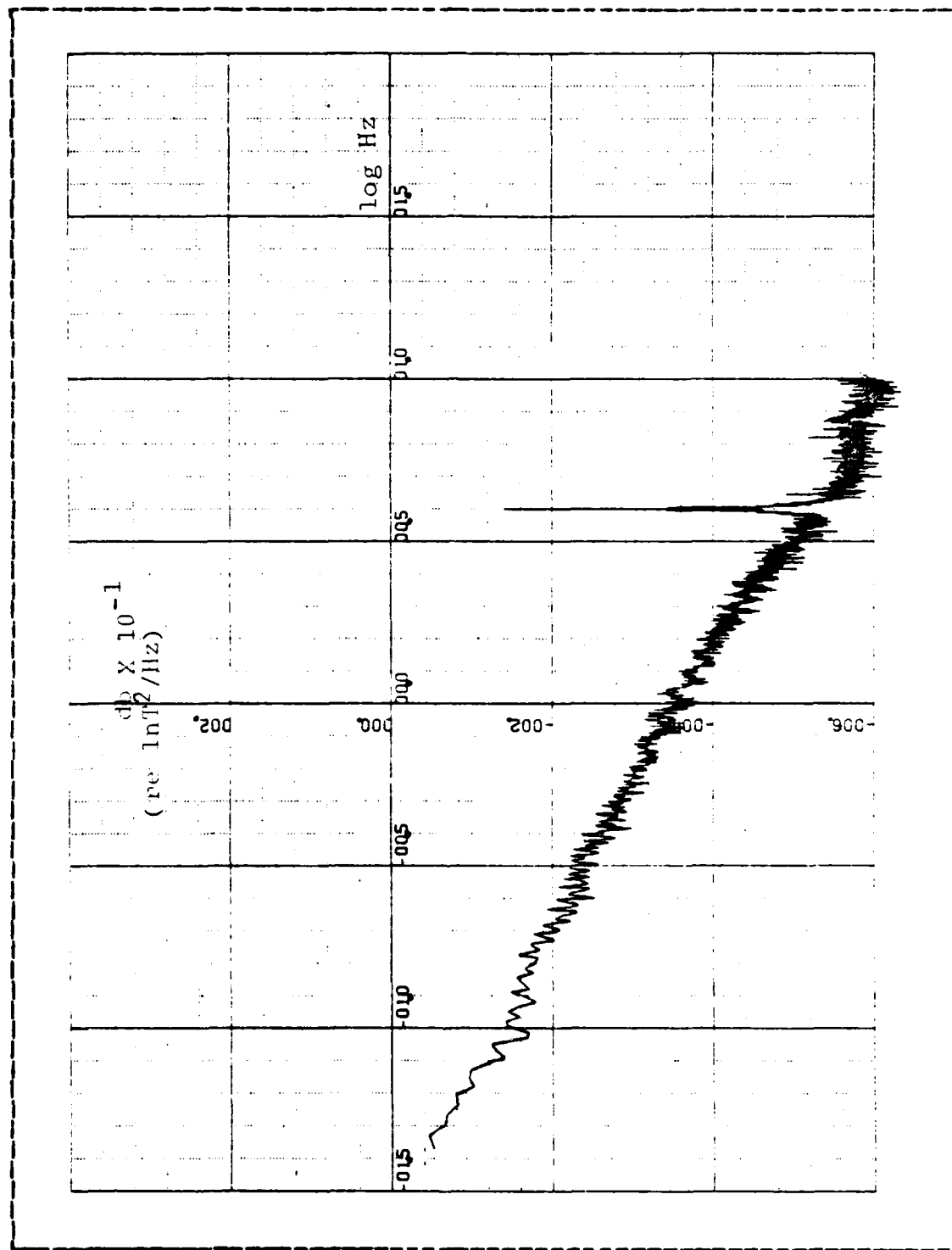
Figure 3.1   PSD, X-Coil, Land Data

34
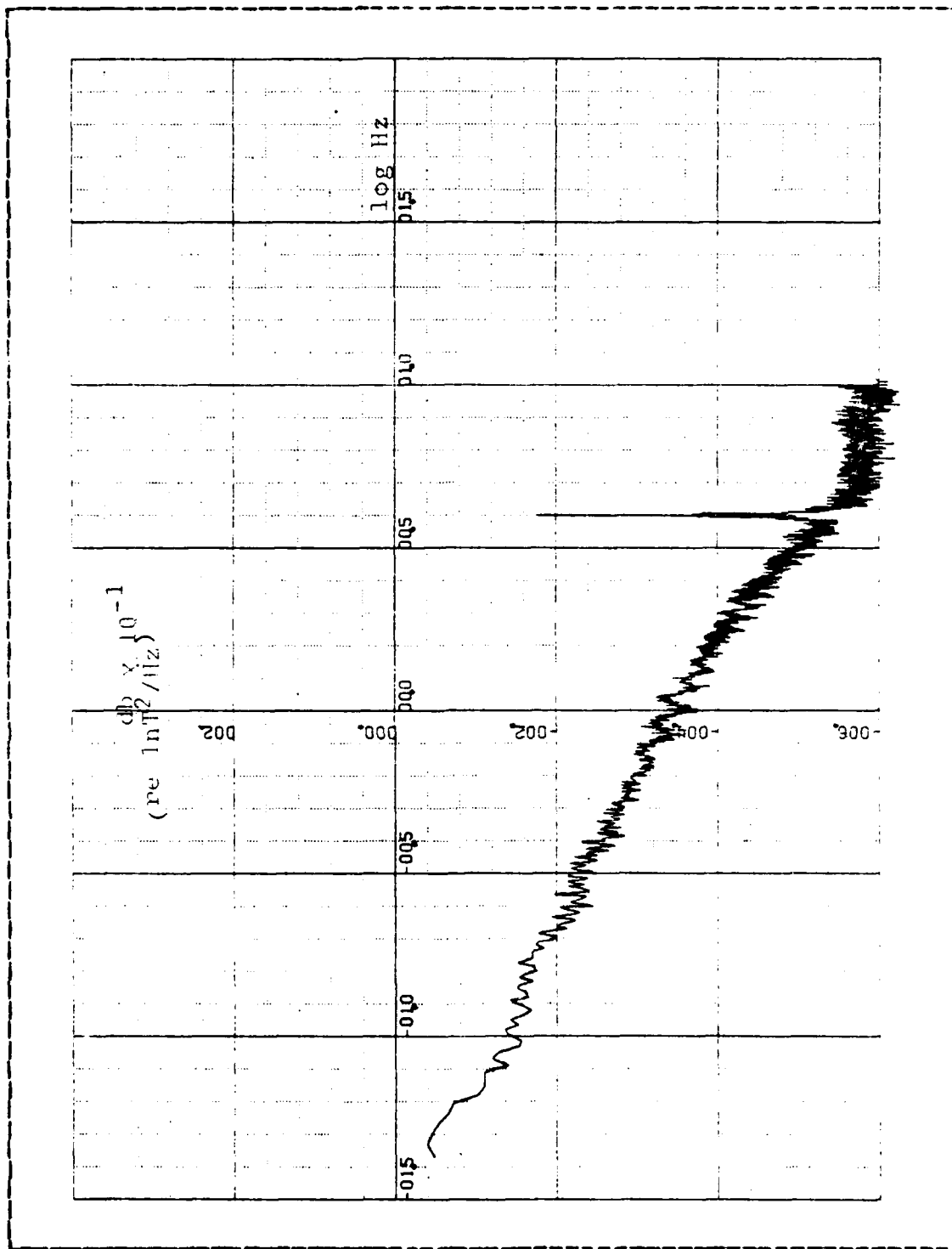
Figure 3.2   PSD, Y-Coil, Land Data

35
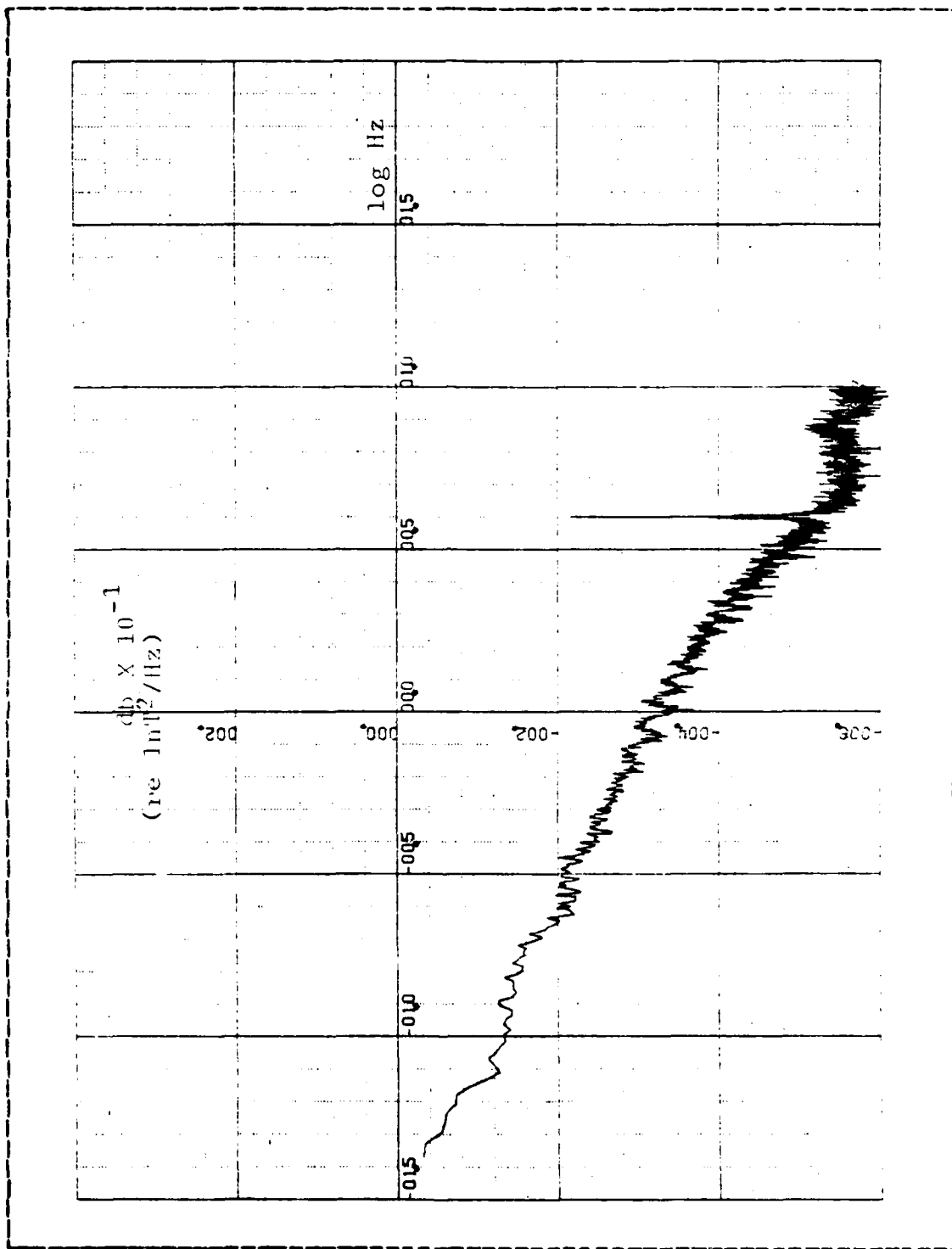
Figure 3.3   PSD, Z-Coil, Land Data
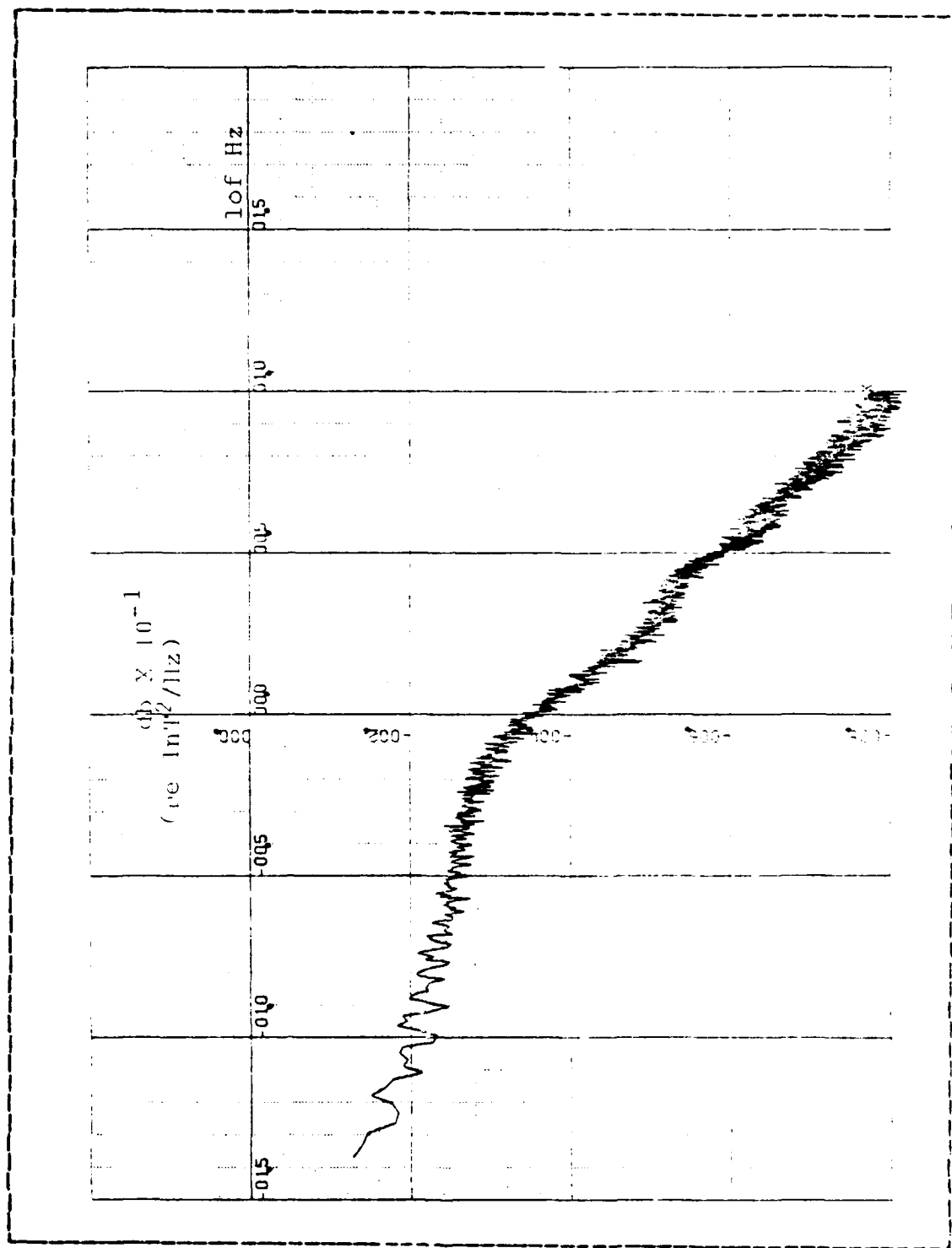
Figure 3.4   PSD, X-Coil, Sea Data

37
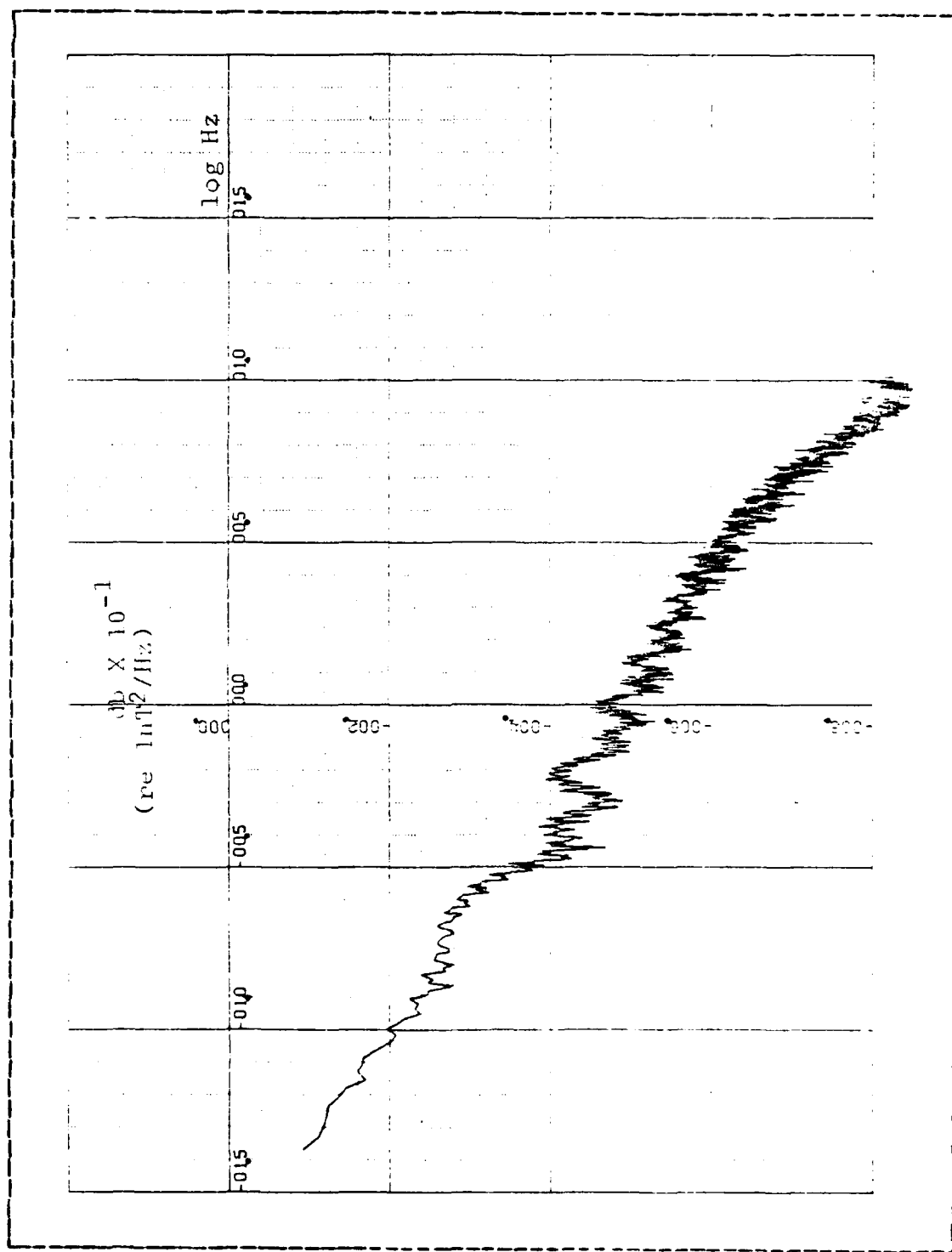
Figure 3.5   PSD, Y-Coil, Sea Data

38

the great differences in magnitude this does not happen.
When the 32 to 64 Hz range is convolved onto the 0 to 32 Hz
range the 60 Hz component will appear at 4 Hz. This destroys
the usefulness of the data in a small region about this
point.

Another point of interest is illustrated by the vertical
component of the sea data recorded on September 16, 1982,
Figure 3.5. During this experiment the Y-coil was oriented
in a vertical rather than the more normal horizontal direc-
tion. Examination of the data shows 10 to 15 dB decrease in
the PSD. This is in agreement with the theory that, because
of the ocean-air interface, geomagnetic waves propagate
vertically in the sea, thus eliminating this component.

B. STOKES PARAMETERS AND THEIR INTERPRETATION

After the collection of the data during June to
September of 1982, the problem of how to interpret it became
a prime concern. During the latter part of this period a
computer program was developed to determine the Power
Spectral Densities (PSD's) by J.M. Schweiger, October 1982,
[Ref. 5].

This program provided the basic structure to read the
data points off of magnetic data tape and, through the use
of a Fast Fourier Transform (FFT) routine and transfer func-
tions, to compute the geomagnetic fluctuations in the
frequency domain. This program provided the basic format
which was expanded and modified to produce other parameters.
The derivations of the equations for these parameters and
their interpretation comprise the remainder of this section.

The first parameter to be discussed is the coherence
between the different channels on land and sea. Coherence
gives a measure of the "singleness" of the source at the
various frequencies. "Singleness" in this context refers to
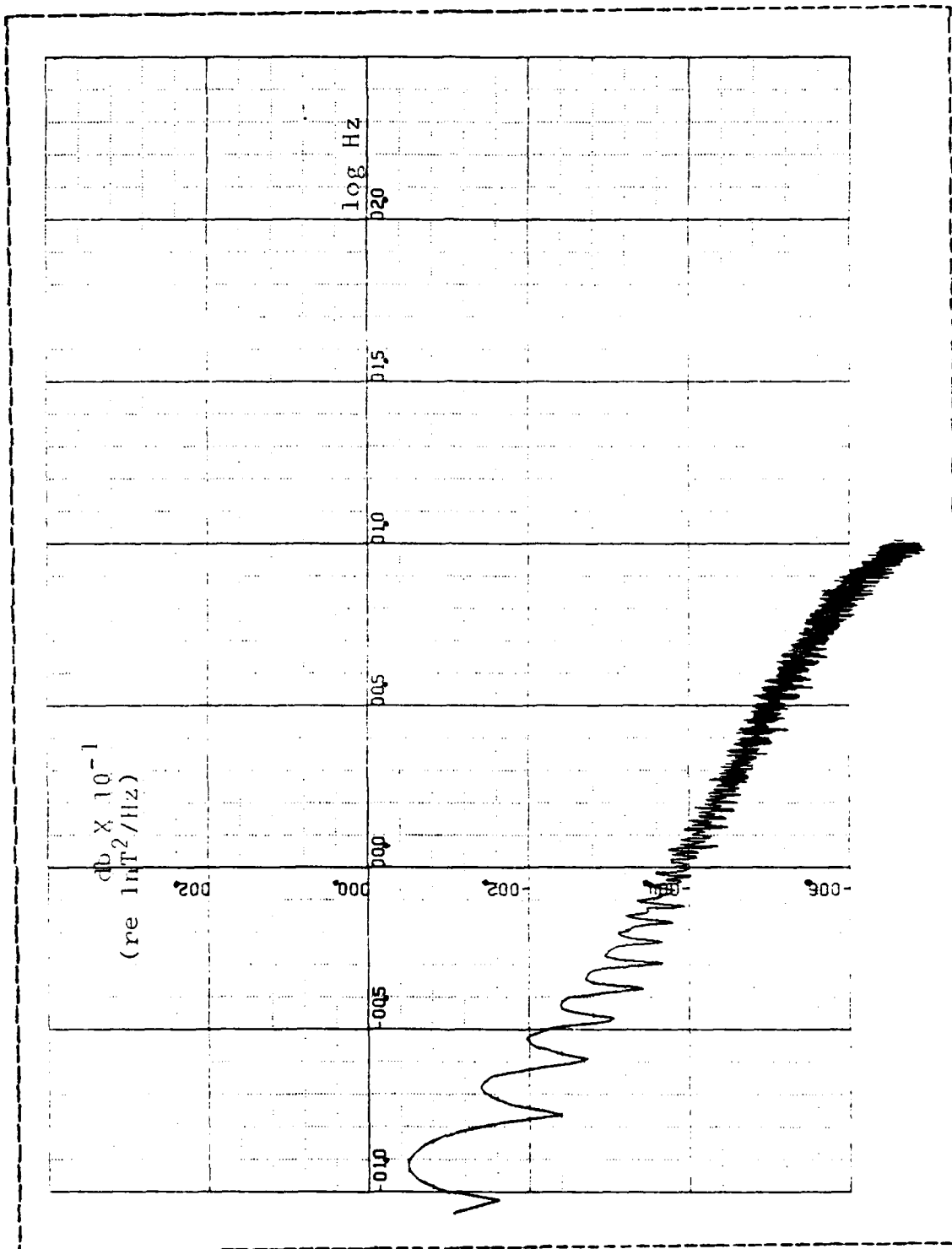
Figure 3.6   PSD, Vertical Component of Sea Data

what percentage of the intensity at a frequency can be said
to come from a single source. To compute the coherence one
first calculates the cross power spectral densities between
the channels. For a given pair of channels X and Y, the
cross power spectral density(S) is defined:

$$S_{xy}(f_j) = 1/N \sum_{n=1}^{N} X(f_j) Y(f_j)$$

In this equation N is the number of blocks of data sent
through the FFT and averaged; $X(f_j)$ and $Y(f_j)$ are the FFT's
along the appropriate axis. The coherence(Γ_{xy}) is defined
as:

$$\Gamma_{xy}(f_j) = \frac{S_{xy}(f_j)}{(S_x(f_j) S_y(f_j))} .$$

For the land data coherences were also determined for the
Y-Z plane and the Z-X plane. Figures 3.7 and 3.8 show
typical land and sea coherences, with all coils oriented in
the horizontal plane. Note that on the land the coherence
stays very close to its maximum value of one until approxi-
mately 7-8 Hz and then starts to decrease while in the case
of the sea data there is more structure at the lower
frequencies. This type of behavior is typical of most of the
data, although the exact frequency of the decline varies.

In addition to coherence, Stokes parameters may be
computed from the auto-spectral densities and cross-spectral
densities. They can be used to interpret the geomagnetic
waves on a bi-Linear basis, a bi-Circular basis or an ellip-
tical basis.

Although other notations are utilized for the Stokes
parameters, the most common notation; s0, s1, s2, s3; will
be employed here [Ref. 9]. The general form of the Stokes
parameters are:

41
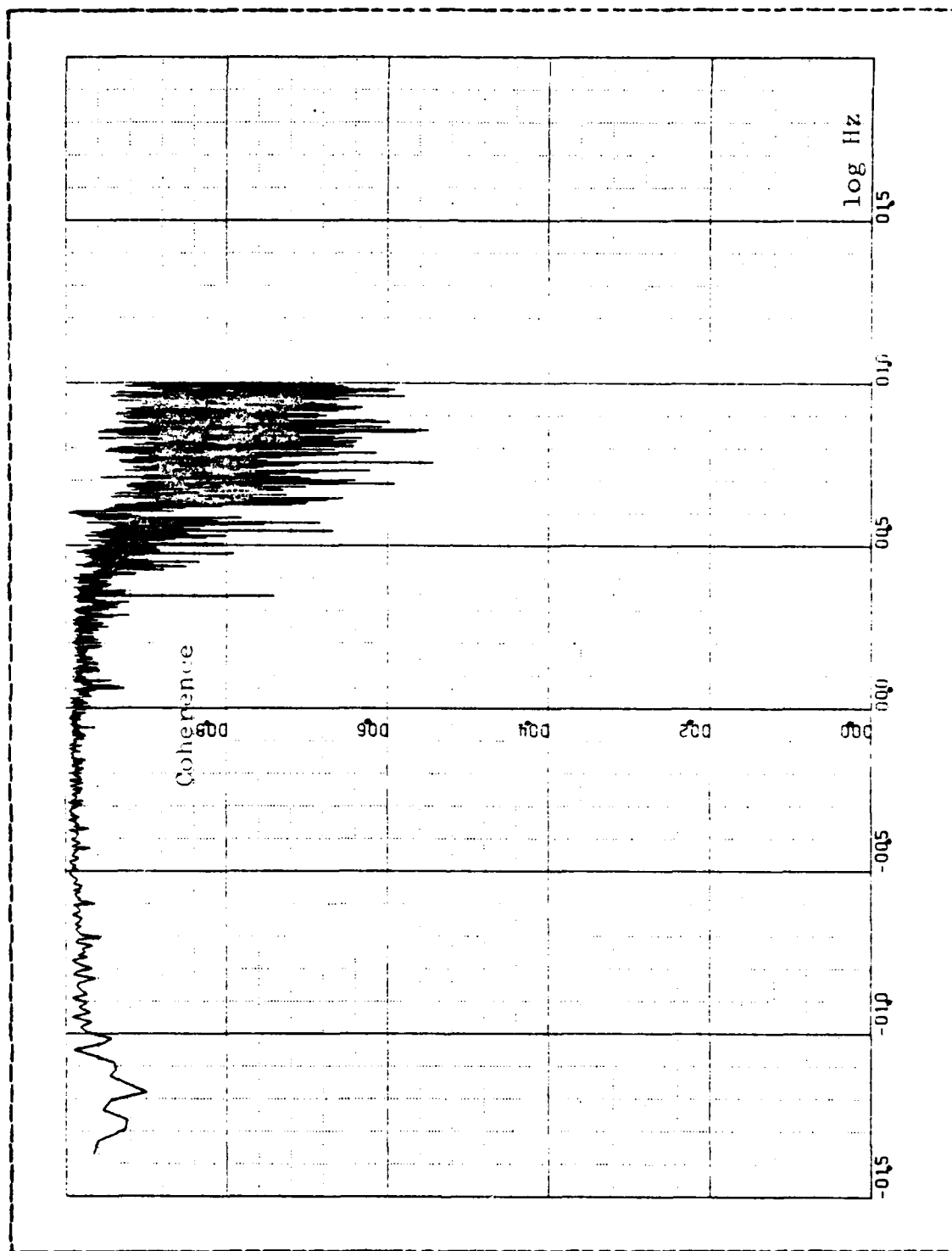
Figure 3.7 Land Coherence, X Vs Y Channels
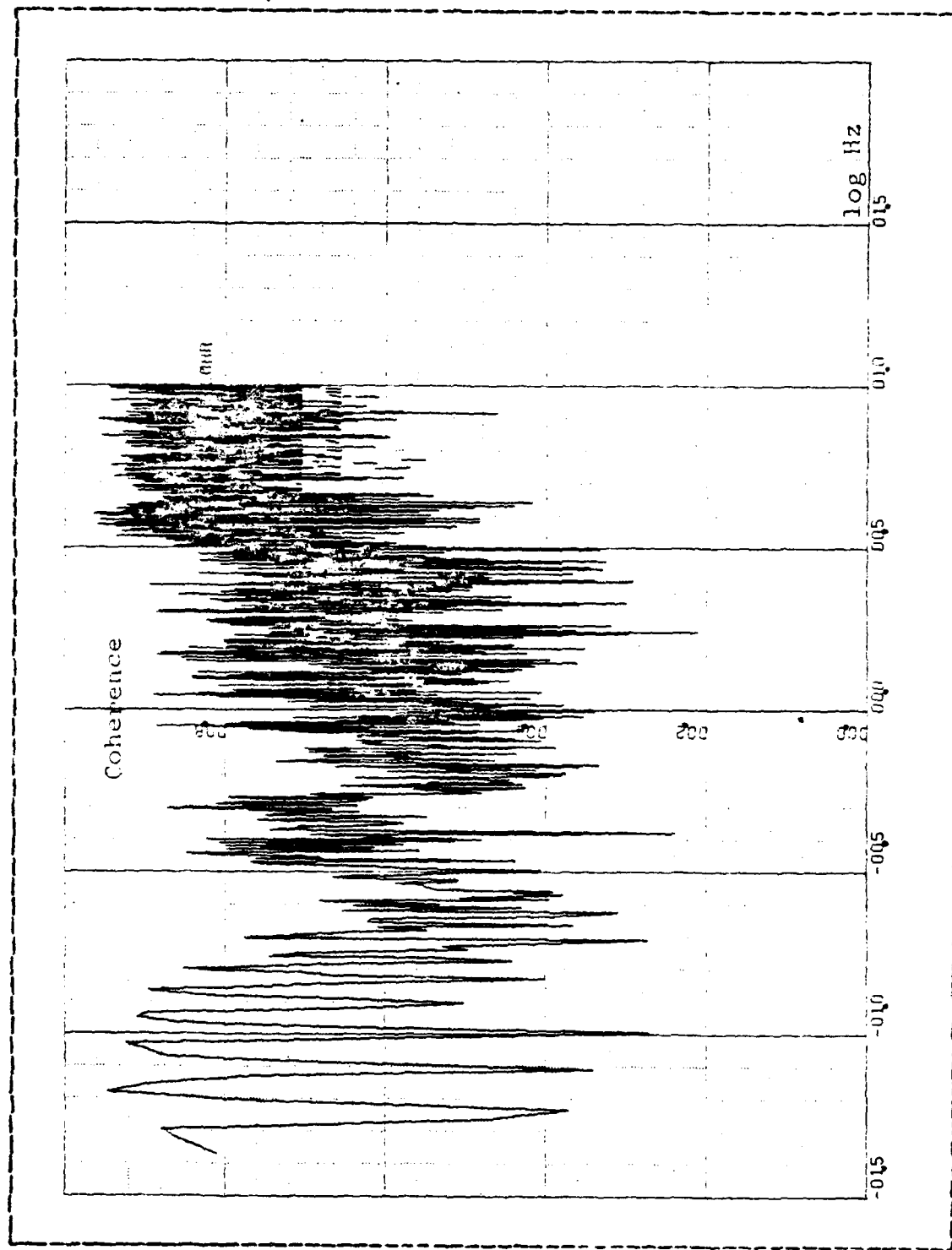
Figure 3.8   Sea Coherence, X Vs Y Channels

43

$$s0 = \langle a1^2 \rangle + \langle a2^2 \rangle$$
$$s1 = \langle a1^2 \rangle - \langle a2^2 \rangle$$
$$s2 = 2\langle a1 a2 \cos\delta \rangle$$
$$s3 = 2\langle a1 a2 \sin\delta \rangle$$

where a1 and a2 are the instantaneous amplitude of the orthogonal components of the magnetic vector and δ is their phase difference. In terms of the auto- and the cross-spectral densities the Stokes parameters can be written:

$$s0 = 2(S_x + S_y)$$
$$s1 = 2(S_x - S_y)$$
$$s2 = 4\,\mathrm{Re}(S_{xy})$$
$$s3 = 4\,\mathrm{Im}(S_{xy})$$

It must be noted that the Stokes parameters were developed originally to describe monochromatic light and can only be applied to our problem after the data has been transformed to the frequency domain.

The bi-Linear basis interpretation of the Stokes parameters can be seen by examining a superposition of two orthogonal linearly polarized waves [Ref. 10]. Computing the Stokes parameters in this basis yields:

$$s0 = 1/2\,(B_x^2 + B_y^2)$$
$$s1 = 1/2\,(B_x^2 - B_y^2)$$
$$s2 = B_x B_y \cos(\theta_x - \theta_y)$$
$$s3 = B_x B_y \sin(\theta_x - \theta_y)$$

Another basis useful for interpretation is the bi-Circular basis. This basis is represented by the superposition of two counter-rotating circularly polarized waves. In this basis the Stokes parameters are:

$$s0 = B_+^2 + B_-^2$$

44
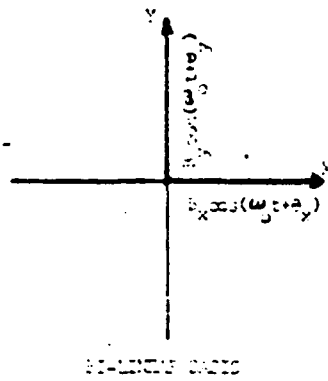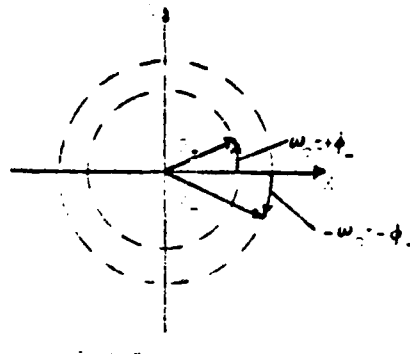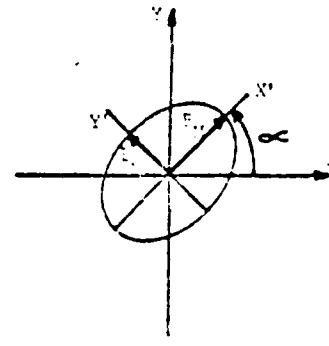
Figure 3.9   Basis for Interpretation

$$s1 = 2B_+ B_- \cos(\phi_+ - \phi_-)$$
$$s2 = 2B_+ B_- \sin(\phi_+ - \phi_-)$$
$$s3 = B_+^2 - B_-^2$$

A final basis of interpretation is the elliptical basis. In this case the basis is modeled by the major and minor axis vectors and the angle formed between the X-axis and the major axis of the ellipse. From this basis the Stokes parameters are:

$$s0 = 1/2\,(B_M + B_m)$$
$$s1 = 1/2\,(B_M - B_m)\cos 2\alpha$$
$$s2 = 1/2\,(B_M - B_m)\sin 2\alpha$$
$$s3 = B_M B_m$$

45

The important point to note from these different basis
sets is that for a given wave form (linear, elliptical, or
cicular) the Stokes parameters, as computed from the spec-
tral densities, are the same in any basis in which they are
computed. This can be easily visualized by taking a circu-
larly or linearly polarized wave and determining the value
of the Stokes parameters in each basis. It seems that these
interpretations are most easily visualized in the elliptical
basis. Consequently, in addition to the Stokes parameters
the angle α was computed to make the interpretation easier.
This angle was calculated from the Stokes parameters s1 and
s2 by the equation:

$$\alpha = 1/2 \; \arctan(s2/s1)$$

Examples of the results of the calculations of the Stokes
parameters and the angle α for land and sea data are
displayed in Figures 3.10 to 3.19. Note that s1, s2, and s3
are normalized by dividing by s0. In addition, for the land
data, the same graphs were produced for the Y-Z plane and
the Z-X plane.

The use of Stokes parameters is based on monochromatic
and polarized waves. To determine the applicability to our
data of the Stokes parameters the degree of polarization
must be found. For a perfectly polarized monochromatic wave

$$s0^2 = s1^2 + s2^2 + s3^2.$$

If the wave is partially polarized then s0 becomes greater
than the sum of the squares of the other three [REF.9]. To
determine how close to the polarized case the data lies, the
degree of polarization (P) can be calculated. It is defined
by,

$$P = \frac{(s1^2 + s2^2 + s3^2)^{1/2}}{s0}.$$

46

Figure 3.10   Land SO, X-Y Plane

47
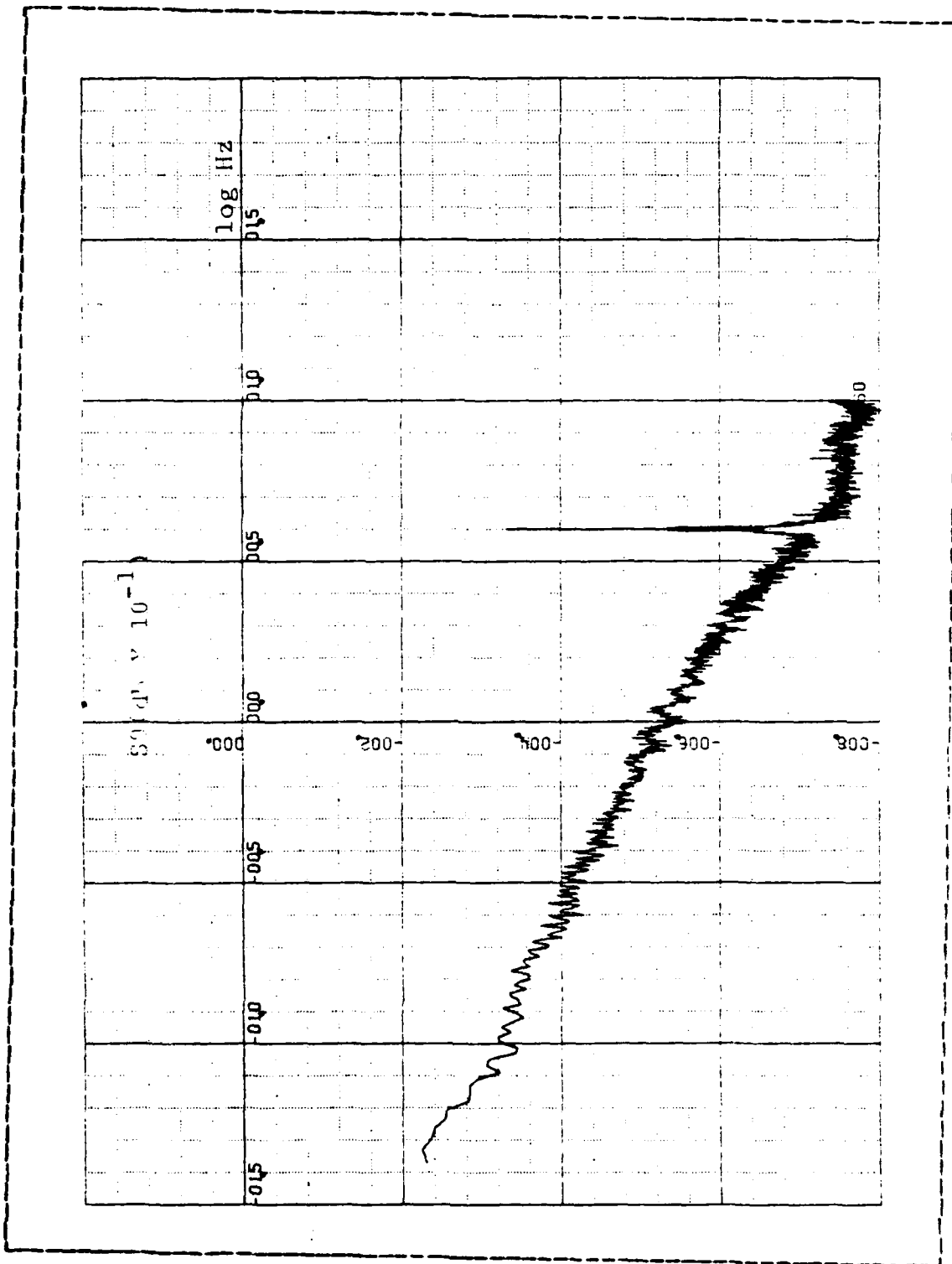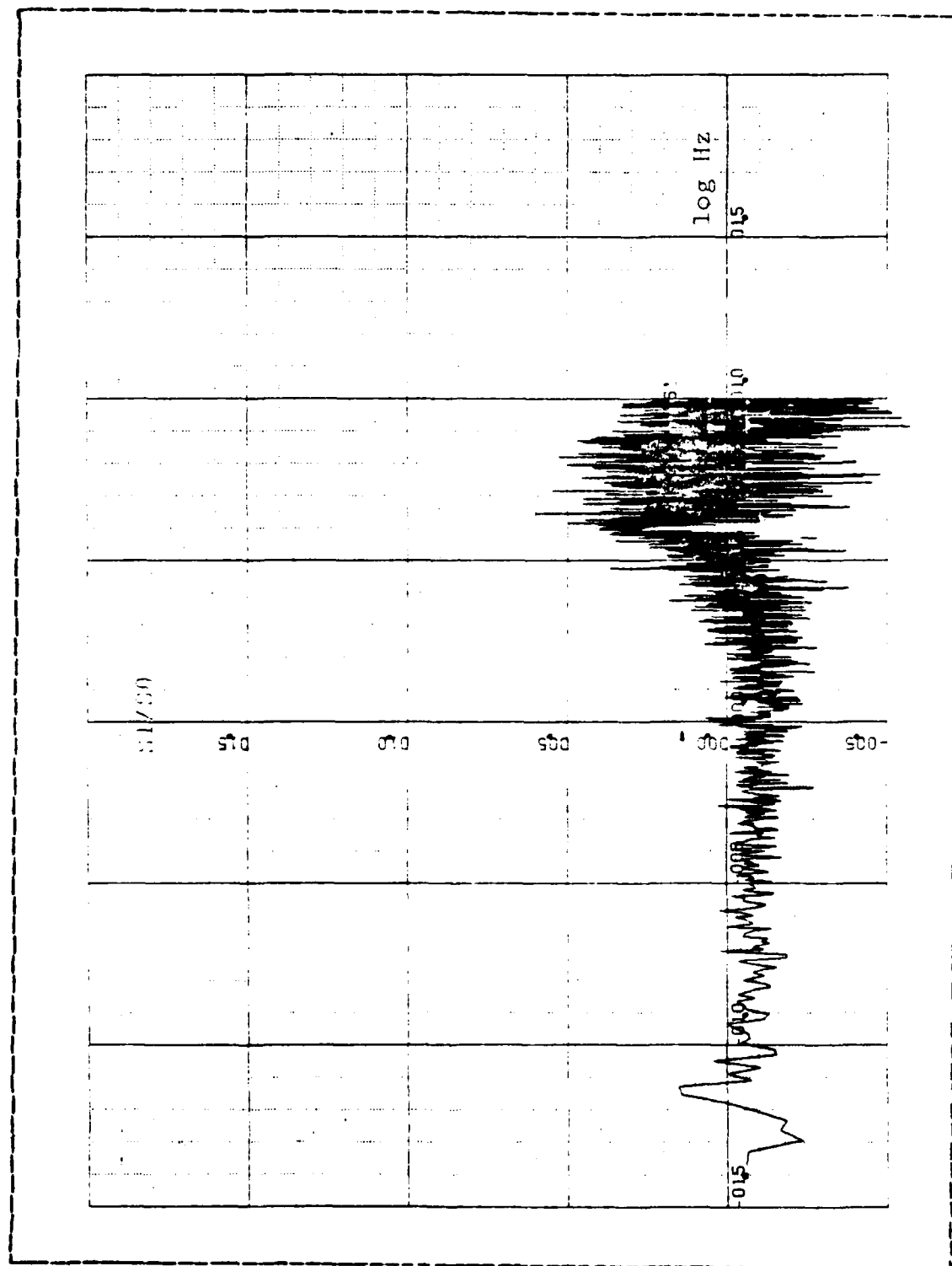
Figure 3.11   Land S1/S0, X-Y Plane
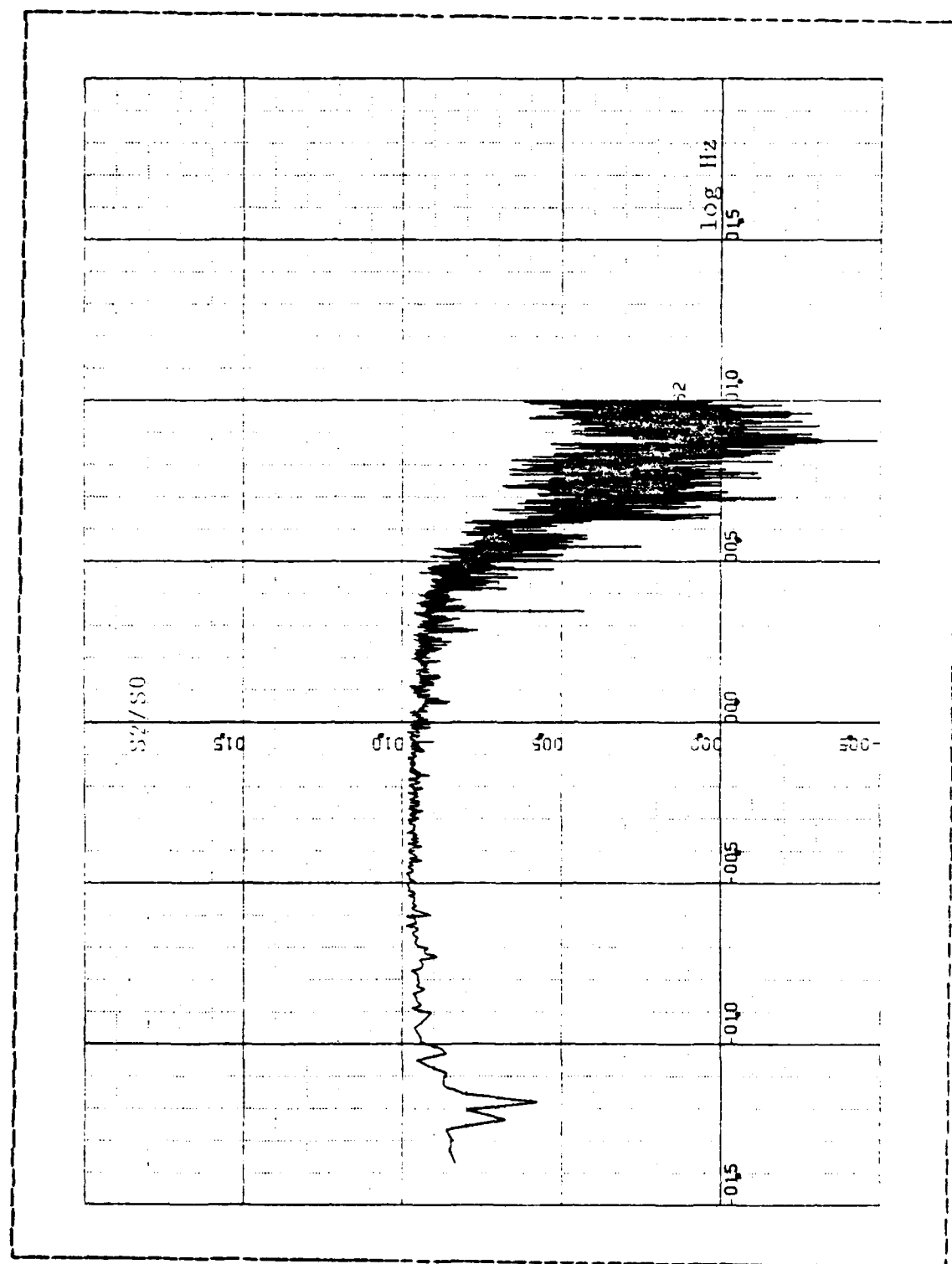
Figure 3.12   Land S2/S0, X-Y Plane

49
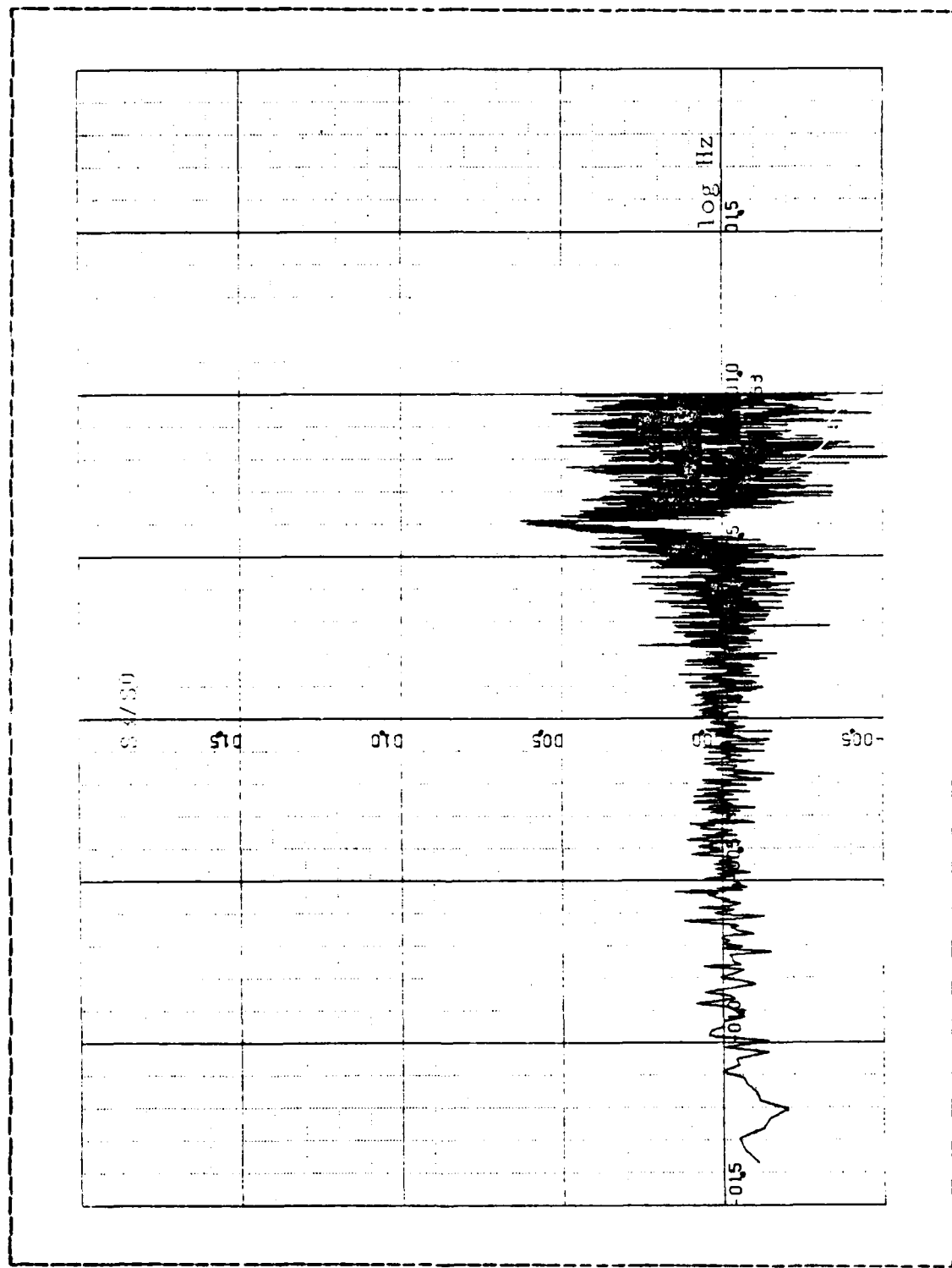
Figure 3.13   Land S3/S0, X-Y Plane
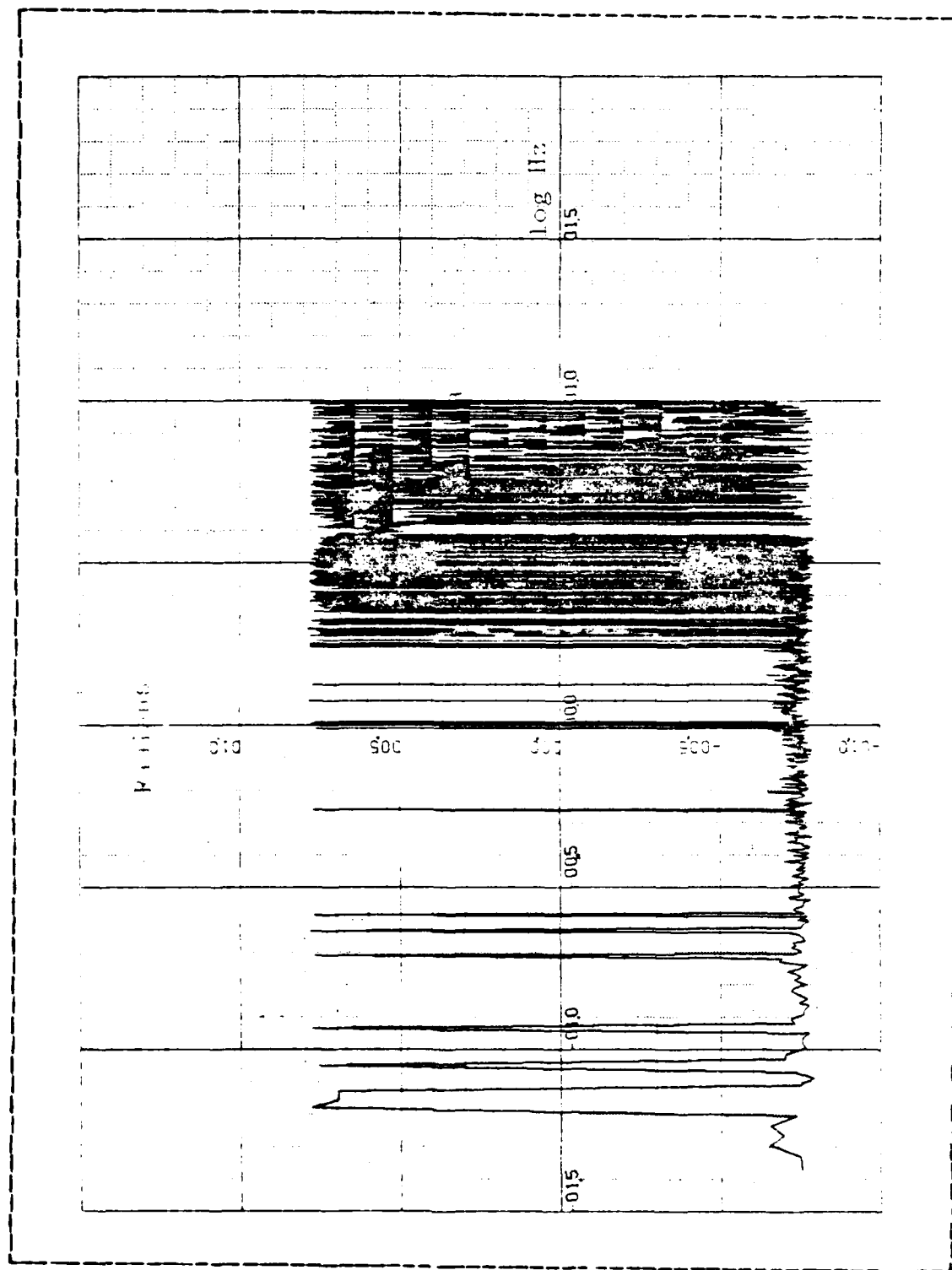
Figure 3.14   Land Angle ∝, X-Y Plane

51

Figure 3.15   Sea SO, X-Y Plane

52
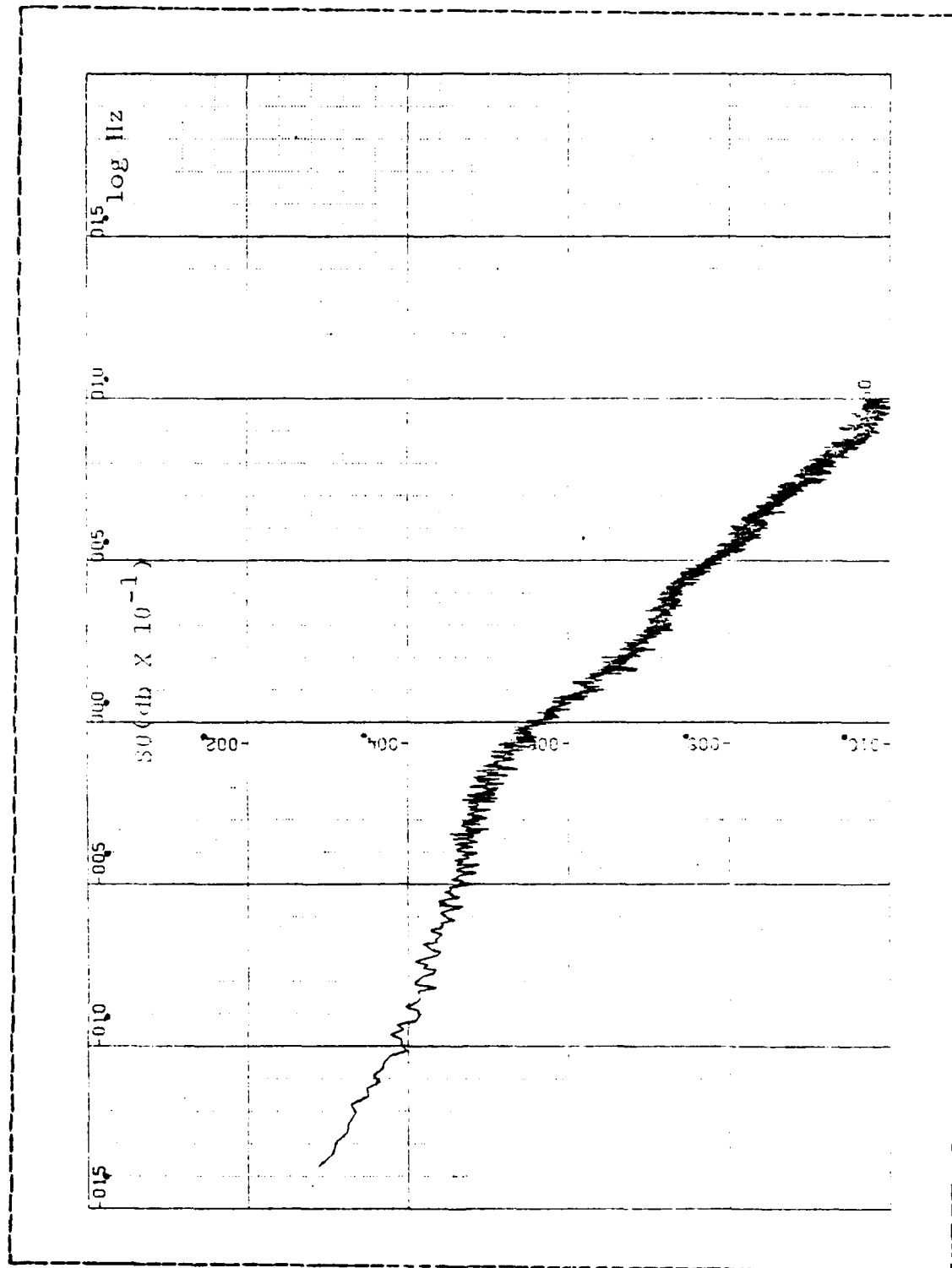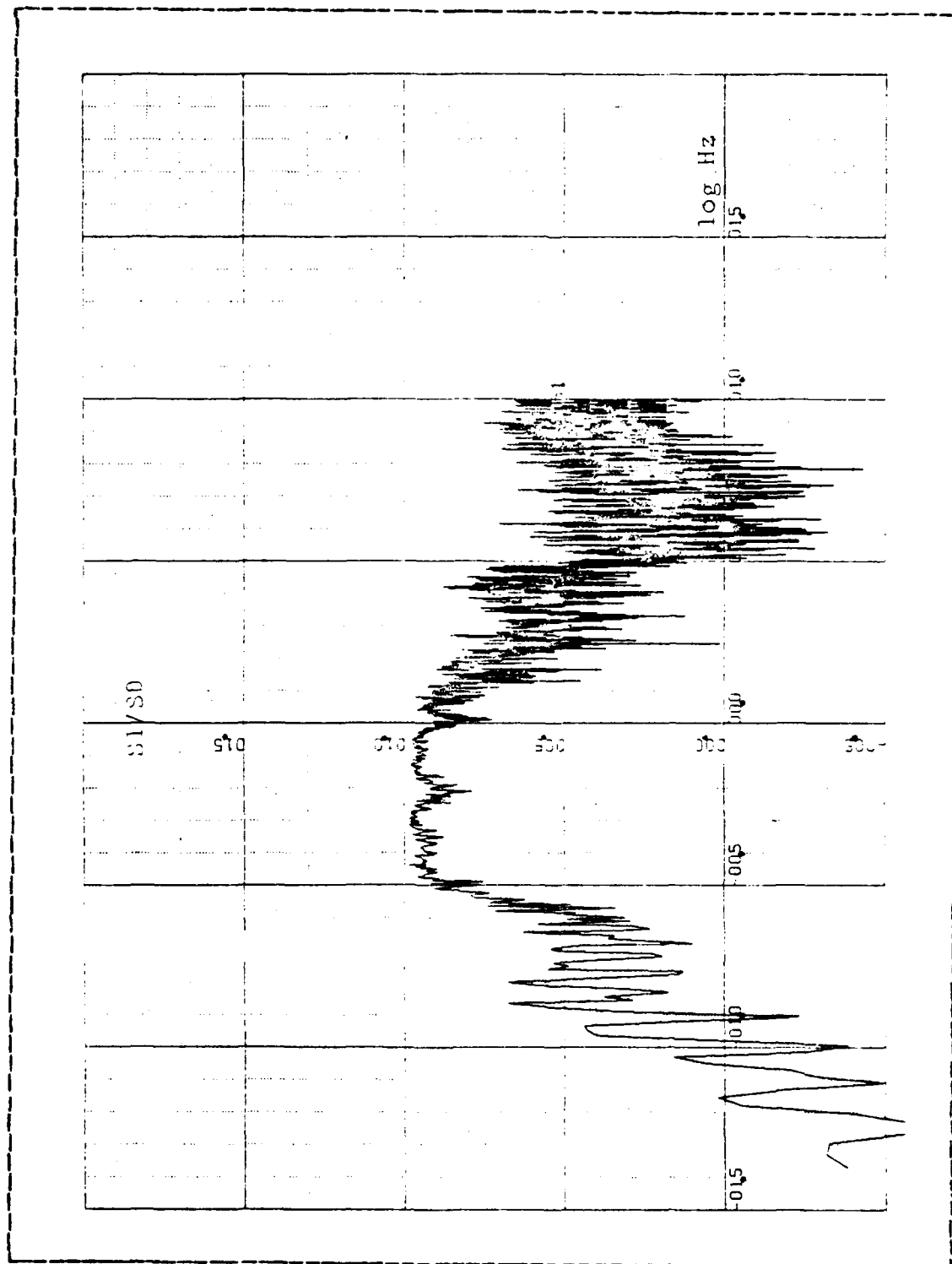
Figure 3.16   Sea S1/S0, X-Y Plane
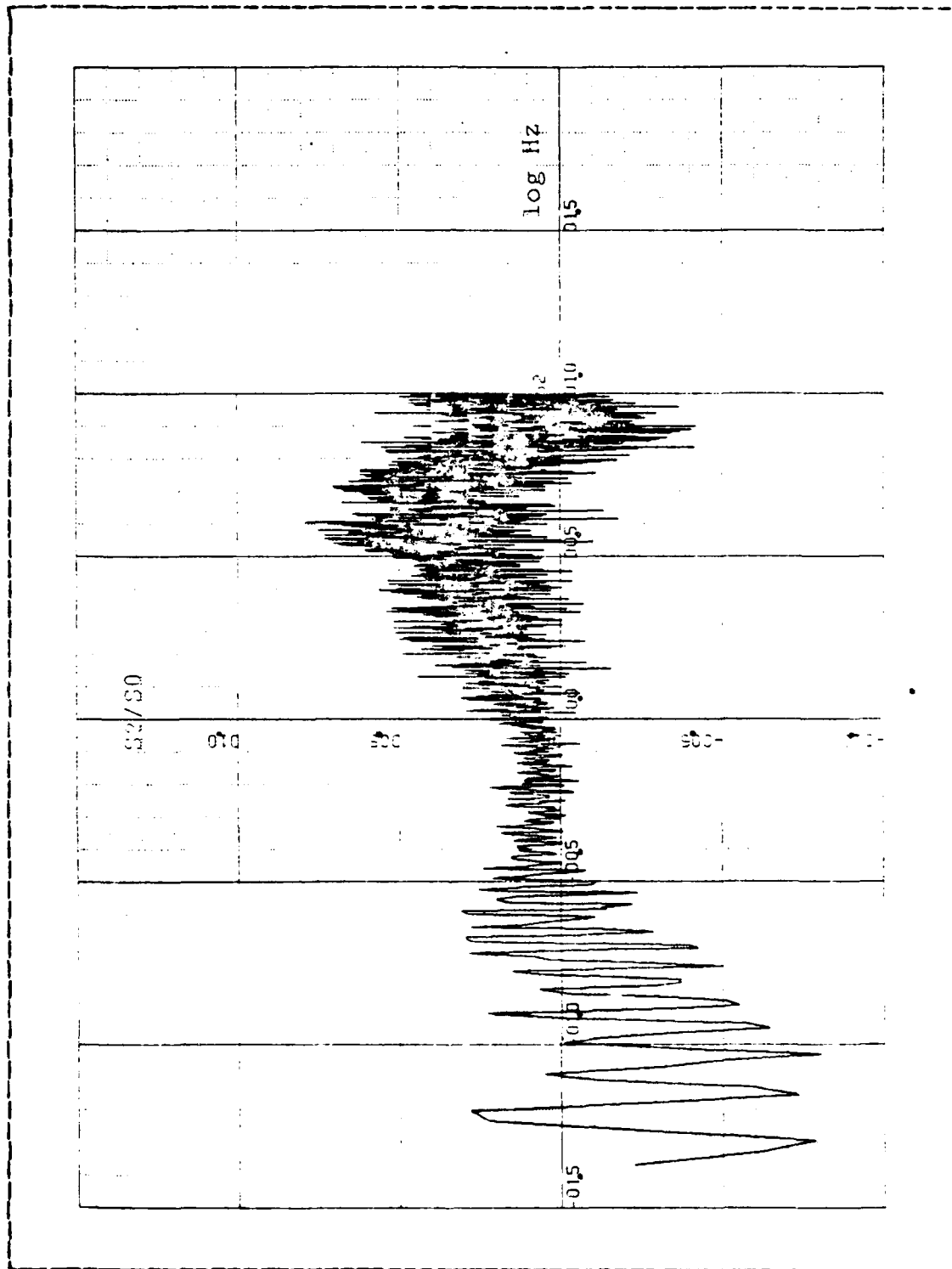
Figure 3.17   Sฑa S2/S0, X-Y Plan
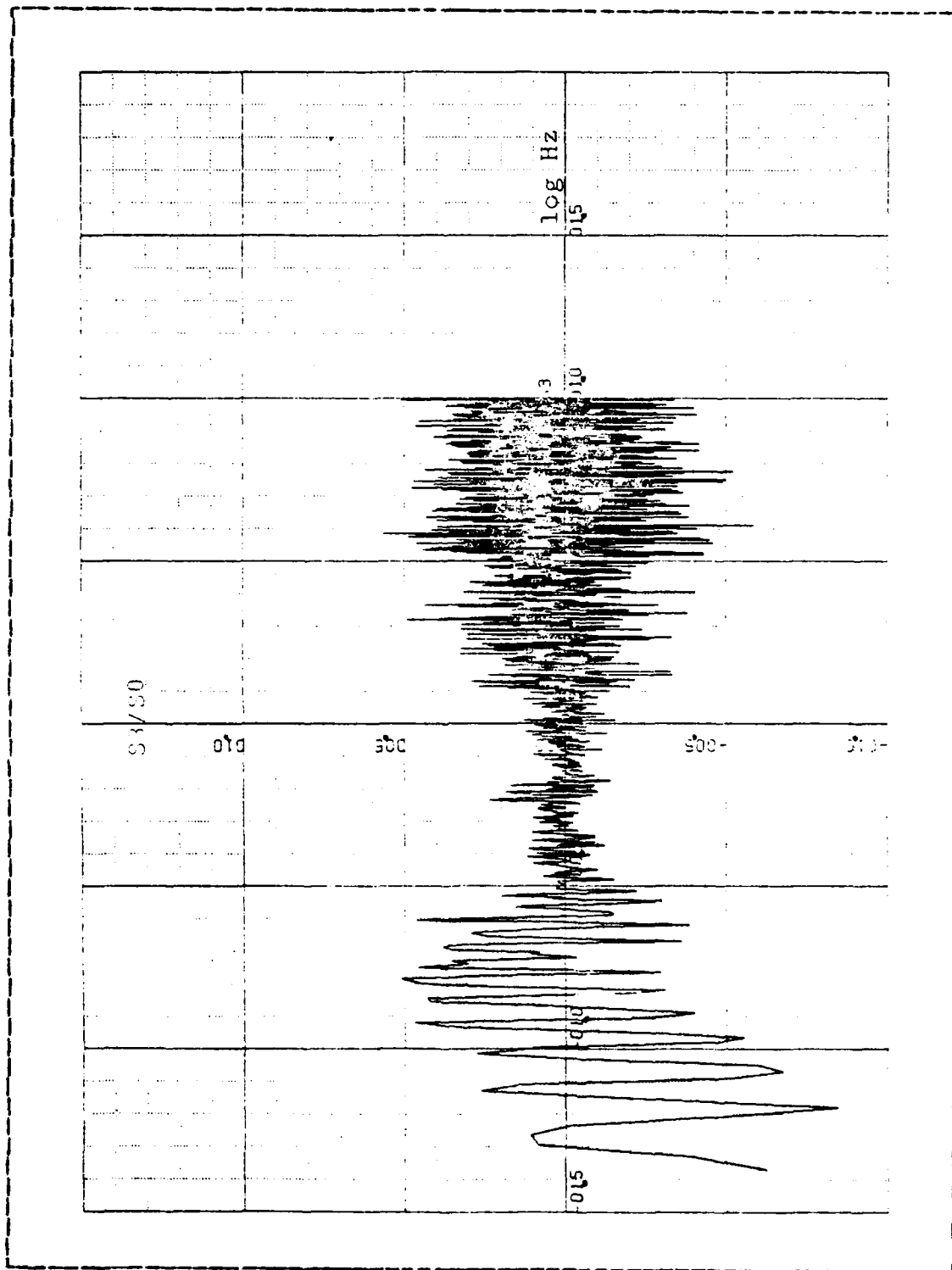
Figure 3.18   Sea S3/S0, X-Y Plane
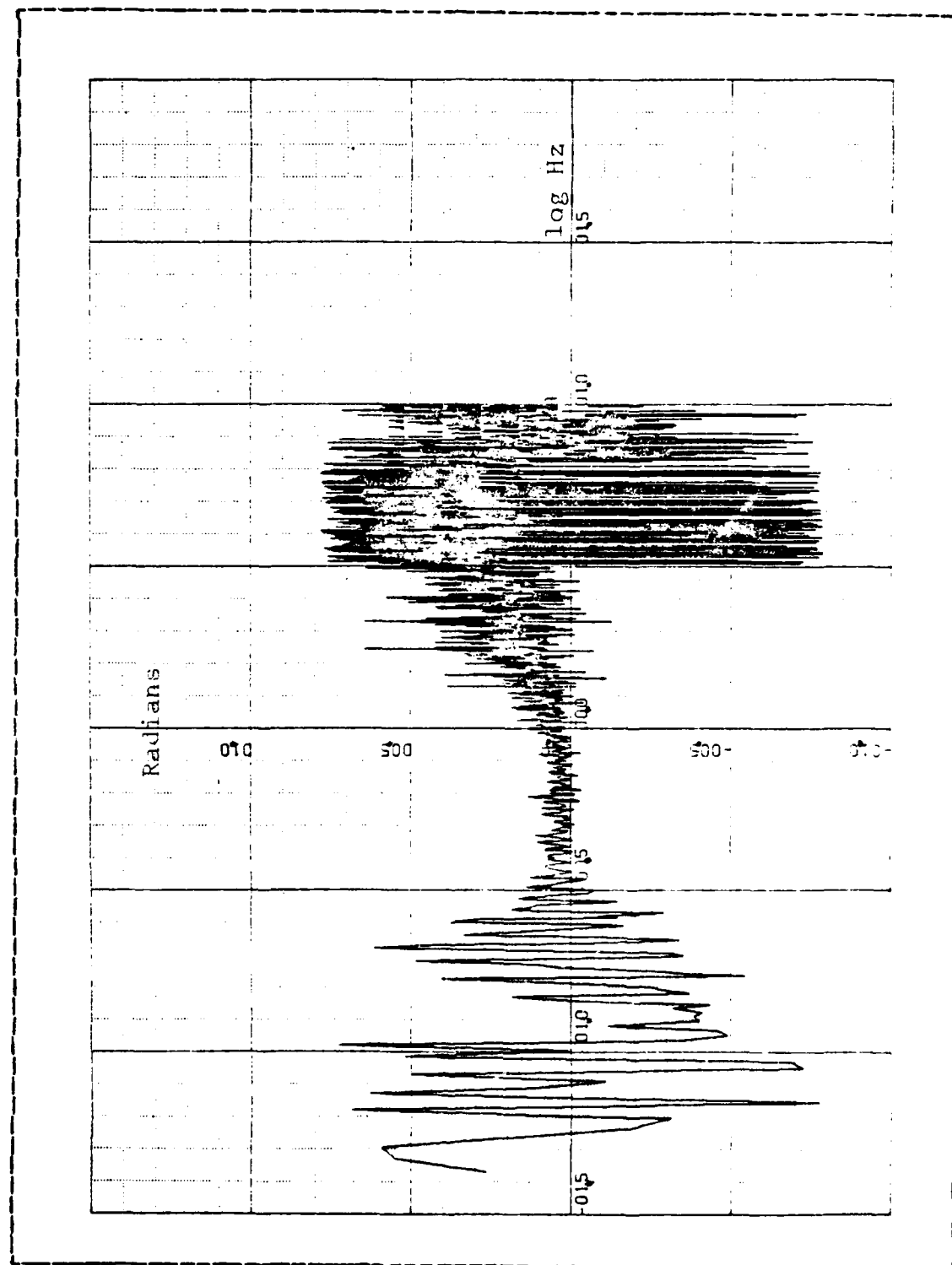
Figure 3.19   Sea Angle α, X-Y Plane

If P is one then the wave is perfectly polarized and any analysis based on the Stokes parameters will be completely accurate.

For values of P less than one the analysis is correspondingly less valid. However, factors that depend only on s1, s2, and s3, such as the angle α and the ellipticity, are not effected by low values of P. In such regions the noise level is much higher and the data is not easily interpreted.

The land and sea data vary in their values of P depending on the time of day and other unknown factors. In general they both show a high degree of polarization through 3 Hz while above this frequency a marked drop off occurs. It was also noted that in the land data the degree of polarization is virtually identical in all three planes. This is apparently due to the fact that the polarization was not oriented along any of the three sensing axis and therefore the proportion of the total intensity that resulted from polarized waves remained relatively constant. (See Figures 3.20-3.23)

One final tool of interpretation of the data is the ellipticity of the wave (E). The ellipticity is defined by the major and minor axis of the ellipse,[Ref. 3]. Specifically E is defined by:

$$\tan E = B_m/B_M$$

This can also be written in terms of the Stokes parameters as:

$$E = 1/2 \arcsin(s3/(s1^2 + s2^2 + s3^2)^{\frac{1}{2}})$$

where E varies from $\pi/4$ to $-\pi/4$. The interpretation of E is illuminated by considering its dependence on s3 and the elliptical basis. If E is zero then the minor axis is zero which means the polarization of the wave is linear. At $E = \pi/4$

57

Figure 3.20   Degree of Polarization, Land, X-Y Plane
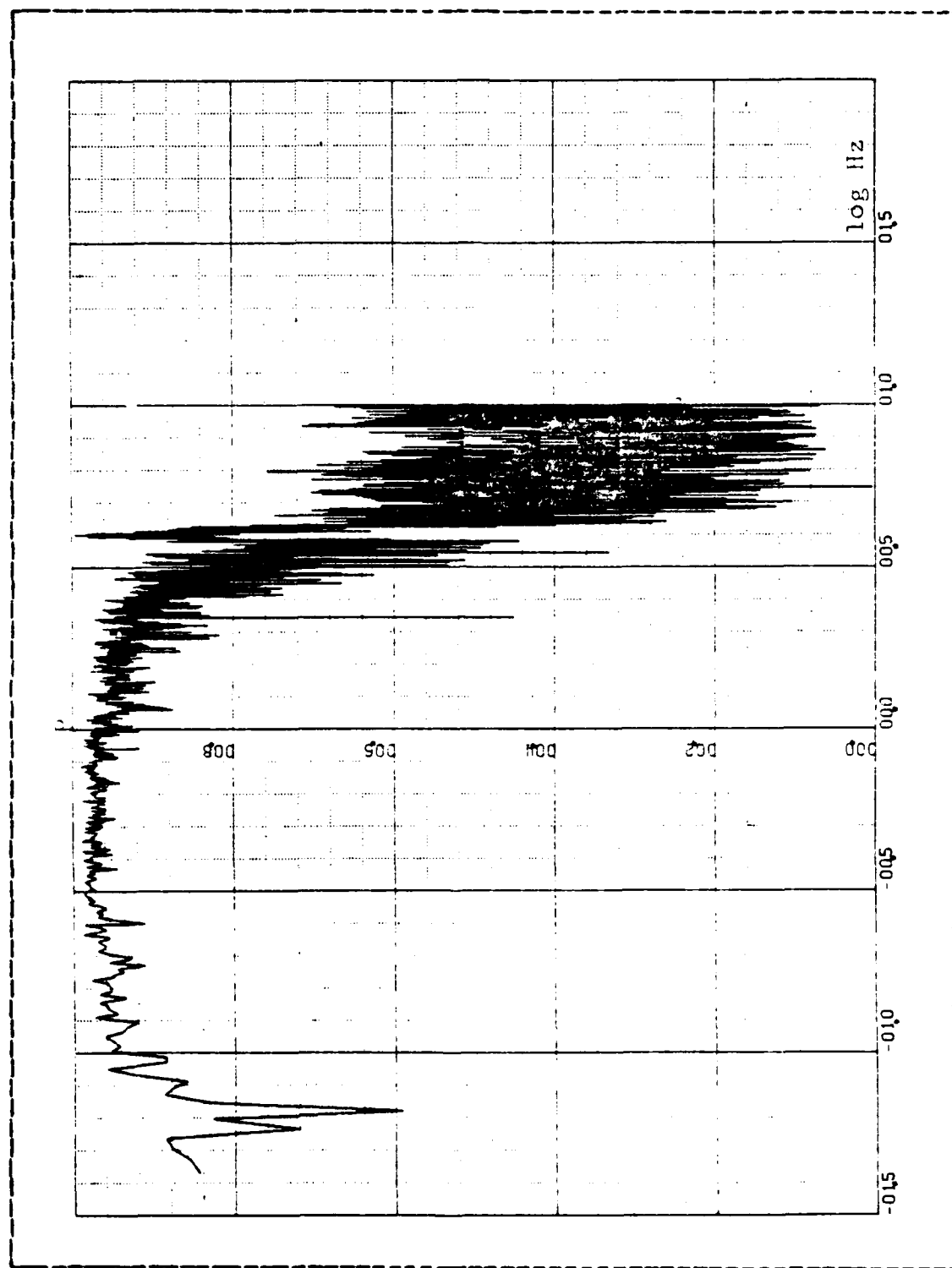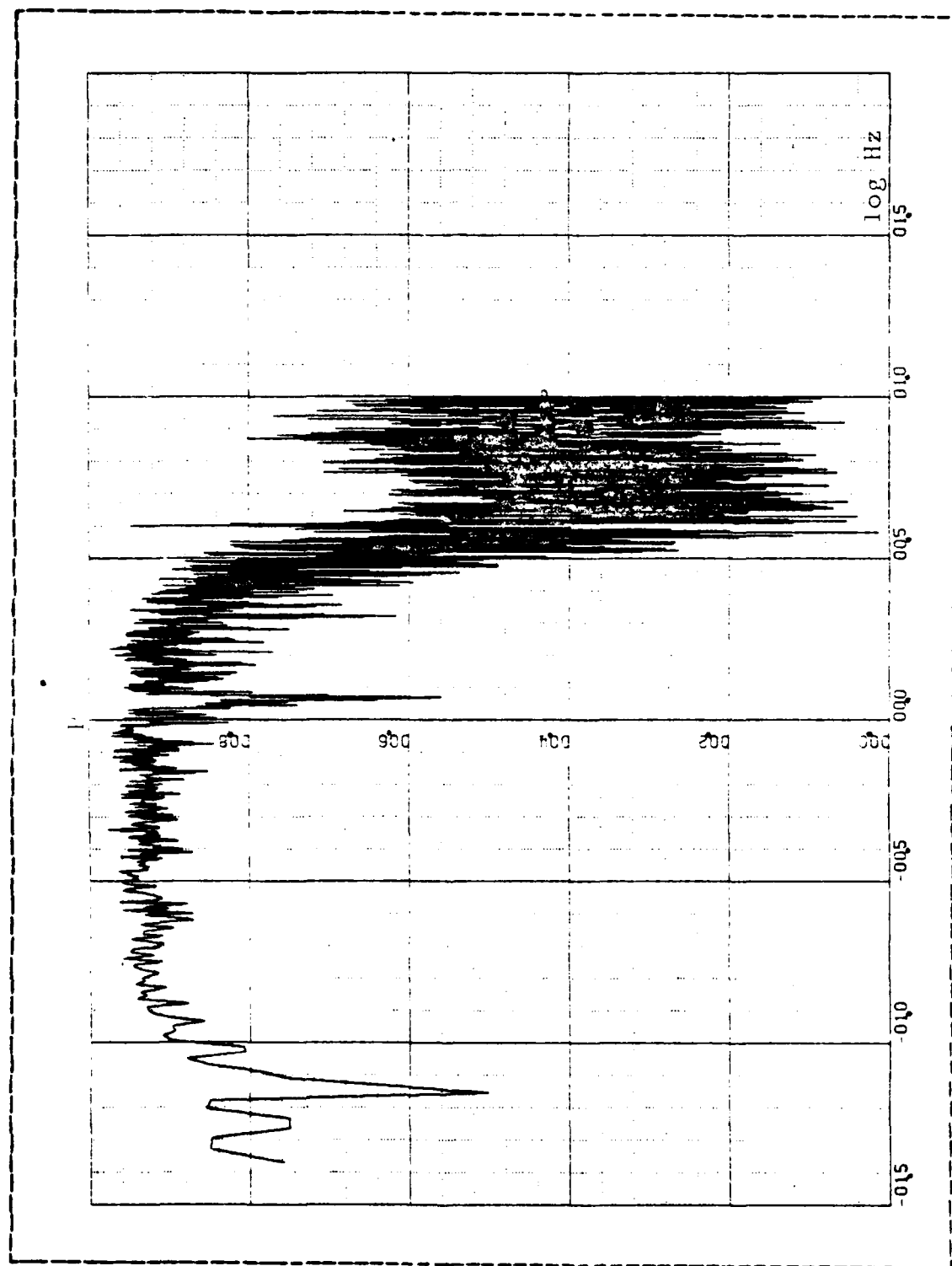
Figure 3.21   Degree of Polarization, Land, Y-Z Plane
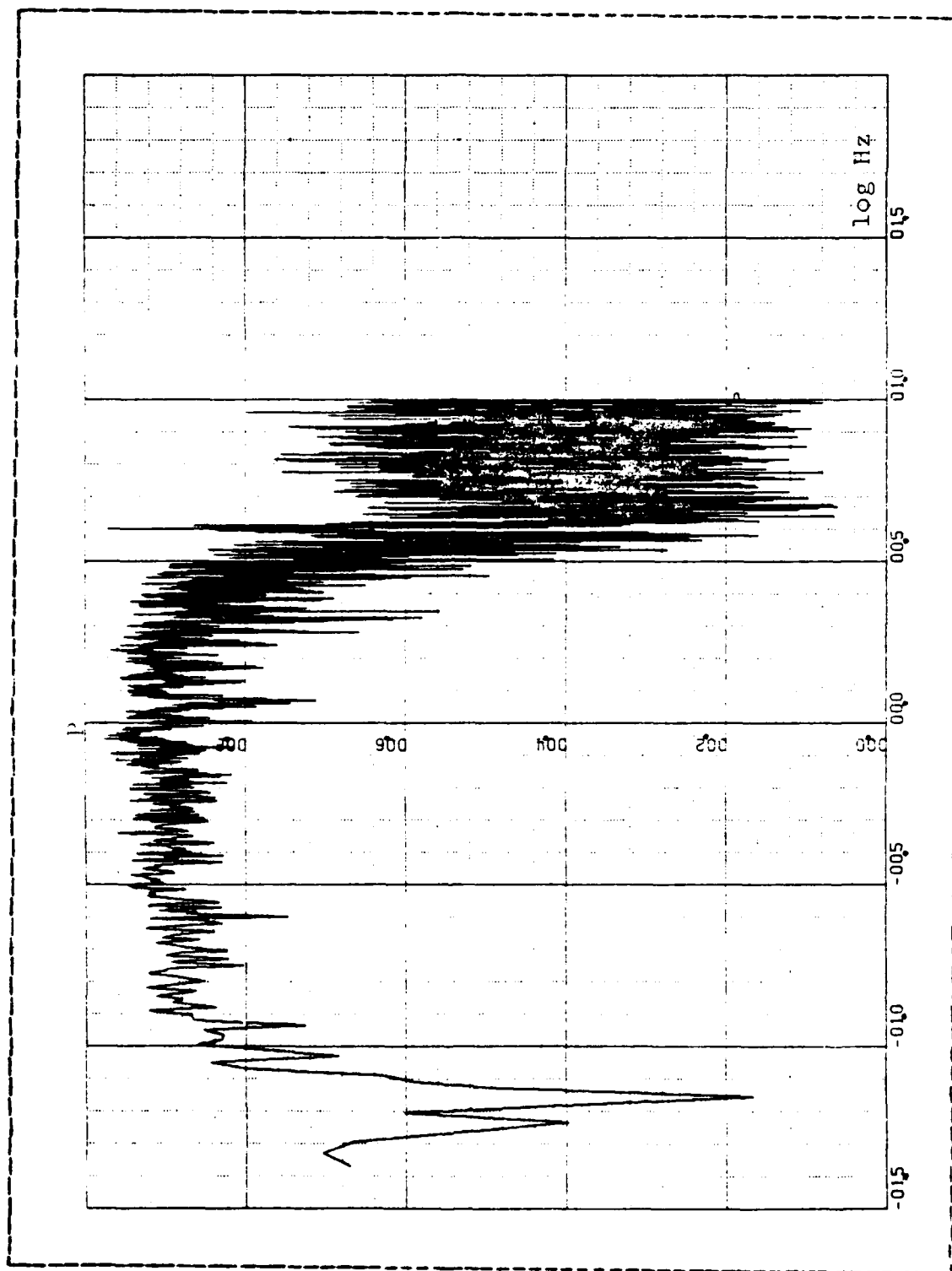
Figure 3.22   Degree of Polarization, Land, Z-X Plane

60
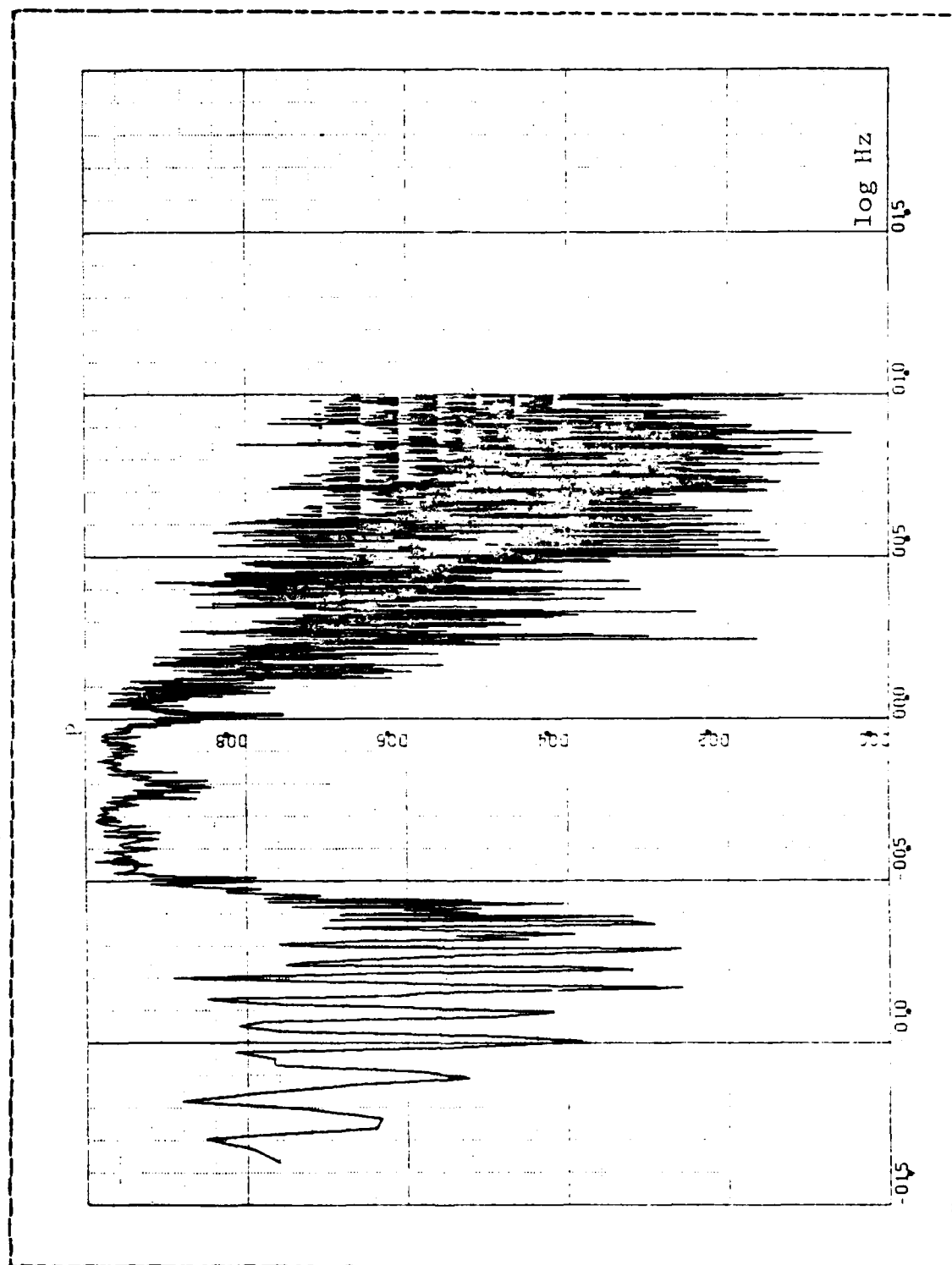
Figure 3.23 Degree of Polarization, Sea

61
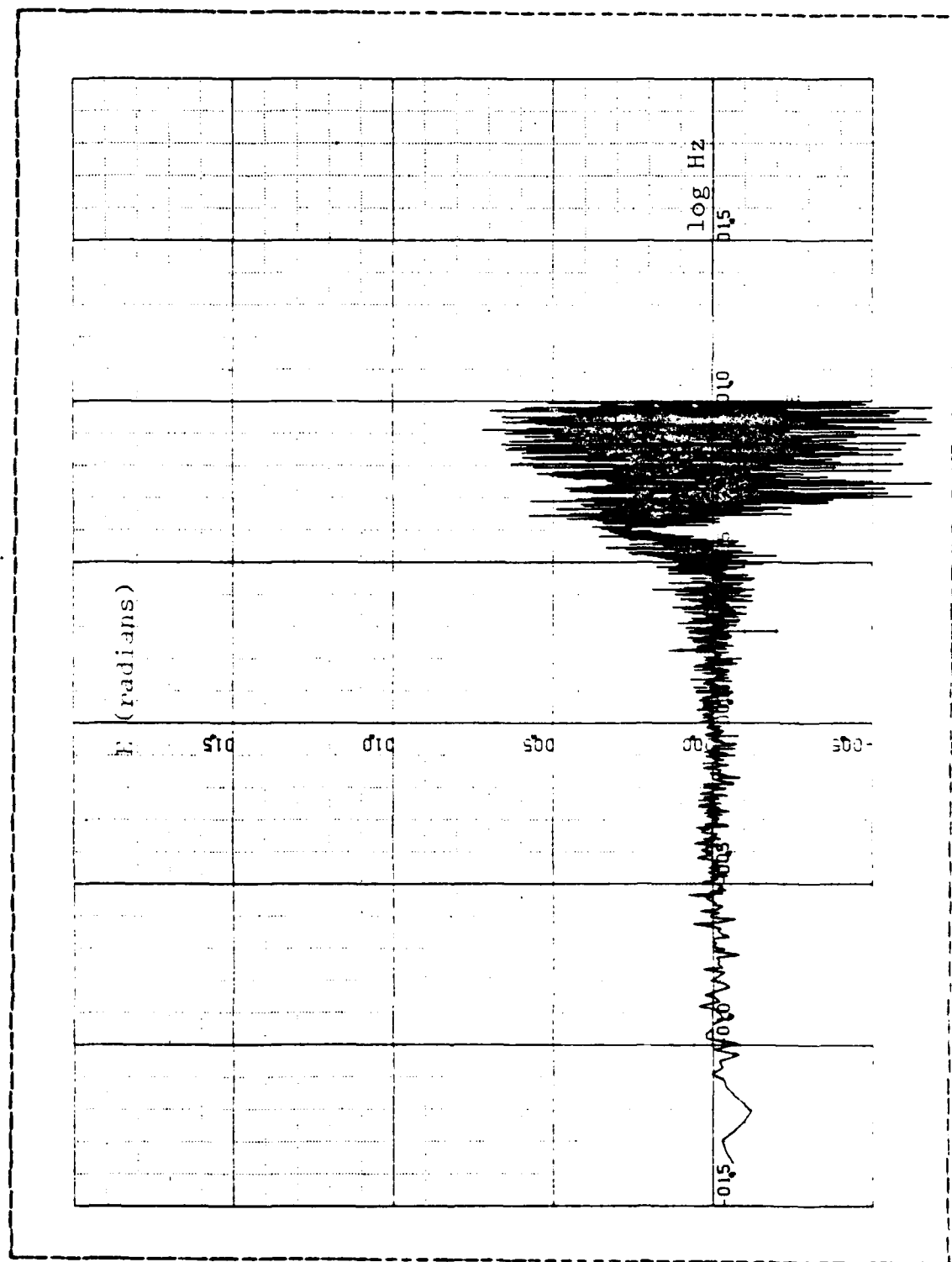
Figure 3.24   Ellipticity, Land, X-Y Plane
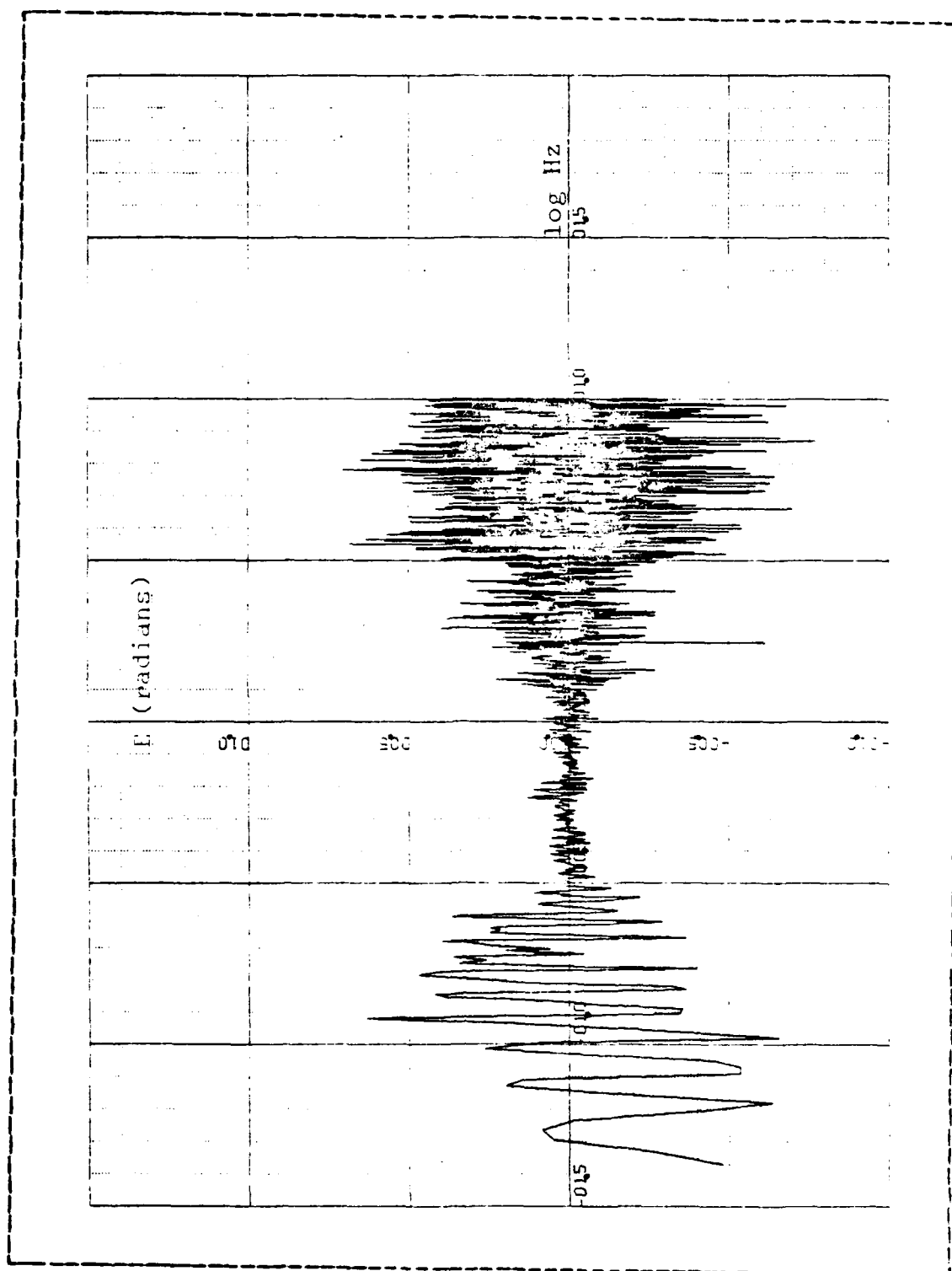
Figure 3.25   Ellipticity, Sea, X-Y Plane

63

the polarization is circular and is rotating in a right-handed sense, and at $E=-\pi/4$ the wave is again circular, but with a left-handed rotation. In between these values of E, the polarization of the wave is an ellipse with the appropriate handedness of the polarization depending on whether E is positive or negative. The smaller the absolute value of the ellipticity the narrower or more linear the ellipse becomes.

From Figures 3.24 and 3.25, the form of these waves for both land and sea data is generally a narrow ellipse with varying left and right handedness in the areas of high polarization while appearing to be more elliptical outside these areas [Ref. 9].

The final result of this investigation is that through the computation of the Stokes parameters the nature of the geomagnetic wave can be determined. Specifically, to find the type of polarization of the wave, one computes the ellipticity and the orientation angle α. The degree of polarization is also needed to establish the degree of validity of the interpretation. Naval Postgraduate School Technical Report #NPS 61-83-005, contains additional plots of all the factors described in this section.

C. COMPUTER PROGRAM DEVELOPEMENT AND DATA PROBLEMS

As noted earlier the ability to process large amounts of data in a timely manner was first put to use in this project in September 1982. The original program has been expanded to compute all of the factors listed in the previous section. It consists of a main program, a FFT subroutine, and a read subroutine. As noted before the FFT subroutine transfers the data into the frequency domain and the read subroutine reads the PCM data from the digital computer tape and places it in the input array. All changes and additions

made were in the main program, therefore only the main program is included in Appendix A. This program, Landxyz, is used to evaluate only the land data. The version of the program used to evaluate the sea data is identical to Landxyz with the following exceptions: sea system transfer functions are used; because the sea system has only two coils, only one plane of interpretive factors is computed.

Although the basic program proved adequate to find the power spectral densities, the growth of the program to include the other calculations created several problems. The Job Control Language (JCL) provides the guidance to the operating system of the computer to tell it how to run batch jobs. Specifically what input and output devices to use and how much memory to allocate to the program during each step of its execution. (In the program the JCL can be identified by the //'s at the start of each line of this code.) During the expansion of the program the amounts of memory in the LINK, GO and PLOT steps in the execution of the program have all expanded. The current JCL is capable of handling up to two hours of data at 32 Hz or one hour of data at 64 Hz.

Sea and land data are initially recorded on analog tape and then decoded and re-recorded onto digital tape in the Near Shore Laboratory of the Naval Postgraduate School. This procedure is discussed in [Ref. 3]. The output of this re-recording is approximately ninty minutes of real time data, from either the sea or land site, on a digital tape with a density of 800 bits per inch (BPI). The storage density proved a great handicap in the rapid expansion of the program. The Church Computer Center has fifteen tape drives, but only one of these is capable of handling a 800 BPI tape. The competition for this one tape drive led to processing times of up to twenty-seven hours. This delay made any programming error extremely costly in terms of time

65

lost. An attempt was made to transfer selected tapes into the memory of the computer, but it was unsuccessful due to minor recording errors on the digital tapes. These recording errors were overcome by the read subroutine in order to be able to work with the data. Time did not permit the presuit of this avenue of improvement but at best only a few tapes could be stored this way because of the vast amount of raw data.

The computer program was validated through the use of a test tape. The test tape was recorded with a sinusoidal input at known frequency and voltage level as measured by a spectrum analyser. When this tape was processed by the Landxyz program, the correct frequency and amplitude were produced, [Ref. 11].

A noise floor tape was produced by replacing the sensing coils with 120 ohm resistors. This tape was then evaluated by the Landxyz program to produce the PSD of the noise floor of the system. Figure 3.26 shows this noise floor superimposed on a land PSD plot.
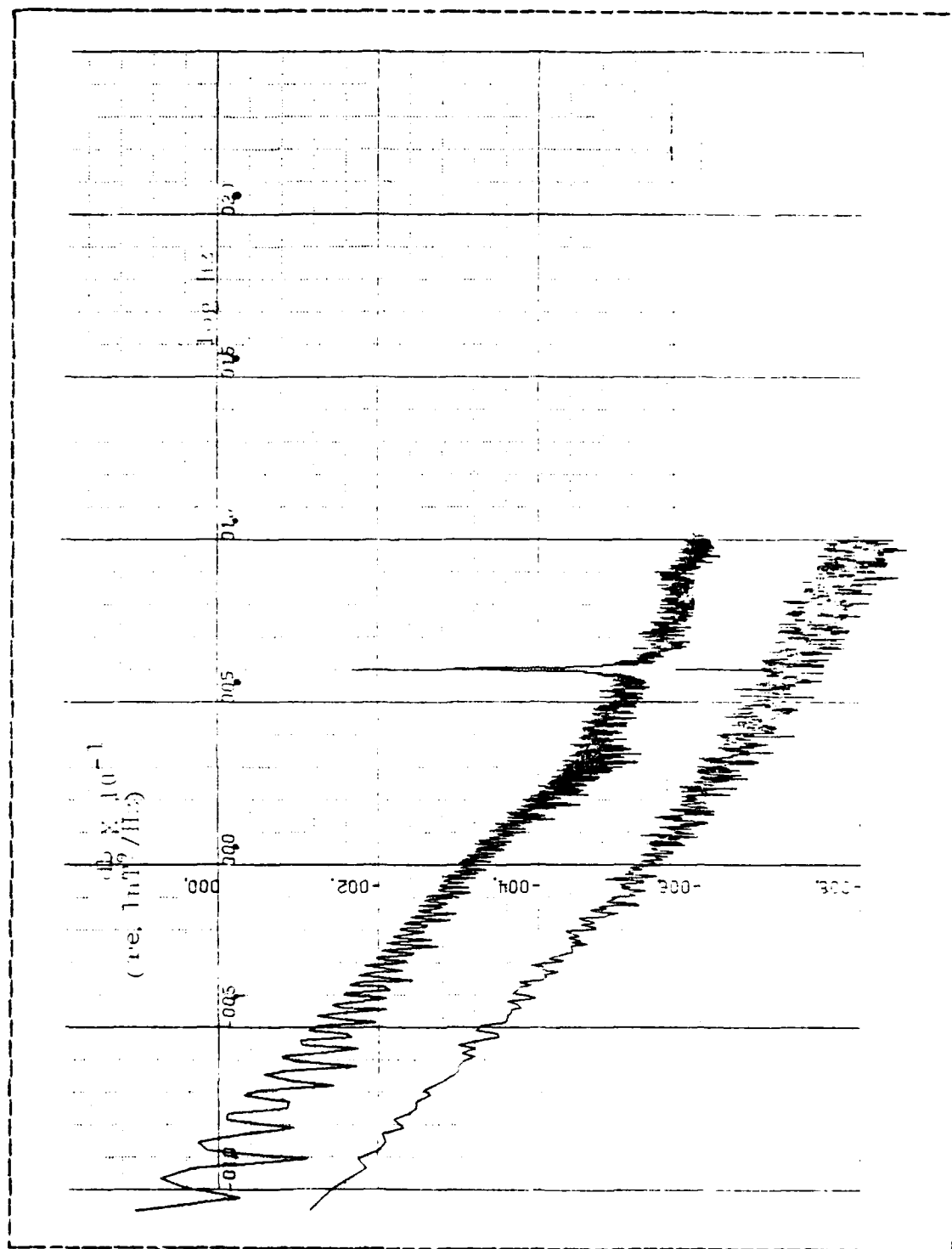
Figure 3.25   Noise Floor PSD

67

IV. CONCLUSIONS AND RECOMMENDATIONS

A. CONCLUSIONS

As stated earlier part of the objective of this thesis was to calibrate, install and operate the land portion of the Naval Postgraduate School's geomagnetic data collection system. This was generally successfully acomplished with the exception of degradation of data produced by using the more noisy La Mesa site rather than the more remote Chew's Ridge site. Exactly how much of an improvement in the quality of the data will result from the move to Chew's Ridge is difficult to predict. It could possibly diminish the 60 Hz component so that data could be obtained in the region of 4 Hz. Overall some 70 hours of land data was collected during this research, of which approximately twenty hours has been evaluated to date.

For the thesis's second objective, the production of a computer program and procedures to interpret the data, the expansion of the basic program to compute the coherences, Stokes parameters, degree of polarization, elliptical orientaion angle, and the ellipticity would appear to have satisfied the requirement. The major drawback to this system is the limited amount of data that can be processed in a reasonable time. At most the current programs are capable of evaluating only 5-6 hours of land and sea data in a twenty-four period. This is primarily due to tape drive availability, but the requirement of the man-hours for decoding, re-recording on digital tape and filing these tapes at the computer center cannot be discounted. The data processing system has reached the stage where large amounts of data can be evaluated but it is not yet ready to operate on a continuous basis.

B. RECOMMENDATIONS

The first recommendation is that the data transmission problem be solved so that the Chew's ridge site can be operated on a continuous basis. This has two advantages; in the improvement in the quality of the sampling environment and in giving a contiuous data stream that can be recorded at appropriate intervals to provide a long term data base from which low frequency trends could be observed.

Improvement could also be made in the area of data processing. Specifically, a new method of data handling is needed. Several alternatives exist, the first being the acquisition of the projects own decoder and digital tape drive to provide a digital tape of a higher density than can now be made. This would make it possible for a two to eight fold reduction in the number of tapes necessary to hold the data and would also give faster turn around time during processing due to the increased number of tape drives available at the computer center. Other data handling schemes are also feasible if the problem of how to read data from the digital tapes into the mass storage system of the computer can be overcome. This would make it possible to run programs in other than the "batch" mode and avoid the use of tape drives to gain access to the data.

APPENDIX A

COMPUTER PROGRAM

```
//LANDXYZ JOB (1573,0129),' POGUE    SMC 1573',CLASS=F
//*MAIN ORG=NPGVM1.1573P,LINES=(99)
//*FORMAT PR,DDNAME=PLOT.SYSVECTR,DEST=LOCAL
// EXEC FRTXCLGP,REGION.GO=3000K
//FORT.SYSIN DD *
      INTEGER*2 IN(16)
C      ARRAY 'IN' IS USED IN READING DATA FROM TAPE
      COMPLEX*8 XX(8192),YY(8192),Z(8192)
      COMPLEX*8 SXY(8192),SYZ(8192),SZX(8192)
C      THE COMPLEX*8 ARRAYS ARE USED TO ORDER INPUT
C      DATA AND INITIALLY REPRESENTS VOLTAGE-TIME
C      SERIES INFORMATION
      DIMENSION TIME(8192),FREQ(8192),WORK(16384),FRQ2(8192)
      DIMENSION ZX(8192),ZY(8192),ZZ(8192)
      DIMENSION SOXY(8192),SOYZ(8192),SOZX(8192)
      DIMENSION S1XY(8192),S1YZ(8192),S1ZX(8192)
      DIMENSION S2XY(8192),S2YZ(8192),S2ZX(8192)
      DIMENSION S3XY(8192),S3YZ(8192),S3ZX(8192)
      DIMENSION COXY(8192),COYZ(8192),COZX(8192)
      DIMENSION AXY(8192),AYZ(8192),AZX(8192)
      DIMENSION PXY(8192),PYZ(8192),PZX(8192)
      DIMENSION DEXY(8192),DEYZ(8192),DEZX(8192)
C      THE 'Z' ARRAYS REPRESENT FREQUENCY DOMAIN (FFT)
C      MAGNITUDE DATA AND ARE EVENTUALLY CONVERTED TO
C      POWER SPECTRAL DENSITY INFORMATION. COXY IS COHERENCE
C      MEASURED X TO Y. AXY IS THE ANGLE BETWEEN THE MAJOR
C      AXIS OF THE ELLIPSE AND THE X AXIS. PXY IS THE DEGREE
C      OF POLARIZATION IN THE X-Y PLANE.
C      DEXY IS THE ELLIPTICITY IN THE X-Y PLANE.
```

70

```
      INTEGER*4  ITB(12)/12*0/
      REAL*4     RTB(28)/28*0.0/
      REAL ALAB(11)/'X','Y','Z','C','S0','S1','S2','S3','A'
     ,'P','E'/
      REAL*8 TITLE(12)
      EQUIVALENCE(TITLE(1),RTB(5))
C        ARRAYS 'ITB','RTB','ALAB',AND 'TITLE' ARE USED IN
C        THE VERTSATEC PLOTTER OUTPUT.
      DATA XX,YY/16384*(0.,0.)/
      DATA Z/8192*(0.,0.)/
      DATA ZX,ZY/16384*0./
      DATA COXY,SOXY/16384*0./
      DATA S2XY,S3XY/16384*0./
      DATA S1XY,S1YZ/16384*0./
      DATA COYZ,SOYZ/16384*0./
      DATA S2YZ,S3YZ/16384*0./
      DATA COZX,SOZX/16384*0./
      DATA S2ZX,S3ZX/16384*0./
      DATA CZ,FREQ/16384*0./
      DATA AXY,AYZ/16384*0./
      DATA AZX,S1ZX/16384*0./
      DATA PXY,PYZ/16384*0./
      DATA PZX,DEXY/16384*0./
      DATA DEZX,DEYZ/16384*0./
      PI2=6.2831853
C        THE FOLLOWING SECTION READS THE DECODED PCM DATA OFF
C        THE DIGITAL TAPE AND FOR EACH CHANNEL SKIPS EVERY
C        OTHER SAMPLE POINT.
C     ISEC=3
C     ITL=ISEC*32
      ITL=300
      DO 55 JJ=1,ITL
      CALL RD(20,IN,200,IREC,IRR)
   55 CONTINUE
```

```
      IFRAME=8192
      NR=16
      FNR=FLOAT(NR)
      DO 70 L1=1,NR
C     THE DO LOOP ENDING WITH STATEMENT 70 ENABLES THE PRO-
C     GRAM TO PROCESS A LARGE AMOUNT OF DATA BY REPEATING
C     THE PROCESS IN BLOCKS. THE DATA POINTS FROM EACH RUN
C     THROUGH THE DO LOOP ARE ADDED TOGETHER AND EVENTUALLY
C     AVERAGED BY THE THE NUMBER OF TIME THROUGH THE LOOP.
C     'NR' REPRESENTS THE NUMBER OF DATA SEQUENCES TO BE
C     AVERAGED
C     1 SEQUENCE CURRENTLY EQUALS 8192 DATA POINTS FOR EACH
C     CHANNEL OR 256 SECONDS AT A SAMPLE RATE OF 32 CPS.
      DO 60 JJ=1,IFRAME
      CALL RD(20,IN,1000,IREC,IRR)
      XX(JJ)=IN(2)
      YY(JJ)=IN(3)
      Z(JJ)=IN(4)
   60 CONTINUE
      WRITE(6,200)IRR,IREC
  200 FORMAT(10X,'IRR=',I5,5X,'IREC=',I6,/)
C         THIS SECTION GENERATES THE TIME AND FREQUENCY
C         ARRAYS AND NORMALIZES THE INPUT PCM DATA TO VOLTAGE
C         IN PREPARATION FOR FAST FOURIER TRANSFORM TO THE
C         FREQUENCY DOMAIN.
      N=8192
      FN=FLOAT(N)
      DELTAT=1./32.
      T=FN*DELTAT
      DELTAF=1.0/T
      DO 20 J=1,N
      TIME(J)=DELTAT*FLOAT(J)
      FREQ(J)=DELTAF*FLOAT(J)
      XX(J)=(XX(J)-2045.5)*10./2045.5
```

```fortran
          XX(J)=REAL(XX(J))
          YY(J)=(YY(J)-2045.5)*10./2045.5
          YY(J)=REAL(YY(J))
          Z(J)=(Z(J)-2045.5)*10./2045.5
          Z(J)=REAL(Z(J))
C        'XX' IS THE X-COIL DATA, 'YY' IS THE Y-COIL DATA,
   20 CONTINUE
          WRITE(6,900)X,Y,ZP
  201 CONTINUE
          DO 21 J=1,N
          FRQ2(J)=ALOG10(FREQ(J))
   21 CONTINUE
C        THE NEXT 3 STATEMENTS PERFORM AN FFT ON THE INPUT
C        TIME SERIES DATA.
          CALL FOURT(XX,N,1,-1,0,WORK)
          CALL FOURT(YY,N,1,-1,0,WORK)
          CALL FOURT(Z,N,1,-1,0,WORK)
C        THIS BLOCK OF STATEMENTS APPLY THE SYSTEM (VOLTAGE TO
C        B-FIELD) TRANSFER FUNCTION TO THE TRANSFORMED
C        FREQUENCY DOMAIN DATA. THIS BLOCK ENDS AT 9.
C        THE TRANSFER FUNCTION CONVERTS VOLTS TO NANOTESLAS.
C        *****WARNING*****
C        THIS TRANSFER FUNCTION IS GOOD FOR MAGNITUDE ONLY.
          DO 9 L=1,N
          FRQ=FREQ(L)
          IF(FRQ.LE.25.)GO TO 1
          XX(L)=XX(L)/28.
          GO TO 8
    1 IF(FRQ.LE.15.)GO TO 2
          XX(L)=XX(L)/(105.5-3.14*FRQ)
          YY(L)=YY(L)/(181.32-7.588*FRQ)
          Z(L)=Z(L)/(177.26-7.484*FRQ)
          GO TO 8
    2 IF(FRQ.LE.10.)GO TO 3
```

73

```fortran
      XX(L)=XX(L)/(5.958*FRQ-30.97)
      YY(L)=YY(L)/(7.166*FRQ-39.99)
      Z(L)=Z(L)/(6.49*FRQ-32.35)
      GO TO 8
    3 IF(FRQ.LE.7.5)GO TO 4
      XX(L)=XX(L)/(3.492*FRQ-6.31)
      YY(L)=YY(L)/(4.252*FRQ-10.85)
      Z(L)=Z(L)/(4.044*FRQ-7.89)
      GO TO 8
    4 IF(FRQ.LE.5.)GO TO 5
      XX(L)=XX(L)/(2.6311*FRQ+0.14667)
      YY(L)=YY(L)/(3.012*FRQ-1.55)
      Z(L)=Z(L)/(3.184*FRQ-1.44)
      GO TO 8
    5 IF(FRQ.LE.3.)GO TO 6
      XX(L)=XX(L)/(2.6311*FRQ+0.14567)
    7 YY(L)=YY(L)/(2.702*FRQ)
      Z(L)=Z(L)/(2.92*FRQ)
      GO TO 8
    6 XX(L)=XX(L)/(2.72*FRQ)
      GO TO 7
    8 CONTINUE
    9 CONTINUE
C        THIS BLOCK, ENDING WITH 30, THE MAGNITUDE OF THE
C        FREQUENCY DOMAIN DATA IS TAKEN AND PLACED IN A REAL
C        ARRAY,'ZX' FOR THE X-COIL,'ZY' FOR THE Y-COIL AND ZZ
C        FOR THE Z-COIL. THIS DATA IS DIVIDED BY THE NUMBER OF
C        SAMPLE POINTS AND SQUARED TO DETERMINE POWER.
      DO 30 I1=1,N
      ZX(I1)=ZX(I1)+(CABS(XX(I1))/FN)**2
      ZY(I1)=ZY(I1)+(CABS(YY(I1))/FN)**2
      ZZ(I1)=ZZ(I1)+(CABS(Z(I1))/FN)**2
      SXY(I1)=SXY(I1)+((XX(I1)/FN)*CONJG(YY(I1)/FN))
      COXY(I1)=COXY(I1)+CABS((XX(I1)/FN)*CONJG(YY(I1)/FN))
```

```
              SYZ(I1)=SYZ(I1)+((YY(I1)/FN)*CONJG(Z(I1)/FN))
              COYZ(I1)=COYZ(I1)+CABS((YY(I1)/FN)*CONJG(Z(I1)/FN))
              SZX(I1)=SZX(I1)+((Z(I1)/FN)*CONJG(XX(I1)/FN))
              COZX(I1)=COZX(I1)+CABS((Z(I1)/FN)*CONJG(XX(I1)/FN))
       30 CONTINUE
       70 CONTINUE
    C        THIS BLOCK AVERAGES THE DATA POINTS ADDED IN BLOCK 30
    C        ABOVE BY 'NR'. AT THIS POINT THE POWER CURVES ARE
    C        CONVERTED INTO POWER SPECTRAL DENSITIES.
    C        THE COHERENCES AND STOKES PARAMETERS ARE
    C        COMPUTED IN ALL THREE PLANES.
             DO 33 I3=1,N
             S2XY(I3)=(REAL(SXY(I3))/FNR)*4.
             S3XY(I3)=(AIMAG(SXY(I3))/FNR)*4.
             S2YZ(I3)=(REAL(SYZ(I3))/FNR)*4.
             S3YZ(I3)=(AIMAG(SYZ(I3))/FNR)*4.
             S2ZX(I3)=(REAL(SZX(I3))/FNR)*4.
             S3ZX(I3)=(AIMAG(SZX(I3))/FNR)*4.
             COXY(I3)=(COXY(I3))/SQRT(ZX(I3)*ZY(I3))
             COYZ(I3)=(COYZ(I3))/SQRT(ZZ(I3)*ZY(I3))
             COZX(I3)=(COZX(I3))/SQRT(ZX(I3)*ZZ(I3))
             ZX(I3)=ZX(I3)*T/FNR
             ZY(I3)=ZY(I3)*T/FNR
             ZZ(I3)=ZZ(I3)*T/FNR
             S1XY(I3)=((ZX(I3)-ZY(I3))/T)*2.
             S1YZ(I3)=((ZY(I3)-ZZ(I3))/T)*2.
             S1ZX(I3)=((ZZ(I3)-ZX(I3))/T)*2.
             SOXY(I3)=((ZX(I3)+ZY(I3))/T)*2.
             SOYZ(I3)=((ZZ(I3)+ZY(I3))/T)*2.
             SOZX(I3)=((ZX(I3)+ZZ(I3))/T)*2.
       33 CONTINUE
    C        THE NEXT DO LOOP CONVERTS THE B-FIELD POWER SPECTRAL
    C        DENSITY INTO DECIBELS REFERENCED TO 1 NANOTESLA **2
    C        PER HERTZ.
```

```
          DO 32 I=1,N
          ZX(I)=10.*ALOG10(ZX(I))
          ZY(I)=10.*ALOG10(ZY(I))
          ZZ(I)=10.*ALOG10(ZZ(I))
       32 CONTINUE
C      THE NEXT BLOCK ELIMINATES THE FIRST 10 DATA POINTS SO
C      THAT THE FREQUENCY IS .04 TO 10 HZ.
C      S1,S2, AND S3 ARE NORMALIZED BY S0.
C      DEGREE OF POLARIZATION, ORIENTATION ANGLE ALPHA,
C      AND THE ELLIPTICITY ARE ALSO COMPUTED.
          DO 950 I4=1,8182
          FREQ(I4)=FREQ(I4+10)
          FRQ2(I4)=FRQ2(I4+10)
          ZX(I4)=ZX(I4+10)
          ZY(I4)=ZY(I4+10)
          ZZ(I4)=ZZ(I4+10)
          COXY(I4)=COXY(I4+10)
          S1XY(I4)=S1XY(I4+10)/S0XY(I4+10)
          S2XY(I4)=S2XY(I4+10)/S0XY(I4+10)
          S3XY(I4)=S3XY(I4+10)/S0XY(I4+10)
          PXY(I4)=SQRT(S1XY(I4)**2+S2XY(I4)**2+S3XY(I4)**2)
          DEXY(I4)=0.5*ARSIN(S3XY(I4)/PXY(I4))
          S0XY(I4)=10.*ALOG10(S0XY(I4+10))
          COYZ(I4)=COYZ(I4+10)
          S1YZ(I4)=S1YZ(I4+10)/S0YZ(I4+10)
          S2YZ(I4)=S2YZ(I4+10)/S0YZ(I4+10)
          S3YZ(I4)=S3YZ(I4+10)/S0YZ(I4+10)
          PYZ(I4)=SQRT(S1YZ(I4)**2+S2YZ(I4)**2+S3YZ(I4)**2)
          DEYZ(I4)=0.5*ARSIN(S3YZ(I4)/PYZ(I4))
          S0YZ(I4)=10.*ALOG10(S0YZ(I4+10))
          COZX(I4)=COZX(I4+10)
          S1ZX(I4)=S1ZX(I4+10)/S0ZX(I4+10)
          S2ZX(I4)=S2ZX(I4+10)/S0ZX(I4+10)
          S3ZX(I4)=S3ZX(I4+10)/S0ZX(I4+10)
```

75

```
            PZX(I4)=SQRT(S1ZX(I4)**2+S2ZX(I4)**2+S3ZX(I4)**2)
            DEZX(I4)=0.5*ARSIN(S3ZX(I4)/PZX(I4))
            SOZX(I4)=10.*ALOG10(SOZX(I4+10))
            AXY(I4)=ATAN(S2XY(I4)/S1XY(I4))/2.
            AYZ(I4)=ATAN(S2YZ(I4)/S1YZ(I4))/2.
            AZX(I4)=ATAN(S2ZX(I4)/S1ZX(I4))/2.
      950 CONTINUE
C
C     VERSATEC PLOTS
C
      NPTS=10./DELTAF +1.
C        'NPTS' DETERMINES NUMBER OF POINTS NECESSARY
C        FOR THE 0 TO 10 HERTZ RANGE TO BE PLOTTED.
C        FOR THE 'ITB' AND 'RTB' VALUES REVIEW THE WRITE-UP
C        FOR THE SUBROUTINE PROCEDURE 'DRAWP'.
      ITB(3)=7
      ITB(4)=5
      ITB(7)=1
      ITB(12)=1
      RTB(1)=0.0
      RTB(2)=0.0
      RTB(3)=ALAB(1)
      READ(5,3000) TITLE
      CALL DRAWP(NPTS,FRQ2,ZX,ITB,RTB)
      RTB(3)=ALAB(2)
      READ(5,3000) TITLE
      CALL DRAWP(NPTS,FRQ2,ZY,ITB,RTB)
      RTB(3)=ALAB(3)
      READ(5,3000) TITLE
      CALL DRAWP(NPTS,FRQ2,ZZ,ITB,RTB)
      RTB(3)=ALAB(4)
      READ(5,3000) TITLE
      CALL DRAWP(NPTS,FRQ2,COXY,ITB,RTB)
      RTB(3)=ALAB(5)
```

```
READ(5,3000) TITLE
CALL DRAWP (NPTS,FRQ2,SOXY,ITB,RTB)
RTB(3)=ALAB(6)
READ(5,3000) TITLE
CALL DRAWP (NPTS,FRQ2,S1XY,ITB,RTB)
RTB(3)=ALAB(7)
READ(5,3000) TITLE
CALL DRAWP (NPTS,FRQ2,S2XY,ITB,RTB)
RTB(3)=ALAB(3)
READ(5,3000) TITLE
CALL DRAWP (NPTS,FRQ2,S3XY,ITB,RTB)
RTB(3)=ALAB(4)
READ(5,3000) TITLE
CALL DRAWP (NPTS,FRQ2,COYZ,ITB,RTB)
RTB(3)=ALAB(5)
READ(5,3000) TITLE
CALL DRAWP (NPTS,FRQ2,SOYZ,ITB,RTB)
RTB(3)=ALAB(6)
READ(5,3000) TITLE
CALL DRAWP (NPTS,FRQ2,S1YZ,ITB,RTB)
RTB(3)=ALAB(7)
READ(5,3000) TITLE
CALL DRAWP (NPTS,FRQ2,S2YZ,ITB,RTB)
RTB(3)=ALAB(8)
READ(5,3000) TITLE
CALL DRAWP (NPTS,FRQ2,S3YZ,ITB,RTB)
RTB(3)=ALAB(4)
READ(5,3000) TITLE
CALL DRAWP (NPTS,FRQ2,COZX,ITB,RTB)
RTB(3)=ALAB(5)
READ(5,3000) TITLE
CALL DRAWP (NPTS,FRQ2,SOZX,ITB,RTB)
RTB(3)=ALAB(6)
READ(5,3000) TITLE
```

```
CALL DRAWP(NPTS,FRQ2,S1ZX,ITB,RTB)
RTB(3)=ALAB(7)
READ(5,3000) TITLE
CALL DRAWP(NPTS,FRQ2,S2ZX,ITB,RTB)
RTB(3)=ALAB(8)
READ(5,3000) TITLE
CALL DRAWP(NPTS,FRQ2,S3ZX,ITB,RTB)
RTB(3)=ALAB(9)
READ(5,3000) TITLE
CALL DRAWP(NPTS,FRQ2,AXY,ITB,RTB)
RTB(3)=ALAB(10)
READ(5,3000) TITLE
CALL DRAWP(NPTS,FRQ2,PXY,ITB,RTB)
RTB(3)=ALAB(11)
READ(5,3000) TITLE
CALL DRAWP(NPTS,FRQ2,DEXY,ITB,RTB)
RTB(3)=ALAB(9)
READ(5,3000) TITLE
CALL DRAWP(NPTS,FRQ2,AYZ,ITB,RTB)
RTB(3)=ALAB(10)
READ(5,3000) TITLE
CALL DRAWP(NPTS,FRQ2,PYZ,ITB,RTB)
RTB(3)=ALAB(11)
READ(5,3000) TITLE
CALL DRAWP(NPTS,FRQ2,DEYZ,ITB,RTB)
RTB(3)=ALAB(9)
READ(5,3000) TITLE
CALL DRAWP(NPTS,FRQ2,AZX,ITB,RTB)
RTB(3)=ALAB(10)
READ(5,3000) TITLE
CALL DRAWP(NPTS,FRQ2,PZX,ITB,RTB)
RTB(3)=ALAB(11)
READ(5,3000) TITLE
CALL DRAWP(NPTS,FRQ2,DEZX,ITB,RTB)
```

79

```
 3300 FORMAT(6A8)
      STOP
      END
//LKED.SYSUT1 DD SPACE=(1024,(200,200))
//GO.SYSIN DD *
```
LA MESA SITE, 16 SEP 82, 1250-1330 LOCAL
PSD OF X-COIL. AMP IN DB REF NT**2/HZ VS HZ
LA MESA SITE, 16 SEP 82, 1250-1330 LOCAL
PSD OF Y-COIL. AMP IN DB REF NT**2/HZ VS HZ
LA MESA SITE, 16 SEP 82, 1250-1330 LOCAL
PSD OF Z-COIL. AMP IN DB REF NT**2/HZ VS HZ
LA MESA SITE, 16 SEP 82, 1250-1330 LOCAL
COHERENCE OF X & Y COILS VS FREQ(HZ)
LA MESA SITE, 16 SEP 82, 1250-1330 LOCAL
S0(10LOG) VS FREQ(HZ)   X-Y PLANE
LA MESA SITE, 16 SEP 82, 1250-1330 LOCAL
S1/S0 VS FREQ(HZ)   X-Y PLANE
LA MESA SITE, 16 SEP 82, 1250-1330 LOCAL
S2/S0 VS FREQ(HZ)   X-Y PLANE
LA MESA SITE, 16 SEP 82, 1250-1330 LOCAL
S3/S0 VS FREQ(HZ)   X-Y PLANE
LA MESA SITE, 16 SEP 82, 1250-1330 LOCAL
COHERENCE OF Y & Z COILS VS FREQ(HZ)
LA MESA SITE, 16 SEP 82, 1250-1330 LOCAL
S0(10LOG) VS FREQ(HZ)   Y-Z PLANE
LA MESA SITE, 16 SEP 82, 1250-1330 LOCAL
S1/S0 VS FREQ(HZ)   Y-Z PLANE
LA MESA SITE, 16 SEP 82, 1250-1330 LOCAL
S2/S0 VS FREQ(HZ)   Y-Z PLANE
LA MESA SITE, 16 SEP 82, 1250-1330 LOCAL
S3/S0 VS FREQ(HZ)   Y-Z PLANE
LA MESA SITE, 16 SEP 82, 1250-1330 LOCAL
COHERENCE OF Z & X COILS VS FREQ(HZ)
LA MESA SITE, 16 SEP 82, 1250-1330 LOCAL

```
SO(10LOG) VS FREQ(HZ)          Z-X PLANE
LA MESA SITE, 16 SEP 82, 1250-1330 LOCAL
S1/SO VS FREQ(HZ)              Z-X PLANE
LA MESA SITE, 16 SEP 82, 1250-1330 LOCAL
S2/SO VS FREQ(HZ)              Z-X PLANE
LA MESA SITE, 16 SEP 82, 1250-1330 LOCAL
S3/SO VS FREQ(HZ)              Z-X PLANE
LA MESA SITE, 16 SEP 82, 1250-1330 LOCAL
AXY VS FREQ(HZ)
LA MESA SITE, 16 SEP 82, 1250-1330 LOCAL
DEGREE OF POLARIZATION VS FREQ(HZ)   X-Y
LA MESA SITE, 16 SEP 82, 1250-1330 LOCAL
ELLITICITY VS FREQ(HZ)         X-Y PLANE
LA MESA SITE, 16 SEP 82, 1250-1330 LOCAL
AYZ VS FREQ(HZ)
LA MESA SITE, 16 SEP 82, 1250-1330 LOCAL
DEGREE OF POLARIZATION VS FREQ(HZ)   Y-Z
LA MESA SITE, 16 SEP 82, 1250-1330 LOCAL
ELLITICITY VS FREQ(HZ)         Y-Z PLANE
LA MESA SITE, 16 SEP 82, 1250-1330 LOCAL
AZX VS FREQ(HZ)
LA MESA SITE, 16 SEP 82, 1250-1330 LOCAL
DEGREE OF POLARIZATION VS FREQ(HZ)   Z-X
LA MESA SITE, 16 SEP 82, 1250-1330 LOCAL
ELLITICITY VS FREQ(HZ)         Z-X PLANE
/*
//GO.FT20F001 DD UNIT=3400-4,VOL=SER=GMDT52,DISP=(OLD,KEEP),
//              LABEL=(1,NL,,IN),
//              DCB=(RECFM=FB,LRECL=32,BLKSIZE=512,DEN=2)
/*
//
```

APPENDIX B

CHEW'S RIDGE SITE PREPARATION

Chew's Ridge is the site of previous land-side geomagnetic data collection. It is located approximately twenty-three air miles southeast of the Naval Postgraduate School on a hilltop 3,300 feet above sea level. It was chosen for its remoteness from the local power grid (3-4 miles) and its virtual "line of sight" RF path to the school. A detailed description of the physical layout and operation of the site can be found in [Ref. 6].

The original intention of this research was to collect data from this remote site to provide the simultaneous data for the sea trials. Preparation of the site and the necessary equipment continued through most of the project. The data transmission from this site to the Naval Postgraduate School receiving location proved impossible with the transmitter/receivers available.

Previous data collected from Chew's Ridge was collected using a Motorola system that suffered from overheating failures when required to operate in a continuous mode. Intially another attempt was made to repair the Motorola unit but after one last failure this proved economically impossible and it was felt that this unit did not have the bandwidth to accomadate the addition of the PCM to the system. Consequently a REPCO Model 810 transmitter-receiver pair was ordered. These on arrived the first of September and initial testing showed that, although they were capable of operating for long periods of time, they did not have the required 20 KHz bandwidth to accomadate the PCM data. Efforts are currently underway to expand the bandwidth to meet the requirements.
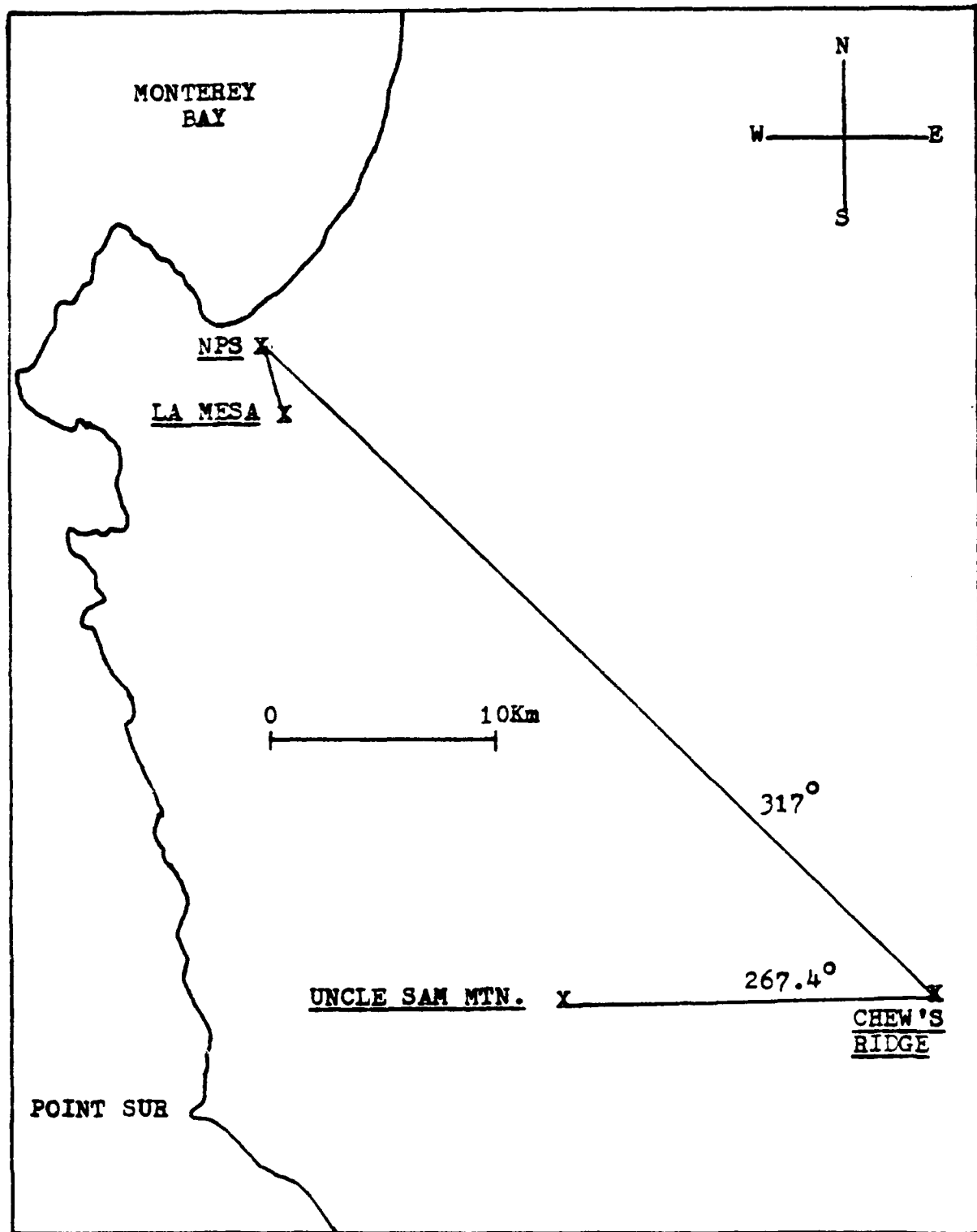
Figure B.1   Geographical Area of Data Collection

To properly orient the sensing coils at this site it is necessary to have an accurate known direction. In order to accomplish this, inquiries were made to the National Forest Service to determine if they have survey data for the area. When it proved nonexistent, a survey by resection was conducted. A theodolite was used to measure relative angles to several prominent terrain features in the area from the Chew's Ridge Site. These measurements were made three times and then averaged. The average relative angles were then drawn on a piece of overlay paper and oriented on a 1:50,000 map of the area. This allowed for the best fit of the data and prevented blunders in the recognition of the terrain features. The most prominent terrain feature (Uncle Sam Mountain) was then chosen for the end of the orienting line. The Grid Azimuth to Uncle Sam Mtn. was then computed from the coordinates of the two locations. Finally the True Azimuth was calculated to be 257.4 degrees. Estimated accuracy of this measurement is one degree.

LIST OF REFERENCES

1. Jacobs, J. A., "Geomagnetic Micropulsations", p. 15-33, Springer-Verlag, 1970.

2. Galejs, J., "Schumann Resonaces", RADIO SCIENCE Journal of Research, v. 69D, n. 8, p. 1043, August 1965.

3. Gritzke, A. R. and Johnson, R. H., "Ocean Floor Geomagnetic Data Collection System", M.S. Thesis, Naval Postgraduate School, Monterey, 1982.

4. Jefimenko, O. D., "Electricity and Magnetism", p. 380, Meredith Publishing Co., 1966.

5. Schweiger, J. M., "Evaluation of Geomagnetic Activity in the MAD Frequency Band (.04 to .06 Hz)", M.S. Thesis, Naval Postgraduate School, Monterey, 1982.

6. Beard, M. W., "Power Spectra of Geomagnetic Fluctuations Between 0.02 And 20 Hz", M.S. Thesis, Naval Postgraduate School, Monterey, 1981.

7. Brigham, E. O., "The Fast Fourier Transforms", p. 93-97, Prentice-Hall Inc., 1974.

8. Clayton, F. W., "Power Spectra of Geomagnetic Fluctuations Between 0.4 And 40 Hz", M.S. Thesis, Naval Postgraduate School, Monterey, 1979.

9. Born, M. and Wolf, E., "Principles of Optics", 4th ed., p. 544-555, Pergamon Press, 1970.

10. Jackson, J. D., "Classical Electrodynamics", 2d ed., p. 273-278, John Wiley & Sons, Inc., 1975.

11. Fisher, J. T., "Coherence in the Horizontal Plane of the Geomagnetic Field in the Frequency Range 0-10 Hz", M.S. Thesis, Naval Postgraduate School, Monterey, 1982.

INITIAL DISTRIBUTION LIST

No. Copies

1. Defense Technical Information Center   2
   Cameron Station
   Alexandria, Virginia 22314

2. Library, Code 0142   2
   Naval Postgraduate School
   Monterey, California 93940

3. Dr. Otto Heinz, Code 61Hz   2
   Department of Physics
   Naval Postgraduate School
   Monterey, California 93940

4. Dr. Andrew R. Ochadlick Jr., Code 610c   2
   Department of Physics
   Naval Postgraduate School
   Monterey, California 93940

5. Dr. Paul Moose, Code 62Me   1
   Department of Electrical Engineering
   Naval Postgraduate School
   Monterey, California 93940

6. Dr. Michael Thomas, Code 61   1
   Department of Physics
   Naval Postgraduate School
   Monterey, California 93940

7. CPT Edward W. Pogue   2
   RR#1, Box 68
   Cleveland, OK 74020

8. LCDR Arnold R. Gritzke, USN   3
   114 Cleveland Avenue
   Lackawanna, New York 14218

9. LT Robert H. Johnson II, USN   1
   46 Grayson Circle
   Willingboro, New Jersey 08046

10. Captain Woodrow Reynolds, Code 68   1
    Department of Oceanography
    Naval Postgraduate School
    Monterey, California 93940

11. Robert C. Smith, Code 61   1
    Department of Physics
    Naval Postgraduate School
    Monterey, California 93940

12. LT Jeffrey M. Schweiger, USN   1
    44 Roundabout Road
    Smithtown, New York 11787

13. Dr. A. C. Fraser-Smith   1
    Radio Science Laboratory
    Stanford Electronics Laboritories
    Stanford University
    Palo Alto, California 94305

14. Dr. David M. Bubenik   1
    Assistant Director,
    Electromagnetic Sciences Laboratory
    SRI International
    333 Ravenswood Avenue
    Menlo Park, California 94025

15. Dr. Robert N. McDonough, 8-368   2
    The Johns Hopkins University
    Applied Physics Laboratory
    Johns Hopkins Road
    Laurel, MD 20801

16. Chief of Naval Research, Code 10001   1
    Department of the Navy
    800 North Quincy Street
    Arlington, VA 22217

17. Chief of Naval Research, Code 411   1
    Department of the Navy
    800 North Quincy Street
    Arlington, VA 22217

18. Chief of Naval Research, Code 420   1
    Department of the Navy
    800 North Quincy Street
    Arlington, VA 22217

19. Mr. William Andahazy   1
    Naval Ship Research and Development Center
    Annapolis Laboratory
    Annapolis, MD 21402

20. Department Chairman, Code 62   1
    Department of Electrical Engineering
    Naval Postgraduate School
    Monterey, California 93940

21. Army Research Office   1
    Department of the Army
    Geosciences Division
    Box 12211
    Research Triangle Park, NC 27709

END

FILMED

5-83

DTIC